

Some pages of this thesis may have been removed for copyright restrictions.

If you have discovered material in Aston Research Explorer which is unlawful e.g. breaches copyright, (either yours or that of a third party) or any other law, including but not limited to those relating to patent, trademark, confidentiality, data protection, obscenity, defamation, libel, then please read our [Takedown policy](#) and contact the service immediately (openaccess@aston.ac.uk)

**AN INVESTIGATION TO DETERMINE THE INFLUENCE OF ILLUMINATION
SOURCES ON COLOUR DISCRIMINATION IN NORMAL SUBJECTS AND
SMOKERS**

KALPEN MISTRY

DOCTOR OF OPTOMETRY (DOptom)

ASTON UNIVERSITY

FEBRUARY 2015

©Kalpen Mistry 2015

Kalpen Mistry asserts his moral right to be identified as the author of the thesis

This copy of the thesis has been supplied on condition that anyone who consults it is understood to recognize that its copyright rests with its author and that no quotation from the thesis and no information derived from it may be published without proper acknowledgement

SUMMARY

Aston University

An Investigation to Determine the Influence of Illumination Sources on Colour Discrimination in Normal Subjects and Smokers

Kalpen Mistry
Doctor of Optometry (DOptom)
2015

Introduction: Accurate colour vision testing requires using the correct illumination. With the plethora of 'daylight' lamps available, is there a cost-effective alternative to the discontinued MacBeth Easel lamp? Smoking is a known risk factor for macula degeneration. As the macula is responsible for colour discrimination, any toxin that affects it has the potential to influence colour discrimination. **Aims:** To find a cost-effective light source for colour vision testing. To investigate the effect of smoking on colour discrimination. To explore how deuteranomalous trichromats compare with normal trichromats. **Methods:** Using the Ishihara colour vision test subjects were classified into the groups: 'Normal/Control', 'Smoker/Test', and 'Case Study' (subjects who failed the screening test and did not smoke). They completed the Farnsworth Munsell 100 Hue test under each of the three light sources: Phillips EcoHalo Twist (tungsten halogen - THL), Kosnic KCF07ALU/GU10-865 (compact fluorescent- CFL), and Deal Guardian Ltd. GU103X2WA4B-60 (light-emitting diode - LED) **Results:** 42 subjects took part in the study: 18 in the Normal/Control group, 18 in the Smoker/Test group, and 6 in the Case Study group. For the Normal/Control group the total error scores (TESs) were significantly lower with the CFL than with the THL ($p = 0.017$) as it was for the Case Study group ($p = 0.009$). No significant differences were found between the Normal/Control group and the Smoker/Test group for each light source. Decision tree analysis found pack years to be a significant variable for TES. **Discussion:** All three light sources were comparable with previous studies. The CFL provided better colour discrimination than the LED despite them both being 6500 K. Deuteranomalous trichromats showed a greatest deviation than normal trichromats using the LED. **Conclusions:** The Kosnic KCF07ALU/GU10-865 is a cost-effective alternative for colour vision testing. Smoking appears to have an effect on colour vision, but requires further investigation.

Keywords: Colour vision, Smoking, Tungsten halogen lamps, Compact fluorescent lamps, Light-emitting diodes

ACKNOWLEDGEMENTS

I would like to extend my gratitude to Mr Babubhai Mistry for his technical assistance in the design and construction of the equipment used. I would like to acknowledge the support of my supervisor Dr Robert Cubbidge, and Dr Mark Dunne for the guidance given. I would also like to thank Milton Keynes General Hospital, Heron Opticians, Hammond & Dummer Opticians, Lesley Arkin Optometrists, Oxford Eye Hospital, and all the subjects that gave up their time to participate in the study.

TABLE OF CONTENTS

SUMMARY.....	2
ACKNOWLEDGEMENTS.....	3
List of Figures.....	10
List of Tables.....	14
List of Abbreviations.....	17
1. INTRODUCTION.....	18
1.1 Light.....	19
1.1.1 Waves.....	19
1.1.2 Photons.....	20
1.1.3 Units used to describe Light.....	21
1.2 Colour.....	22
1.2.1 Munsell Colour Space.....	23
1.2.2 CIE Colour Space.....	24
1.2.3 Uniform Colour Space.....	27
1.3 The Retina.....	28
1.3.1 Retinal Pigment Epithelium.....	29
1.3.2 Photoreceptors.....	30
1.3.3 Horizontal Cells.....	35
1.3.4 Bipolar Cells.....	35
1.3.5 Amacrine Cells.....	36
1.3.6 Retinal Ganglion Cells.....	36
1.3.7 Beyond the Retina.....	37
1.3.8 Macula and Fovea.....	38
1.4 Receptive Fields.....	40
1.4.1 Achromatic Receptive Fields.....	40
1.4.2 Chromatic Receptive Fields.....	44
1.4.3 Colour Constancy.....	48
1.5 The Importance of Colour Vision.....	49
1.5.1 Evolution of Colour Vision.....	49
1.5.2 Colour Vision in Society.....	50
1.5.3 Occupational Requirements.....	51
1.6 Colour Vision Deficiencies.....	53

1.6.1 Congenital Colour Vision Deficiencies.....	53
1.6.1.1 Dichromatism.....	54
1.6.1.2 Anomalous Trichromatism.....	55
1.6.2 Acquired Colour Vision Deficiencies.....	58
1.7 Colour Vision Tests.....	62
1.7.1 Anomaloscopes.....	63
1.7.2 Pseudoisochromatic Plates.....	64
1.7.2.1 Ishihara Plates.....	65
1.7.2.2 Handy, Rand, and Ritter Plates.....	67
1.7.3 Arrangement Tests.....	68
1.7.3.1 Farnsworth-Munsell 100 Hue Test.....	68
1.7.3.2 Farnsworth Dichotomous Test for Colour Blindness.....	72
1.7.4 The City University Test.....	73
1.7.5 Lantern Tests.....	74
1.7.5.1 Holmes-Wright Lantern.....	74
1.7.5.2 Farnsworth Lantern.....	75
1.8 Lamps.....	75
1.8.1 History of Lamps.....	75
1.8.2 Black Bodies, Colour Temperature, and Correlated Colour Temperature.....	76
1.8.3 Incandescent Lamps.....	78
1.8.3.1 General Service Lamps.....	78
1.8.3.2 Tungsten-Halogen Lamps.....	78
1.8.4 Discharge Lamps.....	79
1.8.4.1 Fluorescent Lamps.....	80
1.8.4.2 Mercury Vapour Lamps.....	80
1.8.4.3 Metal Halide Lamps.....	80
1.8.4.4 Sodium Vapour Lamps.....	81
1.8.5 Light-Emitting Diodes.....	81
1.8.6 Sources of Illumination for Colour Discrimination.....	82
1.9 Smoking.....	84
1.9.1 Ocular Pathology secondary to Smoking.....	86
1.9.2 Colour Vision and Smoking.....	88
1.10 Aims of the Study.....	89

2. RESEARCH OBJECTIVES.....	90
2.1 Part 1 Normal/Control Subjects.....	91
2.2 Part 2 Smoker/Test Subjects.....	92
2.3 Part 3 Case Study Subjects.....	93
3. METHODS.....	94
3.1 Materials.....	95
3.1.1 The Lamps.....	95
3.1.2 Examination Box.....	99
3.1.3 Illumination Outputs of the Lamps.....	101
3.2 Subjects.....	102
3.3 Procedure.....	104
4. RESULTS.....	106
4.1 Subjects.....	107
4.2 Total Error Scores.....	108
4.2.1 Normal/Control Subjects.....	108
4.2.1.1 Light Source A – THL.....	108
4.2.1.2 Light Source B – CFL.....	109
4.2.1.3 Light Source C – LED.....	110
4.2.2 Smoker/Test Subjects.....	111
4.2.2.1 Light Source A – THL.....	112
4.2.2.2 Light Source B – CFL.....	113
4.2.2.3 Light Source C – LED.....	114
4.2.3 Summary of the Total Error Score Results.....	115
4.2.4 Analysis of Total Error Scores.....	116
4.2.4.1 Total Error Scores for the Normal/Control Group.....	116
4.2.4.2 Total Error Scores for the Smoker/Test Group.....	117
4.2.4.3 Normal/Control Group Total Error Scores versus Smoker/Test Group Total Error Scores.....	117
4.2.4.4 Decision Tree Analyses of Total Error Scores.....	117
4.3 FM100 Plots.....	120
4.4 Colour Bands.....	122

4.4.1 Colour Band Error Scores.....	123
4.4.1.1 Colour Band Error Scores for the Normal/Control Group.....	123
4.4.1.2 Colour Band Error Scores for the Smoker/Test Group.....	124
4.4.1.3 Normal/Control Group Colour Band Error Scores versus Smoker/Test Group Colour Band Error Scores.....	124
4.4.1.4 Decision Tree Analysis of Colour Band Error Scores.....	125
4.4.1.5 Summary of Decision Tree Analyses of Colour Band Error Scores.....	132
4.4.2 Alternative Colour Band Analysis.....	132
4.4.2.1 Colour Band Frequency of Cap Error Scores greater than four for the Normal/Control Group.....	133
4.4.2.2 Colour Band Frequency of Cap Error Scores greater than four for the Smoker/Test Group.....	133
4.4.2.3 Normal/Control Group Colour Band Frequency of Cap Error Scores greater than four versus Smoker/Test Group Colour Band Frequency of Cap Error Scores greater than four.....	134
4.4.2.4 Decision Tree Analysis of Colour Band Frequency of Cap Error Scores greater than four.....	136
4.4.2.5 Summary of Decision Tree Analyses of Colour Band Frequency of Cap Error Scores greater than four.....	140
4.4.3 Correlation between Mean Error Scores and Frequency of Cap Error Scores greater than four.....	140
4.4.4 Correlation between Pack Years and Colour Vision....	141
4.4.4.1 Correlation between Error Scores and Pack Years.....	141
4.4.4.2 Correlation between Frequency of Cap Error Scores greater than four and Pack Years.....	143
4.5 Case Study – Colour Vision Defects.....	144
4.5.1 Case Study Subjects’ FM100 Plots.....	144

4.5.2 Case Study Group TES Results.....	151
4.5.3 Case Study Group FM100 Plots.....	152
4.5.4 Case Study Group Colour Band Analyses.....	154
4.5.4.1 Case Study Colour Band Error Score Analysis.....	156
4.5.4.2 Case Study Colour Band Frequency of Cap Error Score greater than four Analysis.....	157
4.5.4.3 Correlation between Mean Error Scores and Frequency of Cap Error Scores greater than four.....	157
4.5.5 Case Study Group compared to the Normal/Control Group.....	158
 5 DISCUSSION.....	 162
5.1 Lamps.....	163
5.2 Subjects.....	163
5.2.1 Age.....	163
5.2.2 Pack Years.....	164
5.3 Normal/Control Group.....	165
5.4 Smoker/Test Group.....	166
5.5 Normal/Control versus Smoker/Test.....	167
5.6 Decision Tree Analyses on Total Error Scores.....	167
5.7 Comparing the colour discrimination for different colours.....	168
5.8 FM100 Plots.....	169
5.9 Colour Band Error Scores	170
5.10 Decision Tree Analyses on Colour Band Error Scores.....	172
5.11 Frequency of Cap Error Scores greater than four.....	174
5.12 Decision Tree Analyses on Frequency of Cap Error Scores greater than four	175
5.13 Comparison between Methodologies.....	176
5.14 Correlation between Pack Years and Colour Vision.....	176
5.15 Proposed Mechanism for Colour Vision Defects in Smokers.....	178
5.16 Case Study Group.....	178
5.16.1 Colour Bands	180
5.16.2 Comparing the Case Study Group to the Normal/Control Group.....	181

5.17 Summary of Results.....	183
5.17.1 Normal/Control Group.....	183
5.17.2 Smoker/Test Group.....	183
5.17.3 Smoker/Test compared to the Normal/Control group.....	183
5.17.4 Colour Band Error Scores.....	184
5.17.5 Frequency of Error Scores greater than four.....	184
5.17.6 Correlation between CBES and Pack Years.....	184
5.17.7 Correlation between FES4 and Pack Years.....	184
5.17.8 The best Light Source for Colour Discrimination.....	184
5.17.9 The Effect of Smoking on Colour Vision.....	185
5.17.10 Case Study Group.....	185
5.17.11 The best Light Source for Colour Discrimination.....	185
5.18 Addressing the Questions in the Aims.....	186
6 CONCLUSIONS.....	187
6.1 Impact on of this Study.....	188
6.2 Limitations.....	188
6.3 Future Studies.....	191
References.....	193
Appendix A Ethics Application.....	204
Appendix B Ethics Approval.....	208
Appendix C Consent Form.....	209

FIGURES

Figure 1.1 Electromagnetic spectrum.....	19
Figure 1.2 Additive colour.....	23
Figure 1.3 Munsell Colour System.....	24
Figure 1.4A Colour Matching Functions r , g , and b	25
Figure 1.4B Colour Matching Functions $x(\lambda)$, $y(\lambda)$, and $z(\lambda)$	25
Figure 1.5 CIE Chromaticity Chart.....	26
Figure 1.6 UCS using u and v coordinates.....	28
Figure 1.7 Simple retinal structure.....	29
Figure 1.8 Rod and Cone density with eccentricity.....	30
Figure 1.9 Rods.....	31
Figure 1.10 Opsin spectral sensitivities.....	33
Figure 1.11 Cones.....	34
Figure 1.12 Golgi-stained human horizontal cells.....	35
Figure 1.13 RGC pathways.....	37
Figure 1.14 The inputs from the LGN into the striate cortex (V_1).....	38
Figure 1.15 Location of the fovea.....	39
Figure 1.16A Centre-on RGC responses.....	41
Figure 1.16B Centre-off RGC responses.....	42
Figure 1.17 Overlapping receptive fields of RGCs.....	43
Figure 1.18 Contrast sensitivity functions.....	44
Figure 1.19 Centre-surround chromatic receptive fields.....	45
Figure 1.20 A simplified model of cone interactions to produce three pathways.....	46
Figure 1.21 Hue-discrimination curve.....	48
Figure 1.22 Confusion for dichromats.....	55
Figure 1.23 How colours are matched with a Nagel anomaloscope.....	56
Figure 1.24 Matching results from 127 anomalous trichromats.....	57
Figure 1.25 Ishihara Plate: vanishing plate.....	67
Figure 1.26 The FM100 plot with confusion axes.....	70
Figure 1.27 The positions of the FM100 cap in UCS.....	71
Figure 1.28 D15 plots.....	73
Figure 1.29 The black body locus plotted on CIE Colour Space.....	76
Figure 1.30 Radiation emitted from heated metals (such as tungsten).....	77
Figure 3.1 Lamp A (THL).....	96

Figure 3.2 Spectral Power Distribution of the THL.....	96
Figure 3.3 Lamp B (CFL).....	97
Figure 3.4 Spectral Power Distribution of the CFL.....	98
Figure 3.5 Lamp C (LED).....	98
Figure 3.6 Spectral Power Distribution of the LED.....	99
Figure 3.7 Layout of the lamps.....	100
Figure 3.8 Circuit diagram for the for the illumination system.....	100
Figure 3.9 The Complete examination box.....	101
Figure 3.10 The illumination from the each light source across the testing surface.....	102
Figure 4.1A The distribution of TES for Normal/Control group using light source A.....	109
Figure 4.1B The Q-Q plot for Normal/Control group using light source A....	109
Figure 4.2A The distribution of TES for Normal/Control group using light source B.....	110
Figure 4.2B The Q-Q plot for Normal/Control group using light source B....	110
Figure 4.3A The distribution of TES for Normal/Control group using light source C.....	111
Figure 4.3B The Q-Q plot for Normal/Control group using light source C....	111
Figure 4.4A The distribution of TES for Smoker/Test group using light source A.....	112
Figure 4.4B The Q-Q plot for Smoker/Test group using light source A.....	112
Figure 4.5A The distribution of TES for Smoker/Test group using light source B.....	113
Figure 4.5B The Q-Q plot for Smoker/Test group using light source B.....	113
Figure 4.6A The distribution of TES for Smoker/Test group using light source C.....	114
Figure 4.6B The Q-Q plot for Smoker/Test group using light source C.....	114
Figure 4.7A The mean TES and standard deviations for the Normal/Control group for the three light sources.....	115
Figure 4.7B The mean TES and standard deviations for the Smoker/Test group.....	115

Figure 4.8 The DTA for TES using the light source and pack years as independent variables.....	119
Figure 4.9 A-F FM100 Plots for the Normal/Control group and the Smoker/Test group.....	122
Figure 4.10 A-F Mean Error Scores in each colour band for the Normal/Control group and the Smoker/Test group.....	125
Figure 4.11 The DTA for red-red/yellow CBES using the light source and pack years as independent variables.....	127
Figure 4.12 The DTA for red/yellow-yellow CBES using the light source and pack years as independent variables.....	128
Figure 4.13 The DTA for yellow/green-green CBES using the light source and pack years as independent variables.....	129
Figure 4.14 The DTA for green-green/blue CBES using the light source and pack years as independent variables.....	130
Figure 4.15 The DTA for purple-purple/red CBES using the light source and pack years as independent variables.....	131
Figure 4.16 A-F Frequency of Cap Error Scores greater than four in each colour band for the Normal/Control group and the Smoker/Test group.....	135
Figure 4.17 The DTA for red-red/yellow FCES4 using the light source and pack years as independent variables.....	137
Figure 4.18 The DTA for red/yellow-yellow FCES4 using the light source and pack years as independent variables.....	138
Figure 4.19 The DTA for green-green/blue FCES4 using the light source and pack years as independent variables.....	139
Figure 4.20 A-C: Scatter plots of TES versus pack years.....	142
Figure 4.21 A-C FM100 plots for Subject 1 of the Case Study group.....	145
Figure 4.22 A-C FM100 plots for Subject 2 of the Case Study group.....	146
Figure 4.23 A-C FM100 plots for Subject 3 of the Case Study group.....	147
Figure 4.24 A-C FM100 plots for Subject 4 of the Case Study group.....	148
Figure 4.25 A-C FM100 plots for Subject 5 of the Case Study group.....	149
Figure 4.26 A-C FM100 plots for Subject 6 of the Case Study group.....	150
Figure 4.27 The mean TES and standard deviations for the Case Study group for the three light sources.....	151
Figure 4.28 A-C FM100 Plots for the Case Study group.....	153
Figure 4.29 A-F Case Study colour band charts using error scores and frequency of error scores greater than four.....	155

Figure 4.30 Mean error scores for colour bands for subjects in the Control group and the Case Study group when using Light Source A.....	158
Figure 4.31 Mean error scores for colour bands for subjects in the Control group and the Case Study group when using Light Source B.....	159
Figure 4.32 Mean error scores for colour bands for subjects in the Control group and the Case Study group when using Light Source C.....	159

TABLES

Table 1.1 Chromatic receptive fields identified by Hubel and Weisel.....	45
Table 1.2 A CIE Colour vision standards for transport.....	52
Table 1.2 B Colour perception standards for the armed forces.....	52
Table 1.3 Prevalence of congenital colour vision defects.....	54
Table 1.4 The different characteristics of congenital and acquired colour vision deficiencies.....	58
Table 1.5 Classification of acquired colour vision deficiencies.....	59
Table 1.6 Summary of ACVD secondary to pathology.....	61
Table 1.7 Summary of ACVD secondary to drug use.....	62
Table 1.8 Summary of health consequences associated with smoking and secondhand smoke exposure.....	84
Table 3.1 The Protocols	105
Table 4.1 The distribution of subjects that passed the screening test.....	107
Table 4.2 The distribution of subjects that failed the screening test.....	108
Table 4.3 Summary of the TES results for the Normal/Control group and Smoker/Test group.....	116
Table 4.4 The DTA results for TES using the light source and group as independent variables.....	118
Table 4.5 The DTA results for TES using the light source and pack years as independent variables.....	119
Table 4.6 The CES for each Group and Light source.....	122
Table 4.7 Colour bands.....	122
Table 4.8 Mean Error Scores in each colour band for the Normal/Control group.....	123
Table 4.9 Mean Error Scores in each colour band for the Smoker/Test group.....	124
Table 4.10 The DTA results for the red-red/yellow CBES using the light source and pack years as independent variables.....	126
Table 4.11 The DTA results for the red/yellow-yellow CBES using the light source and pack years as independent variables.....	128
Table 4.12 The DTA results for the yellow/green-green CBES using the light source and pack years as independent variables.....	129

Table 4.13 The DTA results for the green-green/blue CBES using the light source and pack years as independent variables.....	130
Table 4.14 The DTA results for the purple-purple/red CBES using the light source and pack years as independent variables.....	131
Table 4.15 Summary of the DTAs using TES and Mean Error Scores in the colour bands.....	132
Table 4.16 Frequency of Cap Error Scores greater than four in each colour band for the Normal/Control group.....	133
Table 4.17 Frequency of Cap Error Scores greater than four in each colour band for the Smoker/Test group.....	133
Table 4.18 The DTA results for the red-red/yellow FCES4 using the light source and pack years as independent variables.....	136
Table 4.19 The DTA results for the red/yellow-yellow FCES4 using the light source and pack years as independent variables.....	137
Table 4.20 The DTA results for the green-green/blue FCES4 using the light source and pack years as independent variables.....	138
Table 4.21 Summary of the DTAs using the Frequency of Cap Error Scores greater than four in the colour bands.....	140
Table 4.22 Correlation between the CBES and FCES4 for the Normal/Control group and Smoker/Test group.....	140
Table 4.23 Correlation coefficients and probabilities for pack years with Error Scores.....	141
Table 4.24 Correlation coefficients and probabilities for pack years with Frequency of Cap Error Scores greater than four.....	143
Table 4.25 The TES results for the Case Study group.....	151
Table 4.26 Summary of the Kruskal-Wallis tests for the Case study group using Mean Error Scores in the colour bands.....	156
Table 4.27 Summary of the Kruskal-Wallis tests for the Case study group using Frequency of Error Scores greater than four in the colour bands.....	157
Table 4.28 Correlation between the CBES and FCES4 for the Case Study group.....	157
Table 4.29 Summary of the Mann-Witney U tests comparing scores in each colour band for the Normal/Control group and the Case study group for the THL.....	160

Table 4.30 Summary of the Mann-Witney U tests comparing scores in each colour band for the Normal/Control group and the Case study group for the CFL.....	160
Table 4.31 Summary of the Mann-Witney U tests comparing scores in each colour band for the Normal/Control group and the Case study group for the LED.....	161
Table 5.1 The normal TES at 95% confidence limits for the age ranges in this study.....	165
Table 5.2 Cap positions for the axes of confusion.....	180
Table 5.3 Summary of the Mann-Witney U tests showing significant differences comparing scores in each colour band for the Normal/Control group and the Case study group for all three light sources.....	183

ABBREVIATIONS

ACVD	Acquired colour vision defect
ARMD	Age-related macula degeneration
CBES	Colour band error score
CCT	Correlated colour temperature
CCVD	Congenital colour vision defect
CES	Cap error score
CFL	Compact fluorescent lamp
CHAID	Chi-squared Automatic Interaction Detection
CIE	Commission Internationale de l'Eclairage
CRI	Colour rendering index
CT	Colour temperature
CUT	City University Test
D15	Farnsworth Dichotomous test for colour blindness
DTA	Decision tree analysis
FCES4	Frequency of cap error score greater than 4
FM100	Farnsworth Munsell 100-Hue Test
GLS	General Lighting Service lamps
HRR	Hardy, Rand, and Ritter
LED	Light-emitting diode
LGN	Lateral geniculate nucleus
PIC	Pseudoisochromatic
RGC	Retinal ganglion cell
RPE	Retinal pigment epithelium
SPD	Spectral power distribution
TES	Total error score
THL	Tungsten-halogen lamp

1. INTRODUCTION

1.1 Light

1.1.1 Waves

The electromagnetic wave is a transverse wave where the electric wave and the magnetic wave are perpendicular, and it does not require a medium to travel through. Visible light is part of the electromagnetic spectrum that is visible to the human eye. The notion of light travelling as a wave was proposed by Huygens in 1680 [1], and was further strengthened in 1801 by Young's double-slit experiment and the production of the constructive and destructive interference patterns. Waves in motion follow the formula $v = f \cdot \lambda$ (where v is the velocity of the wave, f is its frequency, and λ is its wavelength). For the electromagnetic spectrum the velocity is $c = 3 \times 10^8 \text{ m.s}^{-1}$ in a vacuum. As an electromagnetic wave travels through different media, depending on the refractive index n of that medium ($n = v/c$), its velocity and wavelength alter but its frequency remains constant. However, for the purposes of simplicity, all wavelengths reported hereafter will be λ_{vacuum} . Within the electromagnetic spectrum, light is situated between ultraviolet ($f = 789 \text{ THz}$, $\lambda = 380 \text{ nm}$) and infrared (395 THz , $\lambda = 760 \text{ nm}$). Figure 1.1 shows that light is a small section of the electromagnetic spectrum.

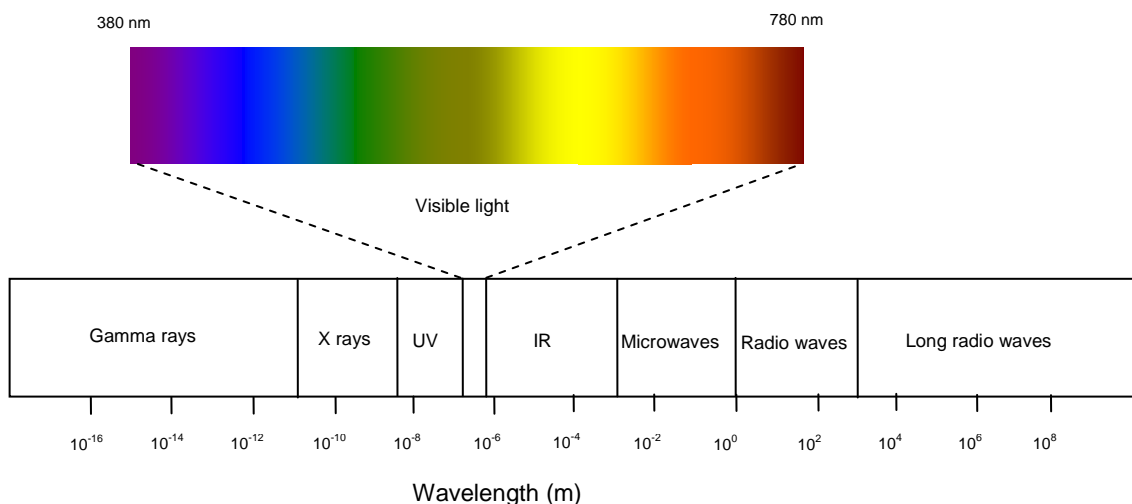


Figure 1.1 Electromagnetic spectrum (K. Mistry).

1.1.2 Photons

Light can also be thought as particles, or quanta, of energy. A photon is a quantum of light. This theory about light was put forward by Planck in 1902 when tackling black body radiation. Compton, in 1923, showed this experimentally as a particle-particle collision resulting in a change in wavelength of X-rays through a graphite sheet: *Compton Effect* [2]. This helps explain some of the interactions between electromagnetic radiation and matter. Planck, in 1900, working with atomic oscillators which emit and absorb electromagnetic waves, deduced that:

$$E = h.f$$

Where E is the quantum of energy, f is the frequency of the radiation, and h is Planck's constant.

Planck's radical assumption was that the energy from the atomic oscillations were discrete values or '*energy packets*', and was extended Einstein in 1905 [1]. This would mean that the higher frequencies of the electromagnetic spectrum carry more energy than the lower frequencies.

Both the wave theory and the particle theory hold true, depending on the circumstances, which led in 1923 to de Broglie's suggestion of a '*wave-particle duality*' [3]. De Broglie proposed that concepts such as energy, momentum, and wavelength can be applied to particles as well as waves, and gave rise to the '*de Broglie wavelength*' [3]:

$$\lambda = h/p$$

Where λ is wavelength of a photon, h is Planck's constant, and p is the magnitude of the relativistic momentum of the particle (in this case the photon).

Light is not alone in exhibiting wave-particle duality, electrons directed at a double slit also produce the constructive and destructive interference patterns [3].

1.1.3 Units used to describe Light

As a source of energy, light *energy* can be measured in joules and its *power* in watts (W). However, when this is adjusted for the sensitivity of the human visual system, the unit of light flow (i.e. luminous flux Φ) is the lumen (lm), and is related to the watt, such that for light where $\lambda = 554$ nm, 621 lm is approximately equal to 1 W [4].

As luminous flux travels in all directions, light is not incident through a two-dimensional angle but rather a three-dimensional angle, or a solid angle ω , measured in steradians (sr) [5]. Therefore a solid angle is to a segment of sphere, what an angle is to a segment of a circle. $\omega = A/r^2$, where A is area on the shell of the sphere, and r is the radius of the sphere. As the surface area of a sphere is $4\pi r^2$, there are 4π sr in a sphere.

The measure of luminous flux through a solid angle is its luminous intensity I . Thus $I = \Phi/\omega$, whose units are $\text{lm}\cdot\text{sr}^{-1}$, also known as candelas (cd).

When considering lighting an area in which a task is undertaken, the amount of luminous flux and the area that is being lit needs to be ascertained. In the same way that pressure is related to force and the area on which it is applied i.e. force per unit area, illuminance E is the luminous flux per unit area. Thus $E = \Phi/A$, and its units are $\text{lm}\cdot\text{m}^{-2}$, also known as lux.

Taking the example of a point source i.e. where A is the surface area of a sphere whose radius is r , and ω is 4π .

As previously stated:

$$I = \Phi/\omega, E = \Phi/A$$

Thus:

$$\Phi = I\cdot\omega$$

$$\Phi = E\cdot A$$

$$I\cdot\omega = E\cdot A$$

$$E = I\cdot\omega/A$$

$$E = I\cdot 4\pi/4\pi r^2$$

$$E = I/r^2$$

This means that illuminance follows an inverse square relationship i.e. when doubling the distance away from the light source, the illuminance decreases by a factor of four; and when tripling the distance away, it decreases by a factor of nine.

When the light source is not a point, but an extended source, then its luminance L needs to be taken into account, which is the lumens per steradian over the perceived area of the source i.e. $L = I/A$, and is measured in cd.m^{-2} .

1.2 Colour

From Figure 1.1 it can be seen that the electromagnetic spectrum ranges from gamma rays to radio waves, and that visible light is just a small section of the spectrum. Within the visible light section violets are at the high frequency-short wavelength end, and reds are at the low frequency-long wavelength end. Thus ultraviolet frequencies are slightly higher than that of violet, and infrared slightly lower than that of red. The term 'hue' is used to describe a distinguishable colour. There are several hundred hues, and white light is made of all the hues equally [6]. The wavelengths of the colours that constitute white light are 380-450 nm for violet, 450-490 nm for blue, 490-560 nm for green 560-590 nm for yellow, 590-630 nm for orange, and 630-780 nm for red [2, 7].

In 1666 Isaac Newton used a prism to split sunlight into overlapping coloured lights. The theory at the time was that the prism transformed the sunlight into the spectrum seen. Newton proposed that refraction through the prism did not introduce colours. He did this by isolating one of the colours using a slit in a screen and then passing that beam through a second prism. As the light did not change colour he concluded that the prism dispersed the sunlight and not transformed it. Newton's second experiment involved splitting the sunlight again into the spectrum as before, and then introducing a second prism to combine the spectrum. He found the resulting beam of light leaving the second prism to be the same 'colour' as the sunlight incident on the first prism, thus demonstrating that the dispersed light can be recombined. His third experiment involved painting the spectrum colours on sectors of a disc and then rapidly rotating the disc. The resultant colour seen was white, thus demonstrating the relationship between the combining lights and the colours produced. An example of utilising this property demonstrated in Newton's third experiment can be seen with a

cathode-ray tube (CRT) projector and the three CRTs (red, green, and blue: the primary colours). The colours are combined in differing quantities to produce the gamut of colours. As shown in Figure 1.2, red plus blue results in magenta, blue plus green results in cyan, green plus red results in yellow, and red plus blue plus green results in white.



Figure 1.2 Additive colour (Jocobolus, Public Domain).

1.2.1 Munsell Colour System

Hue is used to describe the colour [8, 9]. Hue is not interchangeable with wavelength because, as Figure 1.1 shows, yellow light can be described as light of a wavelength of 580 nm, but looking at Figure 1.2, it can also be produced by combining red light (700 nm) and green light (540 nm). The term value is used to describe where on the light-dark scale a sample is. Bright colours are at the top of the scale and darker colours at the bottom. As this is a perceived intensity rather than a physical intensity it has undergone a logarithmic compression. A high value denotes lightness, and is independent of hue. Chroma is used to describe the vividness of a sample. The term chroma can be substituted for saturation [6]. For example pink is desaturated red. These terms are to describe how a stimulus is perceived as opposed to the actual physical characteristics of the stimulus [8]. Even at full saturation, monochromatic yellow is perceived less saturated but brighter than monochromatic blue or red. Hue, value, and chroma were plotted to give the Munsell Colour system in 1905 [10] (see Figure 1.3). This system had over 1200 sample and could be accessed in a three-dimensional model: the Munsell Colour Solid, or in a book with matt and glossy samples [10].



Figure 1.3 Munsell Colour System.

1.2.2 CIE Colour Space

As the Munsell Colour System was a physical entity for observers to refer to, it was dependant on subjective matching, and over time the samples would deteriorate. A new system was devised by Commission Internationale de l'Eclairage (CIE). The CIE was born in 1913, although the seeds were planted many years earlier due to the advances in lighting technologies, with the Commission Internationale de Photométrie in 1903 [11].

By using psychophysical matching experiments in which a reference light is matched with a combination of three primaries. In this situation to be defined as a primary each primary cannot be obtained by the combination of the other two primaries, therefore these do not have to be the blue, green, and red seen in Figure 1.2 [12]. For each reference light the intensities of the primaries are adjusted to produce a colour that is perceived as the same hue as the reference light, although the reference light is a single wavelength, whereas the there are there different wavelengths combined for the match). In a series of experiments carried out by separately by Wright and Guild between 1929 and 1931, they found that not all colours can be produced by the adding blue, green, and red primaries [13, 14]. They found negative values for one of the primaries at a number of reference wavelengths (achieved by adding one of the primaries to the reference light) [12, 13]. This lead to the creation of the 1931 CIE RGB with the primaries: 435.8 nm, 546.1 nm, and 700.0 nm [13, 15, 16]. The negative values found with these primaries were confirmed in

Stiles and Burch in 1955 [17]. In order to maintain positive values for the primaries, a series of experiments were carried out to obtain artificial primaries (rather than the physical primaries) [13, 14]. Figure 1.4A shows the outputs of the primaries (relative to the green source) for each wavelength if RGB primaries were chosen. The values for each source show that the relative intensity of the red light (r) has a negative value when the wavelength of the reference light is 450–525 nm and therefore needs to be added to the reference light. A similar situation is found for the green light (g) between 405 nm and 445 nm. Choosing the artificial, non-physical, primaries, of X, Y, and Z, Figure 1.4B shows the response required from each primary (relative to $y(\lambda)$) for a given reference wavelength. Schrödinger, and then Judd, proposed that the curve $y(\lambda)$ match the photopic luminosity function $v(\lambda)$ [16]. The two reasons for this were to ease the calculations, and to place X and Z on a line with zero luminance [16].

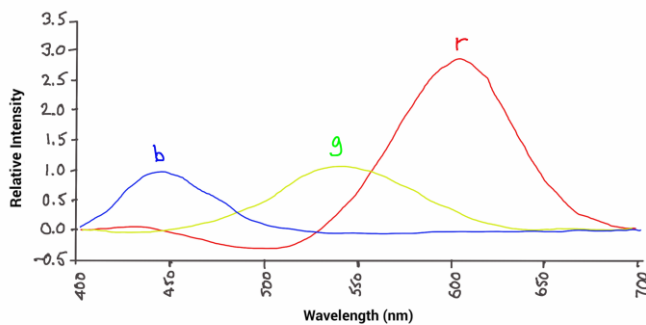


Figure 1.4A Colour Matching Functions r, g, and b (K. Mistry).

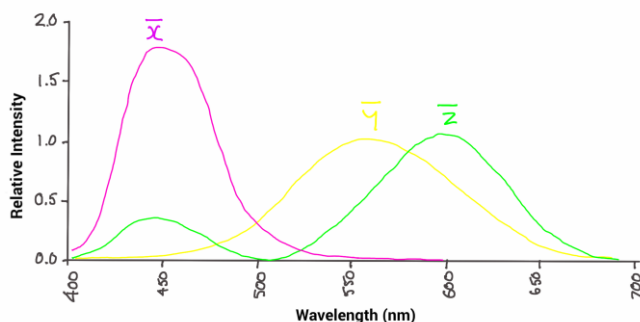


Figure 1.4B Colour Matching Functions $x(\lambda)$, $y(\lambda)$, and $z(\lambda)$ (K. Mistry).

By taking the spectral power distribution (SPD) of the illumination source and then multiplying it by the spectral reflectance of the sample, a SPD of the sample under the illumination source is produced. Each point is multiplied by the points on the function $x(\lambda)$ and the area under the curve gives the tristimulus value for X. This needs to be repeated for $y(\lambda)$ to find Y, and $z(\lambda)$ to find Z [18]. The individual values of x, y, and z are described by the following expressions [18, 19]:

$$x = X/(X+Y+Z)$$

$$y = Y/(X+Y+Z)$$

$$z = Z/(X+Y+Z)$$

Therefore:

$$x+y+z = 1$$

This means that the graph can be plotted using just two coordinates: x, and y; z is not required: $z = 1-(x+y)$ [10]. This makes x and y the chromaticity coordinates, and gives rise to the 1931 CIE Chromaticity Chart also known as CIE Colour Space (see Figure 1.5) [16, 18].



Figure 1.5 CIE Chromaticity Chart (image courtesy of David Pape)

At coordinates (0.33, 0.33) is equal energy white, where there is complete desaturation. Thus saturated (pure) hues are arranged around the edge of the 'horse-shoe shaped' graph, and on Figure 1.5 the numbers represent the wavelengths in the electromagnetic spectrum. As this represents additive colours and there is described by Grassmann's Law of additivity, when adding any two colours on the chart, the resultant colour lies on the straight line that joins the two points [14, 16]. Thus, if source A (0.2, 0.1) is added to source B (0.4, 0.5), then the resulting colour would lie on the straight line that connects (0.2, 0.1) to (0.4, 0.5). The position on the line would depend on the ratio of intensities of sources A and B. Therefore three sources would give a colour gamut; and any colour in that space can be obtained by altering the ratios of the three sources.

1.2.3 Uniform Colour Space

Unfortunately the 1931 CIE colour chart is perceptually irregular. That is that perceptual difference in colour between any two points is not the same throughout the chart. In the 1940s David MacAdam examined how close the coordinates could be before a subject could not distinguish between them. He then plotted the areas: MacAdam's Ellipses, and found that they were different sizes throughout the chart [20]. To address this problem of perceptual irregularity the Uniform Colour Scale (UCS) was introduced in 1976 [21]. Here the coordinates (x, y) were transformed into (u, v), hence the diagram is also referred to as the CIELUV (see Figure 1.6) [21].



Figure 1.6 UCS using u and v coordinates (Adoniscik, Public Domain).

1.3 The Retina

Photoreceptors are connected to retinal pigment epithelium posteriorly and synapse with the Horizontal cells and Bipolar cells anteriorly. As the name suggests, Horizontal cells synapse horizontally throughout the inner nuclear layer with other photoreceptor-Bipolar cell junctions. The Bipolar cells synapse anteriorly with Amacrine cells and Retinal ganglion cells (RGCs). There are another group of supporting cells located here called Müller cells. The axons of the RGCs form the optic nerve. The position of these different cells can be seen in Figure 1.7.



Figure 1.7 Simple retinal structure (Kolb) [22]

1.3.1 Retinal Pigment Epithelium

The Retinal Pigment Epithelium (RPE) is made up of columnar cells, with 4-8 sides, whose bases attach to the Bruch's membrane, and whose apices surround the tops of the photoreceptor outer segments [23, 24]. The RPE cells contain the pigments melanin and lipofuscin [23]. The RPE cells are non-regenerative, and are often misshapen in older eyes as the living cells enlarge to occupy the spaces left by dead one. They number 4-6 million in healthy eyes. Their average density at the fovea is ~ 4000 cells/mm², and this decreases with eccentricity [25].

The RPE may seem like a simple layer of pigmented cells but it has a vital role in maintaining the health of the retina and facilitating visual function. The pigment in the RPE helps improve the clarity of vision by absorbing stray light [23-25]. As the light energy is absorbed the RPE helps diffuse the converted heat energy into the choroidal circulation [26, 27]. The energy from the incident light can cause photo-oxidative damage through the production of free radicals, the RPE forms part of the retina's defence via its melanosomes [28]. The RPE forms part of the blood-retina barrier, thus preventing toxic agents from entering the retina from the choroidal blood vessels [24, 29], and helping regulate the immune response within the retina [30]. As a result the RPE transports nutrients from the choroid to the photoreceptor outer

segments, and transports water, ions, and metabolic waste in the opposite direction [23-25]. As there is a barrier between the photoreceptor outer segments and the choroid, the RPE has to help regulate the electrical charge in the photoreceptor, without which the excitability of the photoreceptors would not be fast enough [9, 25, 31]. When photoreceptors are stimulated by light the visual pigment undergoes an isomerisation; the RPE is responsible for the re-isomerisation of the visual pigment [32]. Over time the photoreceptor outer segments can become damaged, the RPE phagocytoses them and recycles the materials [23, 24]. It is estimated that a single RPE cell in a 70 year life-span will phagocytose 300 million photoreceptor outer segments [23]. Each RPE cell services 20-50 photoreceptors [23, 25]. Signalling molecules and other such factors are secreted by the RPE to allow neighbouring cells to communicate, structural integrity to be maintained, and cellular repair and maintenance to take place [24].

1.3.2 Photoreceptors

There are two types of photoreceptor: rods and cones

Rods are 100-120 μm long and number 110-125 million in a healthy human retina [10, 29]. Figure 1.8 shows the density of rods peaking 18° away from the fovea centralis (foveal pit) and are absent from the foveola (also known as the fovea floor) and the optic disc.



Figure 1.8 Rod and Cone density with eccentricity (Kolb) [22] adapted from Osterberg 1935 [33]

Rods are very sensitive to light and work best in scotopic conditions [34]. Rods have been known to respond to a single quantum of light, which makes them considerably more sensitive than cones [23, 34]. Unfortunately they do not possess good temporal characteristics and respond much slower than cones [34]. They have no colour discrimination. Figure 1.9 shows the anatomy of a rod, and position and the position of the rhodopsin containing discs.

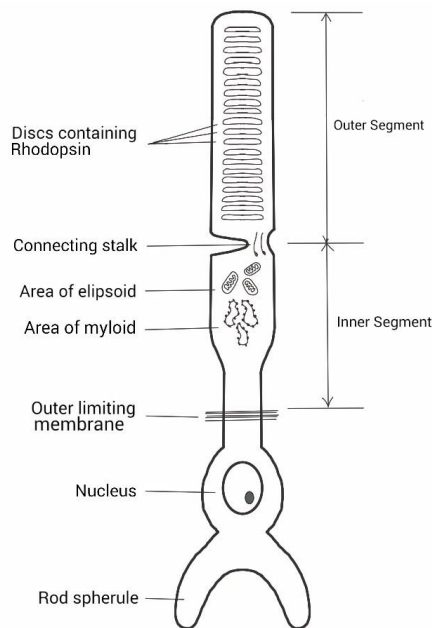


Figure 1.9 Rods (K. Mistry).

They have columnar outer segments and hence are called rods. They enclose 600-1000 discs whose membranes contain the photosensitive pigment rhodopsin [29, 35, 36]. The stack of discs is produced at the base of the outer segment and migrate towards the top where they are shed and phagocytosed by the RPE [24, 29]. There are two cilia in the connecting stalk between the outer and inner segments [29]. The inner segment is split into a further two sections: the outer ellipsoid section contains the basal body with numerous mitochondria, and the inner myloid section contains the endoplasmic reticulum, ribosomes, and Golgi apparatus [29]. Below the outer limiting membrane is the cell body, and spherule at the base of the rod synapses with Horizontal cells and Bipolar cells (see Figure 1.7 and Figure 1.9) [29]. Rods converge on bipolar cells which reduces their spatial resolution, but increases their sensitivity.

Cones are a little shorter than rods and measure 65-75 μm in length [29]. Broadly speaking there are 6.3-6.8 million cones in the healthy retina [10, 29] and they are concentrated in the fovea [23, 37] (see Figure 1.8). The packing of cones peak in the foveola, and then rapidly decrease in density in the central 2 mm of the retina [37]. Their density does not uniformly decrease with eccentricity, but rather in contours that are elongated along the horizontal axis [37]. Song et al found that there is a reduction in cone packing density with age [37]. They are not as sensitive to light as rods but have significantly shorter response times [24]. Cones also have wave guide properties giving them better spatial resolution [35].

Like rods, cones contain photosensitive pigments called iodopsins; however there are three variants of these [36]. Each of these pigments has a different spectral sensitivity function. (see Figure 1.10). The concept of three types of photoreceptor was first hypothesised by Palmer in 1777 [10], but followed up by Young in 1802 and by Helmholtz in 1852 giving rise to the Young-Helmholtz theory of 'The Trivariance of Colour Vision' [38]. For completeness it is worth mentioning a rivalling theory by Hering: in the second half of the nineteenth century Hering proposed a separate red-green pathway from a blue-yellow pathway, and even a black-white pathway; with inhibition aiding colour discrimination. In 1881 Donders proposed that colour vision mediated in zones of the visual pathway; some zones worked with trichromacy, and others with opponency [10]. The three cones that have been found were designated the short-wavelength (also called S or blue), medium-wavelength (M or green), and the long-wavelength (L or red) [19, 39]. There are three opsins (variants of iodopsin) called cyanolabe which has a maximum absorption wavelength of approximately 420 nm (for the S-cone), chlorolabe which has a maximum absorption wavelength of approximately 530 nm (for the M-cone), and erythrolabe which has a maximum absorption wavelength of approximately 560 nm (for the L-cone) [36]. As a result the cones allow for colour discrimination. Although the three cone types are randomly distributed across the retina, the density of S-cones is much lower [40]. S-cones make up approximately 7% of the cones, and are absent from the central 100 μm [41]. L-cones and M-cones are present at a ratio of 2:1 in the central retina; however, the proportions of M- and L-cones vary considerably [37].



Figure 1.10 Opsin spectral sensitivities (courtesy of David Pape)

The genetic coding for the opsins was discovered in the 1980s [10, 42]. The code for the cynolabe was found on chromosome 7q31-32 [42], whereas the codes for the chlorolabe and erythrolabe on the long (q) arm of the X-chromosome (Xq28) [42, 43] (the coding for rhodopsin is found on chromosome 3 [35]). The cynolabe code is made up of 348 amino acids [42], whereas the chlorolabe and erythrolabe codes are both made of 364 amino acids [42]. The codes for the chlorolabe and erythrolabe would be the same but for 15 amino acids [38, 42]. This suggests that chlorolabe and erythrolabes evolved from a mutation in the opsin gene on the X-chromosome more recently [10]. There is very little variation in the gene for cynolabe amongst the population resulting in only a very small variation in its spectral sensitivity [42, 44]. Due to the similarities in the genes for chlorolabe and erythrolabe, and their proximity on the chromosome, there can be cross-overs and misalignments during genetic replication [42, 43], resulting in a greater amount of variation in the pigments amongst the population, and the formation of hybrid genes [42]. Subsequently there is a higher frequency of colour vision defects caused by errors with chlorolabe and erythrolabe, than with cynolabe [42, 45]. The gene for cynolabe shares approximately 42% of its information with rhodopsin, 44% with erythrolabe, and 43% with chlorolabe, suggesting that it evolved after rhodopsin, but before erythrolabe and chlorolabe [10].

Anatomically the cones are a little different to the rods. Most apparent is the difference in the shape of the outer segments (see Figure 1.1). Cones are wider at the base compared to rods, and taper to a rounded tip [29]. Unlike the rods which have membranous discs, the outer wall of the cone is continuous with the pigment-

containing membranes [29]. The inner segment of the cone is very similar to that of the rod, and culminates in the pedicle (rather than a spherule) which synapses with Horizontal cells and Bipolar cells (see Figure 1.7).

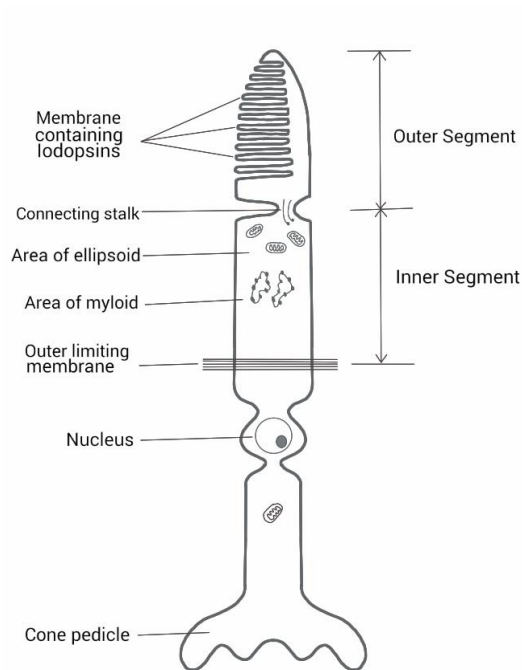


Figure 1.11 Cones (K. Mistry).

There are sensory receptors throughout the body. They are sensitive to different stimuli, such as light, sound, pressure, and heat. The normal response to a stimulus is the depolarisation of the receptor cell. However, the photoreceptors in the eye are depolarised when they are not stimulated i.e. in the dark [35]. When stimulated by light, the photoreceptor hyperpolarises [35]. In the dark the photoreceptor membrane is permeable to sodium and potassium ions; this flow of ions in the dark results in a 'dark current' [35]. Light causes the 'bleaching' of the visual pigment, which results in the closure of the sodium pores, and thus causes the potential difference across the membrane to increase, and for the cell to hyperpolarise [35]. As the cell hyperpolarises the release of the neurotransmitter from the photoreceptors decrease [35]. Both rods and cones release the neurotransmitter glutamate [46]. Per gram, photoreceptors require more oxygen than any other tissue in the body [23].

1.3.3 Horizontal Cells

Horizontal cells run between photoreceptors, and in doing so provide the first level of image enhancement by sharpening contrast and increasing spatial resolution [29]. There are three types of Horizontal cell in the primate retina shown in Figure 1.12: HI, HII, and HIII [47]. HI cells are relatively small and connect mainly M-cones and L-cones, with a few S-cones at one end of the cell, with rods via an axon at the opposite end [48]. HII cells have a shorter axon, and connect with a greater number of S-cones and fewer M-cones and L-cones than the HI, and the axon terminates with only S-cones [48]. The HIII cell is larger than the HI cell, and connects M-cones and L-cone, avoiding the S-cone, and the target of the axon is still to be discovered [48].



Figure 1.12 Golgi-stained human horizontal cells (Kolb) [22]

Image enhancement is achieved by excitation and inhibition of the Horizontal cells produced by releasing the neurotransmitter gamma-aminobutyric acid (GABA) [29, 46] in response to the glutamate released by the photoreceptors [46].

1.3.4 Bipolar Cells

Bipolar cells synapse with photoreceptors and Horizontal cells at one end, and Amacrine cells and RGCs at the other end. Bipolar cells will either connect to rods or cones, but not both [49]. There is one type of Rod bipolar cell, and depending on its location in the retina, it can connect with up to 50 rods [49], and up to four RGCs [29].

This level of convergence from rods down to the bipolar cells is one of the reasons why the rods have such poor spatial resolution. There are 10 types of Cone bipolar cells: seven take input from several cones (diffuse Bipolar cells), whereas the other three have a one-cone-to-one-bipolar cell arrangement [50]. Larger diffuse Bipolar cells can synapse with up to 20 cones, whereas the smaller diffuse Bipolar cells found in the central retina connect to 5-7 cones [51]. The Bipolar cells corresponding to the fovea are midget Bipolar cells, of which there are two types: flat midget Bipolar cells, and invaginating midget Bipolar cells [49]. The other type of one-cone-to-one-bipolar cell is the blue S-cone Bipolar cell [52]. It would be the same as any other midget Bipolar cell but for several wispy dendrites [52]. Like photoreceptors, Bipolar cells are stimulated by the neurotransmitter glutamate [46].

1.3.5 Amacrine Cells

There are at least 25 types of Amacrine cell in the human retina; their classification is based on their dendritic tree size, branching characteristics, and stratification of their dendrites in the inner plexiform layer [52]. They have large cell bodies and numerous long processes which synapse with Bipolar cells and RGCs [29]. Their function, as with Horizontal cells, is to provide a level of image processing via excitation and inhibition to aid image enhancement.

1.3.6 Retinal Ganglion Cells

The RGC is the second neurone of the visual pathway (the first being the Bipolar cell) [29]. There are at least 18 different types of RGCs in the human retina. Another way of classifying them is to divide them into midget cells, parasol cells, bistratified cells, photosensitive ganglion cells, and other ganglion cells. Midget cells are small RGCs that correspond to the parvocellular pathway; they have a slow conduction speed (~2 m/s) and so are also known as tonic cells, but code for colour; they account for approximately 80% of the RGCs [43, 53-55]. Parasol cells are larger RGCs that form part of the magnocellular pathway; they have a greater degree of convergence compared to midget cells but have a faster conduction speed (~4 m/s), and make up approximately 10% of RGCs [53, 54]. Parasol RGCs are also known as phasic cells, they respond better than midget cell in low contrast, but do not carry the same level of information on colour [55]. This is because the tonic cells have three spectral types

(red-centre, green-centre, and blue-centre) whereas the phasic cells combine red-cones and green-cones and so do not have colour opponents in the image processing [10, 55]. Bistratified RGCs project into the koniocellular pathway, they are also known as blue-yellow ganglion cells [40, 56]. There is not as much known about this pathway, and there seems to be some uncertainty on how their receptive fields work [56]. Photosensitive ganglion cells carry some information which is required for maintaining the circadian rhythm, and for pupillary light reflexes. They have been linked to the concept of 'blind sight' i.e. a subconscious visual pathway [40, 56].

1.3.7 Beyond the Retina

RGC axons leave the eye through the optic disc, and the majority terminate in the lateral geniculate nucleus (LGN) (see Figure 1.13).



Figure 1.13 RGC pathways: *M* is the magnocellular pathway, *P* is the parvocellular pathway, *B/Y* is the koniocellular pathway, *LGN* is the lateral geniculate nucleus, and *S* in the superior colliculus (Kolb) [22]

The LGN consists of 6 layers. Layers 1 and 2 (ventral layers) have input from the magnocellular pathway. The remaining layers (dorsal layers) receive input from the parvocellular pathway. The ventral layers of the LGN project to the layers 4C α of the striate cortex (V_1) [35]. From there they project to 4B. The dorsal layers of the LGN

project layers 4A and 4C β , from where they project to layer 2 and 3 (see Figure 1.14) [35, 57]. Only layers 1, 4A, and 4C do not project out of the cortex [35].

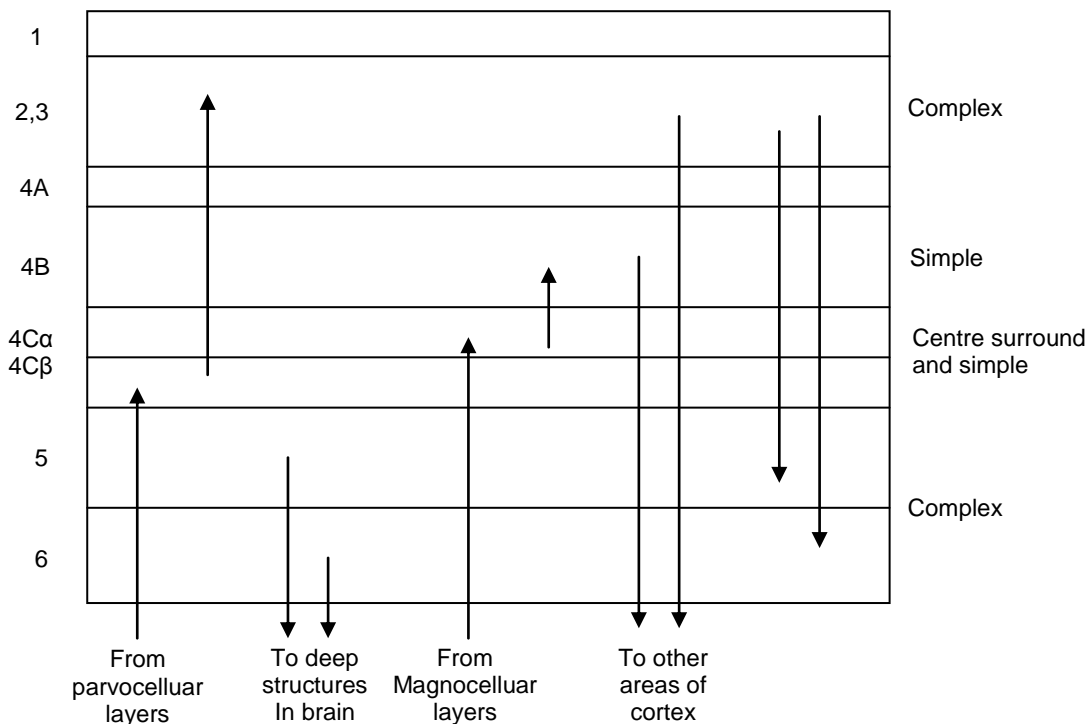


Figure 1.14 The inputs from the LGN into the striate cortex (V_1) adapted from work by Hubel [35] (K. Mistry).

1.3.8 Macula and Fovea

Figure 1.8 shows that the density of photoreceptors varies with eccentricity from the fovea [33]. It can be seen that the cone density is highest at the fovea and then rapidly decreases with eccentricity [33]. The centre of the fovea lies approximately 15.5° temporal, and 5.6° inferior the centre of the disc [58].

The fovea itself is about 1.5 mm (1500 μm) in diameter [9, 29] and subtends approximately 5° [9]. The foveal avascular zone is 622 μm in diameter, but be 400-700 μm [59], and is a rod-free area. (as indicated by the arrows on Figures 15A and 15B). The floor of the depressed area is the fovea centralis, and the walls of the depression seen in the fovea are called the clivus [29]. The foveal centralis is 400 μm in diameter [9]. The arrow on Figure 1.15B also shows the direction of light into the eye. Throughout the rest of the retina the light must travel through the nerve fibre layer, RGCs, Amacrine cells, Bipolar cells, Horizontal cells, and any other supporting

cells such as Müller cells, before reaching the photoreceptors. However, in the fovea centralis this is not the case, thus maximising the sharpness, or acuity, of the vision in this area [9, 29]. There are about 147,000 cones per mm² in the fovea centralis [29], and it is this density, like the pixel density on a digital camera sensor, that determines the potential acuity of the eye [9]. The fovea is avascular and relies on the capillaries in the choroid for its blood supply [29].



Figure 1.15 Location of the fovea. *A* shows a location of the fovea centralis of a right eye, on the right-hand side of the picture is the optic nerve head. *B* is a cross-section through the same region taken with an optical coherence tomographer (OCT) (Kolb [22])

Macula lutea (often referred to as just the 'macula') is a yellowish area which starts 3 mm temporal to the optic nerve head and extends a further 5-6 mm [23, 60]. The yellowish colouration is due to the carotenoid pigment xanthophyll, and is found in the layers between the photoreceptor cell bodies and the RGCs [61]. Conditions that affect the macula (e.g. age-related macula degeneration, macula oedema, diabetic maculopathy, Stargart's disease) not only have a deleterious effect on visual acuity, but can also alter colour perception due to the disruption caused to the way the cones function [10, 62].

1.4 Receptive Fields

Anatomically a receptive field of a particular cell refers to the group of cells that form its input e.g. the receptive field of a bipolar cell would refer to the photoreceptors from which it gains its input. However, a special case is made in vision for receptive fields to refer to the area in space that a cell responds to [9, 35, 38]. The first retinal receptive fields to be described in this way were of the RGC. Visual receptive fields are not confined to the retina, they can also be mapped in the LGN, and in the visual cortex. The receptive fields become more complex as the visual pathway progresses [35]. The simplest receptive field to describe is that of a photoreceptor; this is the area of space from which light causes the photoreceptor to hyperpolarise. Taking the example of a RGC, the cell's receptive field can be found by measuring which areas need to be stimulated in order to elicit a response from the cell [9]. The receptive field can be described in 2 ways; either an area on the retina, or as an angle subtended on the retina [35]. The latter is more practical as it accounts for the relationship between the size of a target and the distance away from the eye [35], and it also relates well to the clinical measure that is visual acuity.

1.4.1 Achromatic Receptive Fields

During the 1950s Stephen Kuffler recorded the responses and measured the receptive fields of cat RGC [63, 64]. He found that by using a small light, not only could he increase the firing of the RGCs, but he could also suppress them [63, 64]. This led to the discovery of 'on-off' receptive fields. A centre-on, surround-off receptive field describes a receptive field in which the cell will fire when the stimulus is in the central part of the field, but the RGC will be inhibited if a part of non-central receptive field is stimulated (see Figure 1.16A) [35, 64, 65].

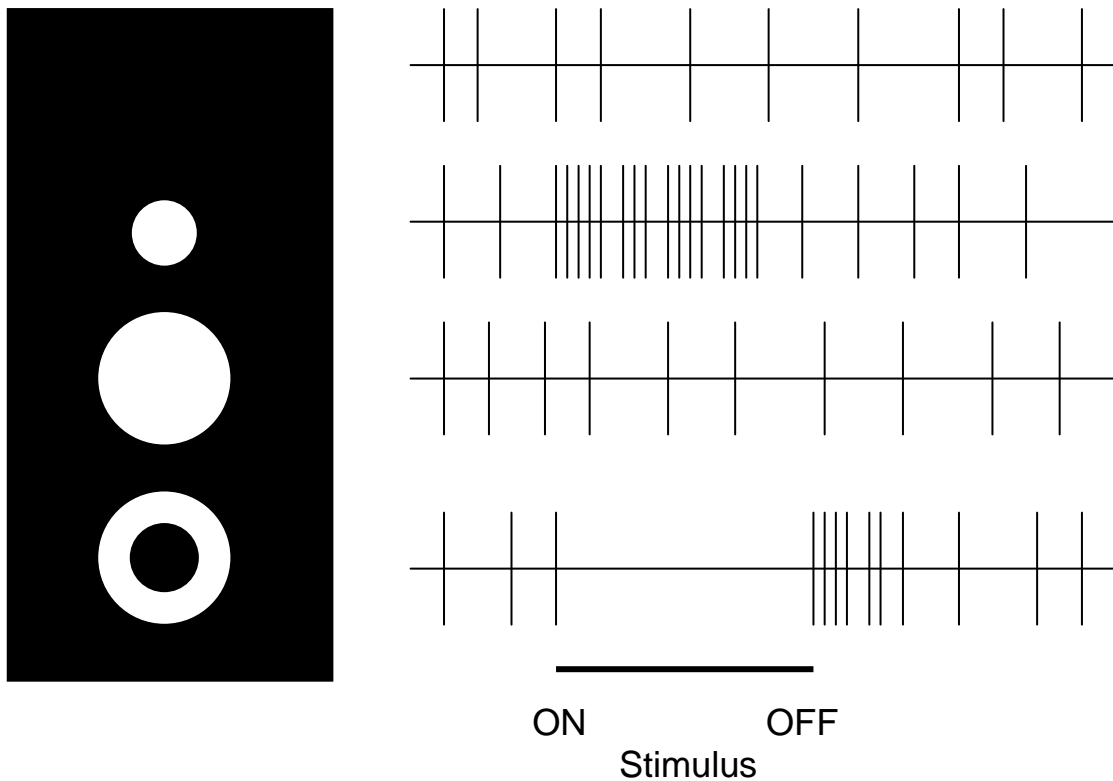


Figure 1.16A. 4 different stimuli (left) and the responses of a centre-on RGC (right). Of note are the similar responses of the RGC to 'no spot' and the 'large spot' stimuli, the increased firing of the RGC to the 'small spot' stimulus, the inhibition of the RGC to the 'annular' stimulus, and a period of increased firing when the 'annular' stimulus was removed [63] (K. Mistry).

Kuffler discovered that in addition to centre-on surround-off receptive fields, there were centre-off, surround-on receptive fields (see Figure 1.16B) [63]. Centre-off receptive fields are as important as centre-on receptive fields because the visual world is made up of both light and dark objects [64].

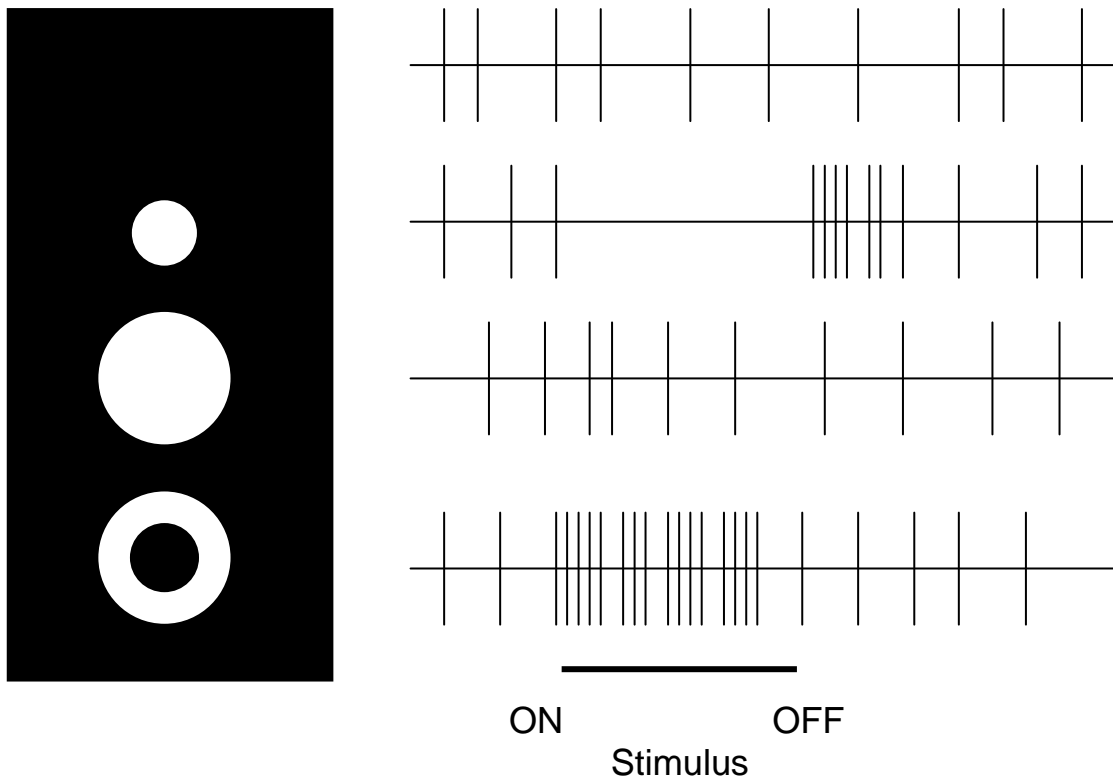


Figure 1.16B. 4 different stimuli (left) and the responses of a centre-off RGC (right). Of note are the similar responses of the RGC to 'no spot' and the 'large spot' stimuli, the increased firing of the RGC to the 'annular' stimulus, the inhibition of the RGC to the 'small spot' stimulus, and a period of increased firing when the 'small spot' stimulus was removed [63] (K. Mistry).

From Figures 16A and 16B it can be seen that the size of the stimulus used is crucial to the responses of the RGC, and may explain why the neurophysiologists before Kuffler, who used diffuse lights, were unsuccessful in recording the receptive fields of RGCs [63]. The hypothesis for the production of these centre-surround receptive fields lies with the excitation and inhibition caused by the Horizontal and the Amacrine cells [35, 64].

RGC receptive fields are not distinct entities such that where one receptive field ends another starts. The receptive field of one RGC overlaps with its neighbour (see Figure 1.17). Thus a spot of light influences a number of RGCs, some are excited and some are inhibited [35].

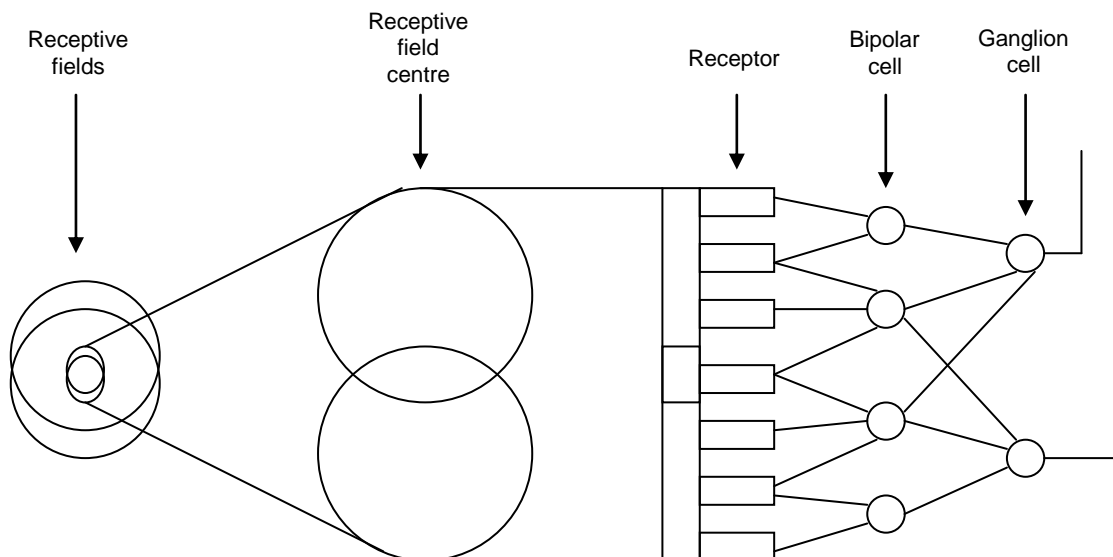


Figure 1.17 Overlapping receptive fields of RGCs (adapted from Eye, Brain, and Vision by Hubel [35]) (K. Mistry).

These centre-surround receptive fields allow the visual system to detect relative changes in brightness rather than the absolute values. This allows a person to perceive the same shades of grey under different sources of illumination as being the same even though the amount of light being reflected back, the luminance, is different [35]. An example of this is the appearance of newspaper print indoors and outdoors; the print still looks black-on-white despite the measurements with a light meter being different in the two environments. The eye can be deceived in perceiving an object as being darker than it actually is by increasing the intensity of the surrounding luminance. One situation where this is employed is a CRT television; here when the television is off, the screen looks grey; however, when turned on the blacks in the picture are no darker than the grey when the television is off, but are perceived as being darker. Thus the visual system is designed to detect changes and edges. This can be seen when looking at the contrast sensitivity function: there is a reduction in sensitivity below 4 cycles per degree, and this reduction is more pronounced in sine-wave gratings when compared to square-wave gratings (see Figure 1.18) [66]. This means that below 4 cycles per degree, the contrast of the grating has to be increased in order for it to be detected, which would suggest some level of inhibition is taking place reducing the visibility of the larger gratings. The contrast sensitivity for the square wave grating at the lower frequencies is higher as the waveform can be constructed from a series of sine waves of higher frequencies (as shown by Fourier theory) some of which have a higher sensitivity [66].

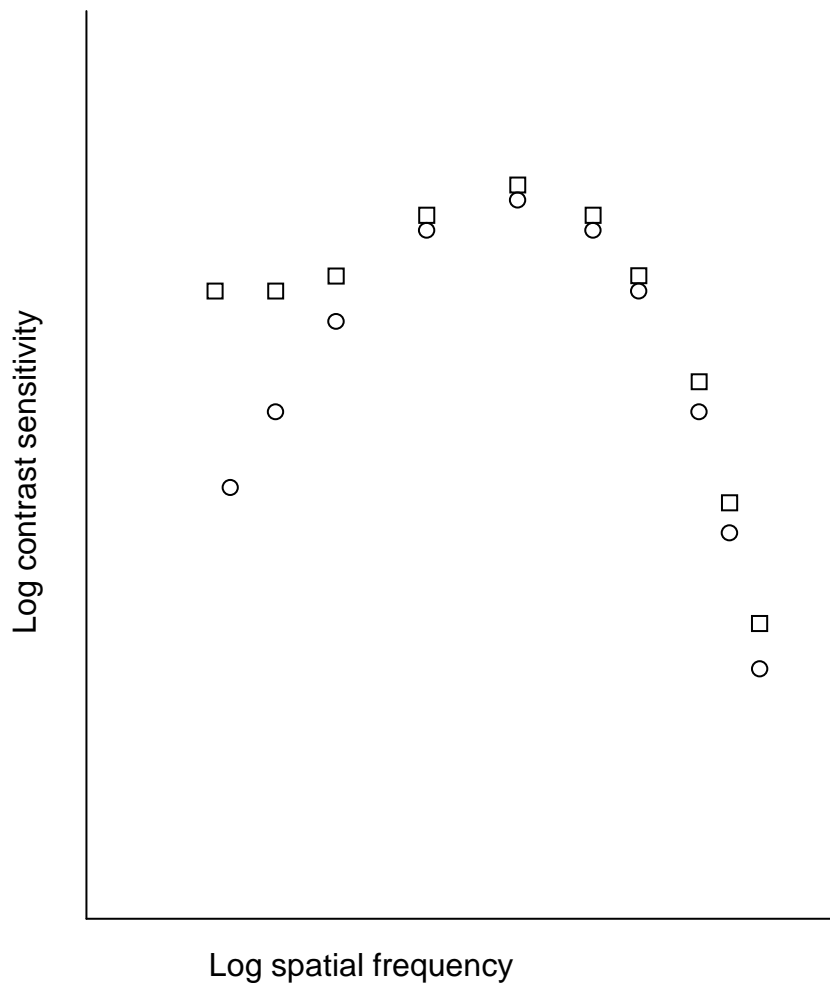


Figure 1.18 Contrast sensitivity functions of sine-wave gratings (○) and square-wave gratings (□), adapted from Campbell et al 1968 [66] (K. Mistry).

1.4.2 Chromatic Receptive Fields

However, receptive fields are not just confined to the achromatic visual system. As a single cone cannot be responsible for colour discrimination, chromatic processing must take place when the output of the cones are compared and contrasted [39]. There are colour opponent RGCs that produce these comparisons [39]. If cone spectra were the only active mechanism, then accurate hue discrimination would be biased towards the longer wavelengths, as cone spectra are not evenly spaced with respect to wavelength (see Figure 1.10). In 1956 Svaetichin found colour-opponent cells in the retinae of fish. He found three types of cells: ones that hyperpolarised to light regardless of wavelength, those that hyperpolarised to green light and depolarised to red light, and cells which hyperpolarised to blue light and depolarised to yellow light [5, 35]. These results come closer to Hering's model rather than the

Young-Helmholtz model, and therefore supports Donder's proposal. Similar results to those found by Svaetichin were found by De Valois in 1958 on macaque monkeys (more closely related to humans than fish) [35]. He also found two types of opponent cells: red-green, and blue-yellow, with there being a cancellation response of the red-green cell when both red and green lights were shone, and a cancellation response of the blue-yellow cell when both blue and yellow lights were shone [35]. In 1966 Hubel and Weisel used small spots of light rather than diffuse lights and found centre-surround receptive fields. They felt that for a receptive field in which red light excited the centre and green light inhibited the surround, that both red (L) and green (M) cones were active over the entire receptive field rather than solely supplying their designated areas (see Figure 1.19) [38]. The receptive fields identified by Hubel and Weisel can be seen in Table 1.1 [35, 39]:

Centre	Surround
Red excitation	Green inhibition
Red inhibition	Green excitation
Green excitation	Red inhibition
Green inhibition	Red excitation
Blue excitation	Red + Green inhibition
Blue inhibition	Red + Green excitation
Red + Green excitation	Blue inhibition
Red + Green inhibition	Blue excitation

Table 1.1 Chromatic receptive fields identified by Hubel and Weisel [35, 39]



Figure 1.19 Centre-surround chromatic receptive fields (Kolb) [22].

Later work has shown that the red-green opponent fields are mediated through the horizontal cells in the retina from L- and M-cones [67]. This shows that the photoreceptors act as filters for the following mechanisms, which achieve chromatic discrimination by comparing the magnitudes of the receptor outputs. The red-green opponent channel is produced by a subtractive comparison of the M- and L-cones [68]. The blue-yellow opponent channel is produced by an additive combination of the M- and L-cones being subtracted from the S-cone (see Figure 1.20) [68, 69], however, this area requires further study [39]. It has been suggested that the additive combination of the M- and L-cones provides a non-opponent brightness channel [70].

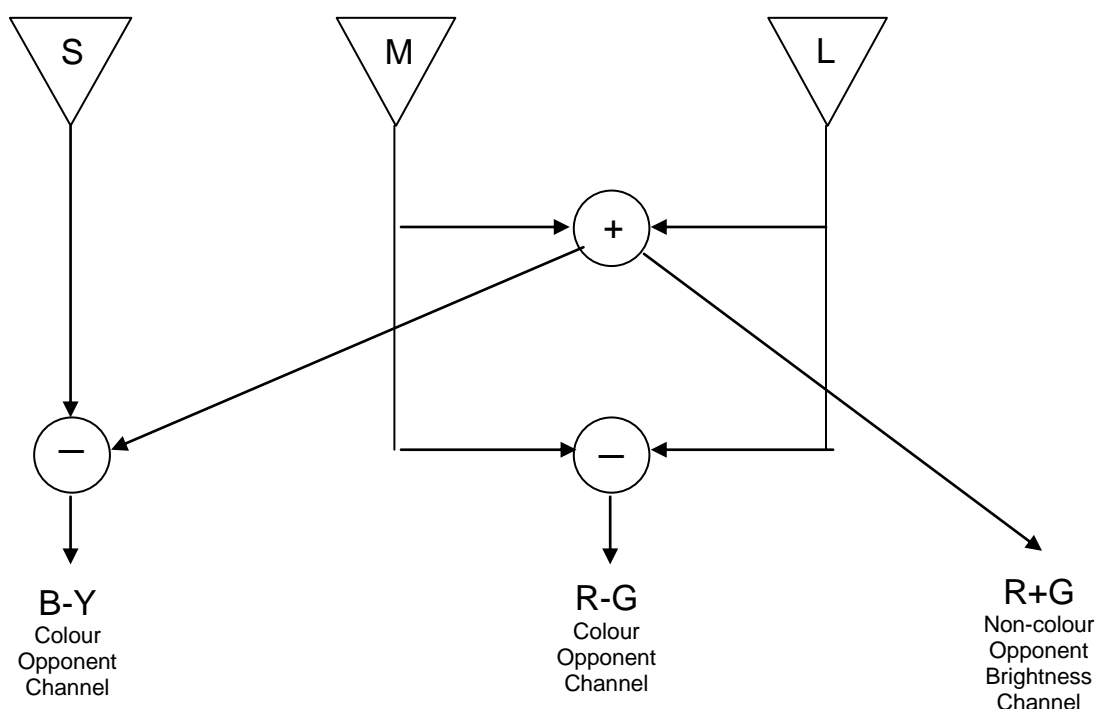


Figure 1.20 A simplified model of cone interactions to produce three pathways, adapted from Schwartz 1998 [71] (K. Mistry).

The structure of chromatic receptive fields seen in the LGN are similar to that found in the RGCs [38]. The colour-opponent receptive fields of the cells in the retina and the LGN may not be designed to make colour contrast comparisons due to the disparity between the high density of L-M opponent midget RGCs and the low chromatic spatial acuity [39], but rather they detect luminance contrast instead [35, 38].

The next port-of-call in the visual pathway is the striate cortex (V_1). As seen in Figure 1.14, the parvocellular pathway enters the striate cortex in layer 4A and 4C β , and goes on to layers 2 and 3, and show some chromatic sensitivity [57, 68]. Colour opponent cells make up large proportion of the cells in the LGN, however, this is not the case in V_1 [53]. Work by Hubel and Horton in 1981, and Humphrey and Hendrickson in 1983, identified blob-like structures in the striate cortex that responded to colour, but the receptive fields were considerably more complex than those found in the LGN [35, 39]. In 1984 Hubel and Livingstone found that the most common chromatic receptive field type was one with red excitation and green inhibition in the centre, combined with red inhibition and green excitation in the surround i.e. double-opponent cells [38, 72]. These cells have receptive fields similar to the cells found by Daw in 1967 in the retinae of goldfish [39, 53]. These cells did not respond to white light, suggesting that they were involved in the detection of chromatic contrast [9]. This would suggest that the Young-Helmholtz theory provides an explanation at the photoreceptor level, whereas the Hering theory describes the processing beyond the photoreceptors [38, 43]. Unfortunately this is not universally accepted as studies by Thorell et al [73], and Lennie et al [68] that failed to find these cells [39, 74]. The colour sensitive cells in V_1 are likely to consist of single-opponent cells for signalling the colour of a receptive field, and double-opponent cells for the higher processing required for colour contrast, and colour constancy [39].

Beyond V_1 , colour coding is less clear. Colour information is projected in to V_2 , V_4 , and posterior inferior temporal cortex [38, 39, 43]. The *blobs* in V_1 project to thin stripes in V_2 [39]. There is some suggestion that hue-mapping (linking red to orange, orange to yellow, yellow to lime etc) takes place in V_2 [38]. V_4 may be responsible for higher colour processing such as colour constancy [9, 10]. This processing, in V_4 , takes place in a collection of cells termed “globs” [39]. Some stroke patients with damage to the ventral cortex (involving V_4) have an acquired defective colour vision and even achromatopsia, suggesting that V_4 has a significant role in colour processing [75].

Colour-opponent receptive fields go some way to explaining why colour discrimination is so good. A ‘hue-discrimination curve’ can be plotted using a 2° field split in two: one half has a reference wavelength, and the wavelength of the second half is increased or decreased from that of the reference until the difference is only just noticeable [76]. For a given wavelength λ , the just-noticeable change in

wavelength below λ ($\delta\lambda_1$) and the just-noticeable change in wavelength above λ ($\delta\lambda_2$) are measured. By taking the average of these two increments i.e. $\frac{1}{2}(\lambda - \delta\lambda_1) + \frac{1}{2}(\delta\lambda_2 - \lambda)$, a value for $\Delta\lambda$ can be plotted for each wavelength λ (see Figure 1.21). The hue-discrimination curve shows that the visual system, at certain wavelengths, is sensitive enough to discrimination to within 2 nm, with the sensitivity peaking around 490 nm and 590 nm. The three minima on the curve (445 nm, 490 nm, and 590 nm) correspond to the spectral regions where two cones are being stimulated differentially [10].



Figure 1.21 Hue-discrimination curve [22].

1.4.3 Colour Constancy

The double-opponent receptive fields, along with the higher processing done in other cortical areas (such as V_4 [10]), result in the ability to recognise colours as being the same despite different spectral reflectances [35, 39]. For example, a red car looks red both on a bright sunny day, and on an overcast day despite the light reflected back off the red car being very different (due to the different spectral compositions of the light incident on the car). This ability cannot be explained by the cone outputs on their own, as there is a function that is related to the relative reflectances of the surfaces in the entire scene, allowing for a perceptual adjustment to be made [39]. This was demonstrated by Land in the 1950s using a Mondrian-type painting and three coloured projectors (red, green, and blue) [35]. With the painting only being illuminated by the projectors he set the intensities of the lights such that the light reflected back off the green square had a spectrum of x . He would then illuminate the orange such that the light reflected back had a spectrum of x . Such that when the rest of the picture is covered, the reflected spectra are the same and the squares appear the same colour. When the rest of the picture is uncovered, rather than the

green square and the orange square appearing the same colour, the green square appeared green, and the orange square appeared orange [35]. This seemed to work regardless of the settings on the projectors (provided they were all on) [35]. This means that colours can be distinguished under different sources of illumination. A similar phenomenon was demonstrated by fish according Ingle in 1985, suggesting that it was not a late development in the evolution of colour vision [35].

1.5 Importance of Colour Vision

Colour vision is not only used by humans, but also by other animals and plants, for the purposes such as communication, protection, attracting mates, warning potential predators, and provides the observer with valuable information about their environment [10].

1.5.1 Evolution of Colour Vision

The natural world contains a myriad of colours. Colour vision has evolved as an essential tool for survival for many diurnal animals. The sophistication of colour vision goes beyond just colour detection even in lower animals such as fish and bees. For example, flowers are brightly coloured to attract potential pollinators such as bees, birds, bats, butterflies, and moths [10]. A greater attraction increases the chance of passing on genetic material. The reproductive drive is not confined to flowers; the brightly coloured plumage of a peacock helps it find a mate. When searching for food, colours help distinguish one plant, berry, or fruit from another. For those organisms that hunt others, colour vision helps in the detection of its prey. The mechanism of camouflage, where an organism can blend in to its surroundings, helps one creature hide from another. This can be a defensive, in the case of a stick-insect or a caterpillar; or predatory, for example, the colour of a green tree-dwelling python sitting in the canopy, or a tiger lying observing its next meal in the long dried grass [10]. Some poisonous creatures make themselves more conspicuous by using bright colours to warn away potential predators [10]. Other non-poisonous creatures in the same habitat may adopt the colours of their poisonous neighbours to deter predators [10].

In the higher primates the important colour-based skills of red-green discrimination emerged because they have a largely fruit-based diet. These high levels of discrimination were of a distinct advantage when selecting and picking the fruits which were ready to eat. As the evolutionary processes progressed and tree dwelling primates became bipeds, they developed separate populations of cones sensitive to longer wavelengths. The reason for this can only be speculated as being due to the different spectral composition of the forests compared with the open savannahs that the ancestors of modern man migrated to [77].

1.5.2 Colour Vision in Society

In society colour vision tasks can be categorised into comparative, connotative, denotative, and aesthetic [19, 78]. Comparative tasks involve judging whether colours are the same or different, for example, mixing paints or dyes to a specified colour [19, 78]. Connotative tasks involve colour coding [19, 78]. Examples of connotative colour coding include railway signal lights, resistor colour codes, ripeness of fruit [19, 78]. Here a colour is assigned a specific meaning. Denotative colours are used to mark out, highlight, and organise materials [19, 78]. This makes the information easier to access, for example, the use of highlighters to indicate text that is important, using colours to tell how hot an object is, and the use of black-on-yellow for patients with visual impairment. With the ubiquitous use of display screens capable of displaying lots of information, denotative colour is essential to stop the user being visually overloaded [10]. Road traffic signals fall into this category because the driver will know whether to stop or go dependant on the position of the light that is on, and so colour vision is not essential [79]. One could argue that that road traffic signals are connotative at night if the whole traffic light cannot be seen, in which case the colour of the light that is on becomes more important as its position is not known. Finally aesthetic colour tasks are there to create an emotional response [19, 78]. The colour of a waiting room maybe chosen to keep patients calm before a procedure, the colour of restaurant to create a romantic ambience, or the bold colours in children's play areas.

1.5.3 Occupational Requirements

Today colour vision is used in decision making by skilled professionals which include railway personnel, pilots, engineers, deck officers, vehicle drivers, signals personnel in the armed forces, and quality controllers in the print and paint industries. Here the colour judgement of the subject is critical, and any uncertainty can lead to dangerous or expensive errors. For example, a pilot needs to be able to discriminate between desaturated blues, and greys that appear in the sky, sea, horizon, and on the ground, often under non-optimal viewing conditions [78]. There are a number of occupations where normal colour vision is a requirement: commercial airline pilots, air traffic controllers, technical and maintenance staff at international airports, aircraft pilots and engineers in the armed forces, naval officers on service ships and all submarine personnel, masters and watch keepers on merchant marine vessels, customs and excise officers, train drivers, railway engineers and maintenance staff, workers in industrial colour quality assurance and colour matching, workers in fine art reproduction and photography, and some electrical and electronic engineers [10, 78]. Some of these industries require special colour vision tests to be administered especially when the occupation requires the recognition of coloured signals [80]. Beyond this there are occupations which accept some people with slight colour vision defects: fire-fighters, police officers, some electrical and electronic engineers, some ranks in the armed services, hospital laboratory technicians, merchant seamen [10, 78]. Finally there are a number of occupations in which colour vision deficiencies provide a distinct disadvantage, but there is lack of uniformity in the guidelines: art teaching, bacteriology, botany, chemistry, interior design, histopathology, horticulture, geology, metallurgy and diamond grading [10]. This last set of occupations highlight the role of denotative colour tasks. Note that the lists of occupations above are examples, and not exhaustive. The CIE have produced colour vision standards for transport, and for the armed forces (summarised in Tables 2A and 2B) [81].

Standard	Test Results	Application
Standard 1: Normal Colour vision	Pass Ishihara or Holmes-Wright Lantern type B	High risk activities when correct recognition of colour signals or codes is safety critical
Standard 2: Defective Colour Vision A (Slight deutan deficiency, protans excluded)	Fail Ishihara but pass an approved lantern test. Nagal anomaloscope to identify protans where required	Low risk activities requiring the recognition of signal lights at a 'moderate' distance
Standard 3: Defective Colour Vision B (Slight-moderate red-green deficiency)	Fail Ishihara, but pass Farnsworth D15	Low risk activities requiring the recognition of pigment colours or large signal lights at a 'short' distance in photopic conditions

Table 1.2A CIE Colour vision standards for transport [81]

Standard	Test Specification
CP1: Superior colour discrimination	No errors with the Holmes-Wright lantern at low brightness in scotopic conditions
CP2: Normal colour vision	No errors on the first 17 plate of the Ishihara 38-plate edition
CP3: Slight red-green deficiency	No errors with the Holmes-Wright lantern type A at high brightness in scotopic conditions
CP4: Adequate colour discrimination	Correct recognition of coloured wires, resistors, or stationary tabs used in different trades
CP5: Severe colour deficiency (Royal Navy only)	Unable to obtain CP1-4

Table 1.2B Colour perception standards for the armed forces [81]

1.6 Colour Vision Deficiencies

1.6.1 Congenital Colour Vision Deficiencies

Huddart in 1777 recounted the problems caused by a colour vision abnormality to the work of a shoemaker called Harris [10], but it was not until the 1790s when John Dalton carried out more detailed work in the area of colour vision deficiencies [10, 42]. Dalton found that his own ability to name and distinguish colours differed from other people [10]. He was unable to differentiate red, orange, yellow, and green, naming them all as red. He subsequently concluded that he could not see long-wavelength (red) light. Dalton found that not only did his brother have a similar problem, but so did four other members of Harris' family [10]. Dalton's theory on the matter was that his vitreous was tinted blue, and had been absorbing the longer wavelengths, however, his own post-mortem examination disproved this [10, 42]. The term 'Daltonism' was used to describe individuals with colour vision defects. This was later replaced by 'colour blindness' by Brewster to refer to blindness to one or more colours, and then replaced by 'colour deficiency' or 'dyschromatopsia' by Von Kries in 1897 [10]. In 1881, work by John William Scott [10], and Baron Rayleigh [5, 10], reclassified people with colour vision problems into dichromats, and anomalous trichromats [5, 10]. Dichromats (like Dalton) have two out of the three photopigments, whereas anomalous trichromats have all three photopigments, but there is an abnormality in one of them [19, 45]. Depending on which photopigment is either missing or defective, a further classification is made i.e. for cyanolabe (blue or S-cone) the prefix 'tritan' is used, for chlorolabe (green or M-cone) the prefix 'deutan' is used, and for erythrolabe (red or L-cone) the prefix 'protan' is used [19, 45]. As can be seen in Table 1.3 the prevalence of congenital colour vision defects (CCVDs) is significantly higher in males than females, and the most common defect is deuteranomalous; this is due to the genes for chlorolabe and erythrolabe being on the X chromosome and being recessive [10]. This inheritance was shown in the large pedigree published by Horner in 1876 [10].

Type of variation	Subdivision	Colour matching variables	Approximate Prevalence	
			M (%)	F (%)
Normal		3	92	99.5
Monochromats	Rod	1	Rare	Rare
	Cone	1	Rare	Rare
Dichromats	Protanope	2	1	0.01
	Deuteranope	2	1	0.01
	Tritanope	2	0.0001	0.0001
Anomalous trichromats	Protanomalous	3	1	0.03
	Deuteranomalous	3	5	0.35
	Tritanomalous	3	Rare	Rare

Table 1.3 Prevalence of congenital colour vision defects (CCVDs) [19, 45]

1.6.1.1 Dichromatism

As dichromats only have two out of the three photopigments, their ability to distinguish hues is greatly reduced since colour opponency is greatly hampered. In 1935, Pitt estimated that a person with normal colour vision can distinguish 150 hues, whereas a protanope can distinguish 30, and a deuteranope only 17 [10].

When taking the example of a protanope, where the erythrolabe is missing, it can be seen from Figure 1.10, that beyond the spectral sensitivity of cyanolabe (i.e. beyond a wavelength of ~530 nm), all distinguishing decisions are made from the output of the chlorolabe (M-cone), rather than the comparison of outputs of M-cones with L-cones [19]. This means that beyond 534 nm (the peak sensitivity chlorolabe), for a light of constant brightness to a normal trichromat, as the wavelength increases, the perceived brightness of a light to a protanope decreases [19]. A similar problem can be seen when either of the other 2 pigments is missing. When this is practically applied using colour matching tests the confusion loci for dichromats can be plotted in CIE Colour Space. These produce areas where colours appear the same: isochromatic to the dichromat, but referred to as pseudoisochromatic as the colours are differentiable to a normal trichromat [10, 19]. These confusion loci, or pseudoisochromatic lines, can be seen in Figure 1.22; they converge to a point

outside the CIE Colour Space diagram. The x-y co-ordinates of these points are: 0.17, 0.00 for a tritanope, 1.40, -0.40 for a deuteranope, and 0.75, 0.25 for a protanope [10, 19].

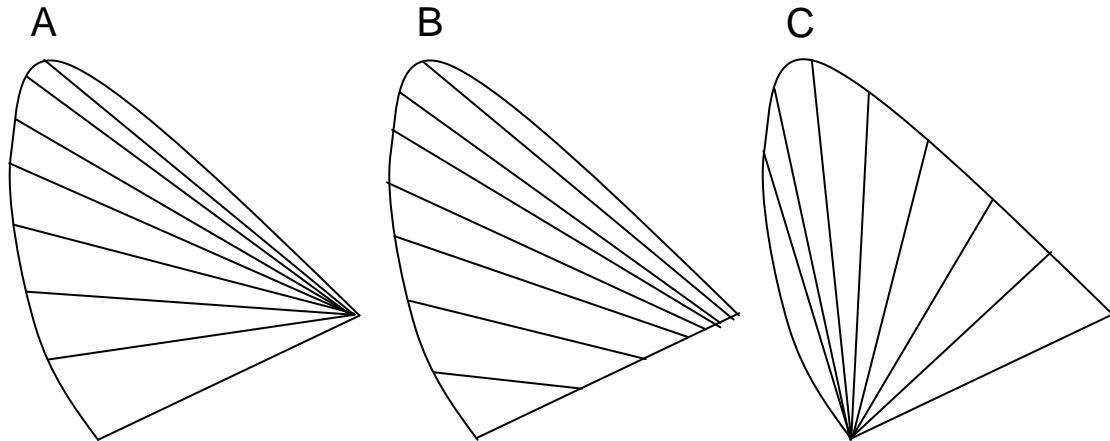


Figure 1.22 Confusion for dichromats: (a) protanope, (b) deuteranope, and (c) tritanope (adapted from *Diagnosis of Defective Colour Vision* by Birch [10]).

Dichromats can be severely affected by their colour vision deficiency. Steward and Cole found that 86% reported difficulties with coloured goods, 68% reported problems with during household repairs/maintenance and with hobbies, and 38% difficulty with food stuffs (recognising whether meat is cooked, or fruit is ripe) [82].

1.6.1.2 Anomalous Trichromatism

Although anomalous trichromats were first described by Rayleigh in 1881, it was not until Nagel constructed an anomaloscope in 1907 that they could be quantitatively studied. The Nagel anomaloscope uses a split field; one half is yellow, and the other is yellow made by mixing red and green (based of the Rayleigh equation 'Red + Green \equiv Yellow' [83]). The subject is required to adjust the intensities of the red and green lights such that they appear to match the yellow light The matching ranges for red-green CCVDs can be seen in Figure 1.23 [84].

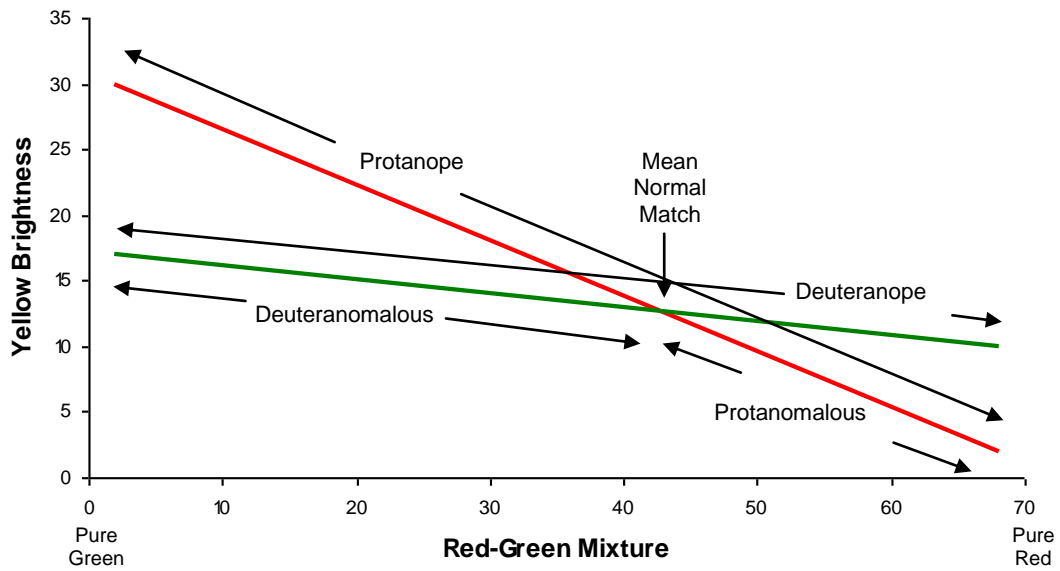


Figure 1.23 How colours are matched with a Nagel anomaloscope [84] (K. Mistry).

The initial question posed was concerning whether anomalous trichromats were extreme cases of 'normals' or a distinct group in their own right. Forshaw in 1954 came to the conclusion, at least for deuteranomalous subjects, that anomalous trichromats were a distinct group [5]. The distinction for protanomalous trichromats was more difficult to make [5]. The results of such an experiment can be seen in Figure 1.24 [10].

occupation, and also feeling restricted in their choice of occupation [82]. However, there is a great amount of variation in degree of deficiencies for anomalous trichromats ranging from almost normal colour vision to that which is similar to a dichromat (see Figure 1.24) [10].

The consequences of poor colour vision can impact not only an individual's occupational choices, but also their safety. In 1989, a survey carried out by Steward and Cole on 102 subjects with colour vision defects found that 49% of dichromats and 18% of anomalous trichromats had difficulties with distinguishing traffic lights. 43% of dichromats and 29% of anomalous trichromats said that their colour vision deficiency had an impact on their choice of career [82].

1.6.2 Acquired Colour Vision Deficiencies

Unlike CCVDs which are present from birth, acquired defects (ACVDs) appear and can alter through a person's lifetime. An ACVD can be unilateral whereas CCVDs are always bilateral. The pseudoisochromatic areas in ACVDs do not follow the predictable axes that are present in CCVDs. The prevalence of ACVDs are equal for males and females. The general differences in congenital and acquired defects are summarised in Table 1.4. They can appear as a result of pathology (general and ocular), intracranial injury, and drug use in certain cases [10]. As ACVDs vary over time, the characteristics of the deficiency can be used to monitor the underlying condition, or even to predict the progression of pathology or toxicity [62].

Congenital	Acquired
Present at birth	Onset after birth
Type and severity constant throughout life	Type and severity changes with time
Type of deficiency can be classified and diagnosed precisely	Not easy to classify Characteristics may be similar to the combination of congenital deficiencies
Both eye equally affected	Monocular differences in severity frequently occur
Visual acuity and visual fields are normal (with the exception of monochromats)	Reduced visual acuity and/or visual field defects
Predominantly red-green	Predominantly tritan
Higher prevalence in males	Equal prevalence in males and females

Table 1.4 The different characteristics of congenital and acquired colour vision deficiencies [10, 62, 85].

Quite often ‘Kollner’s Rule’ is misinterpreted as saying that acquired blue-yellow colour vision deficiencies are due to retinal disease, and acquired red-green deficiencies are due to optic nerve disease; however, the truth is a little less precise [10]. It would appear that blue-yellow and red-green acquired deficiencies do not appear in isolation, and that both defects are present, but in different quantities [10]. There are exceptions to Kollner’s Rule: cone receptor dystrophies often result in red-green defects, and dominantly inherited juvenile optic atrophy results in tritan defects [10].

Kollner’s Rule (1912)

“Blue-yellow blindness: blue and yellow change their appearance first, green and red are preserved. Acquired ‘blue-yellow blindness’ especially develops in disease of the retina and total colour blindness only results in combination with ‘progressive red-green blindness’.

Progressive red-green blindness: Colour vision is totally disturbed. Blue-yellow vision is changed but deterioration is most striking is for red and green. This type of colour blindness can be found in diseases of the conductive pathways reaching from the inner layers of the retina to the cortex.”

Kollner’s Rule as cited by Marré (1973) [86].

Acquired colour vision defects can be classified into 3 types (see Table 1.5):

Type 1	Red-green	Similar to protan defects Wavelength of maximum luminous efficiency displaced to shorter wavelengths
Type 2	Red-green	Similar to deutan defects No reduction of relative luminous efficiency for short wavelengths
Type 3a	Blue	Similar to tritan defect Reduction of relative luminous efficiency at both spectral limits
Type 3b	Blue	Similar to tritan defect Displaced relative luminous efficiency to shorter wavelengths (pseudo-protanomaly)

Table 1.5 Classification of acquired colour vision deficiencies [10].

Changes to the crystalline lens (cataract) which occur as the age of a person advances increase its absorption of the shorter wavelengths of light, which results in a type 3 defect [62]. A study conducted by Beirne et al comparing the colour vision of

older subjects with younger ones found that the younger subjects had better colour discrimination even when the younger subjects were tested whilst looking through tinted lenses that simulated the yellowing effect of an aging crystalline lens [87]. This would suggest that there are other factors, such as pupil size, and macula pigment density, that cause colour vision to deteriorate as a person ages [87].

Moving through the eye to the retina, age-related macula degeneration (ARMD), when severe, results in a type 3 defect [10, 88]; however there were no definitive defects found in subjects with mild ARMD with a degree of false positives [88]. Type 3 defects were also reported in subjects with central serous retinopathy (CSR) [10, 89] (a self-limiting condition in which the fluid accumulates beneath Bruch's membrane resulting in a detachment of the sensory retina at the macula [90]).

Retinitis pigmentosa (RP) is a group of inherited disorders (which may be autosomal dominant, autosomal recessive, or X-linked) that results in the progressive loss of RPE function, rods, and cones (to a lesser degree) [10, 90]. Some RP variants can result in a severe type 3b defect, whereas others can be unaffected [10].

Glaucoma is a progressive optic neuropathy in which there are characteristic optic nerve head changes, and corresponding visual field loss [90-92]. Approximately 20-40% of sufferers have normal colour vision, 30-50% have a blue-yellow defect, 5% have a red-green defect, and 20-30% have a general loss of colour discrimination [85, 93]. Studies into colour vision and ocular hypertension (high intraocular pressure without glaucomatous optic nerve head changes or visual field loss [90]) have found normal colour vision in this group, however abnormal tritan colour matches have been found in ocular hypertensive subjects that did progress to having glaucoma [94, 95].

Diabetes affects approximately 2% of the population [10, 90] and can cause pathological changes to the retinal vasculature, such as microaneurysms, and haemorrhages, resulting in exudates, retinal oedema, hypoxia, and neovascularisation [90, 96]. Diabetic eye disease is the most common cause of blindness in adults under 65 in the developed world [10, 90]. Colour vision defects tend to be type 3, and colour vision is generally poor in individuals with diabetic maculopathy due to the oedema [10]. Although colour vision testing alone cannot be used to screen for diabetic retinopathy [96].

Optic neuritis is an inflammatory or demyelinating process affecting the optic nerve [90, 97], and is often associated with multiple sclerosis. A study carried out by Schneck and Haegerstrom-Portnoy of colour vision defects in optic neuritis found that only 6.8% of sufferers had normal colour vision during the acute phase, whereas 60.8% had normal colour vision after 6 months [97]. In the acute group 40.8% had a blue-yellow defect, 29.6% had a red-green defect, and 29.6% had a non-selective defect [97]. Of the group with the blue-yellow defect, 63% recovered, 14.3% developed a red-green defect, and 6.1% developed a non-selective defect by 6 months [97]. Of those in the red-green defect group 54.9% recovered, 15.5% developed a blue-yellow defect, and 9.8% developed a non-selective defect by 6 months [97]. And finally of the non-selective defect group 63.4% recovered, 9.8% developed a blue-yellow defect, and 16.9% developed a red-green defect by 6 months [97]. This highlights the potential for variability in a colour vision defect amongst people with optic neuritis.

Intracranial lesions and brain injuries can lead to colour vision deficiencies of all types, and can in certain cases, result in cerebral achromatopsia (complete colour blindness) [10, 98].

Although not exhaustive, Table 1.6 shows the variety of conditions and their ACVDs.

Drug	Defect
Cataract	Type 3
ARMD	Type 3
CSR	Type 3
RP	Type 3b
Glaucoma	Blue-Yellow Red-Green General Loss
Diabetes	Type 3
Optic Neuritis	Blue-Yellow Red-Green Non-Selective
Intra-cranial Lesions	All types inc. Achromatopsia

Table 1.6 Summary of ACVD secondary to pathology

There are a number of drugs that can cause colour vision defects: digoxin and digitoxin can cause red-green defects as well as tritan defects in the form of yellow-tinting [99, 100], sildenafil citrate can cause a plasma-level dependant tritan-like defect, chloroquine can cause a protan-like defect as it accumulates in the retina, ethambutol can cause a red-green defect as well as disturbances to tritan discrimination, and some anti-epileptic medication can impair tritan discrimination [62]. The drugs, carbamazepine, tiagabine, valporic acid, and vigabatrin used in the treatment of epilepsy, resulted in the development of a blue-yellow defect [101-103]. Even oral contraceptives can influence colour vision [104]. The recreational drugs: cocaine, amphetamine may cause a blue-yellow defect [105]. The list of drugs shown in Table 1.7 is not exhaustive.

Drug	Defect
Amphetamine	Blue-Yellow
Carbamazepine	Blue-Yellow
Chloroquine	Protan
Cocaine	Blue-Yellow
Digitoxin	Red-Green + Tritan
Digoxin	Red-Green + Tritan
Ethambutol	Red-Green
Sildenafil citrate	Tritan
Tiagabin	Blue-Yellow
Valporate	Blue-Yellow
Vigabatrin	Blue-Yellow

Table 1.7 Summary of ACVD secondary to drug use

1.7 Colour Vision Tests

There are a number of colour vision tests available, some are suitable for clinical screening, and others can be used in research and for the monitoring of pathology. This was started by John Dalton's coloured ribbon test, and was expanded by August Seebeck in 1837 who had 300 coloured papers which needed to be grouped [10]. Occupational colour vision testing had been carried out as early as 1858 for railway workers in France [10]. In 1875 ten people were killed when the steamship 'Isaac Bell' collided with a tug boat off the coast of Norfolk (Virginia, USA), as the tug boat

captain could not distinguish between the red and green navigation lights [10, 81]. This was the first accident attributed to colour vision defects. A second accident took place later that year on a railway line in Sweden when two trains collided resulting in the deaths of nine people [81]. The cause of the accident was assumed to be a colour vision deficiency, although no evidence was found [81]. Following these incidences the Holmgren test, which involved the arrangement of coloured wools, was introduced to screen railway personnel and recruits for the armed forces [81]. It was not until 1891 that Edridge-Green designed the first lantern test [10].

1.7.1 Anomaloscopes

All anomaloscopes are based on the work done by Rayleigh 1881 [5]. They use a 2° bipartite field [10]. Rayleigh used the sodium line (589 nm) for yellow, lithium (670 nm) for red, and thorium (535 nm) for green [83], whereas the Nagel anomaloscope Mk1 uses a 2.5° field, and the green mercury line (546 nm) instead of thorium [10, 83, 106]. Although no longer available, the Nagel anomaloscope Mk1 is considered to be the 'gold standard' for diagnosing protan and deutan colour vision defects [83]. In its place are the Neitz OT, which uses interference filters (whereas the Nagel anomaloscope Mk1 used a prism dispersive method), and the Oculus Heidelberg Mk1, which uses light-emitting diodes (LEDs) and interference filters [83]. To ascertain the severity of a defect for the Nagel anomaloscope Mk1, a red-green discrimination index (RGI) is calculated [106]:

$$\text{RGI} = 1 - (R - MR)/73$$

Where R is the matching range obtained, MR is the mean normal matching range for the instrument, and 73 is the number of units in the red-green matching range. An RGI of approaching one is found for normal trichromats, and an RGI of zero is found for dichromats (see Table 1.3) [106].

These anomaloscopes are only useful for investigating the Rayleigh equation (red-green matching to yellow). To investigate tritan defects, the Mooreland equation (Blue + Green \equiv Blue/Green, and Blue + Yellow \equiv White) needs to be used [83, 107]. Both the Oculus Heidelberg Mk2 [83] and the Pickford-Nicholson [10, 85] anomaloscopes utilise this. The Engelking-Trendelenberg match 470 nm (blue) + 570 nm (green) = 489 nm (blue/green) is used by the Nagel anomaloscope Mk 2 [83].

There is one more equation to mention and that is the Mooreland 2 equation; this was devised because of the spectral green match is more desaturated compared to the spectral blue-green, the absorption of the crystalline lens, and the influence of xanthophyll (the macular pigment) [83].

1.7.2 Pseudoisochromatic Plates

Pseudoisochromatic (PIC) plates exploit the colour confusion that takes place to produce colour camouflage [10]. It takes advantage of the brain's desire to see patterns by placing similar coloured spots or patches (i.e. within Macadam's ellipses/confusion areas) together such that a figure or shape can be seen. If the adjacent coloured spots are too disparate then the brain does not connect them, and so any line in the figure or shape would be broken. There are a number of methods employed by PIC plates: demonstration/malingerer's plate, disappearing/vanishing plates, ambiguous/alteration plates, combination plates, diagnostic/classification plates, quantitative plates, and hidden plates [83].

The demonstration/malingerer's plate is the only plate where the figure and the background are not isoluminant [83]. Therefore colour vision is not required in order to see the figure [83]. This means that all subjects with sufficient visual acuity should get this figure correct based on luminance cues alone. This plate is there to test whether the subject understands what is being asked of them, and also helps identify malingering individuals [83].

In the disappearing/vanishing plates the colours used in the background and that on the figure are close to or on the dichromatic confusion lines [83]. As protan and deutan confusion lines are so close together, there is a certain amount of overlap [83]. If the protan and deutan confusion lines are chosen then a subject with normal colour vision or a tritan defect will see the figure, whereas a subject with a protan or deutan type deficiency will not [83].

Ambiguous/alteration plates are designed such that a subject with normal colour vision will see a different figure to that seen by a subject with the colour defect that the test is designed for [83]. For example if the number seen by a subject with normal colour vision is '5', then by having the spots in the gap between the top bar of the '5'

and the rounded section such that the colours appear the same as the rest of the '5' to a subject with defective colour vision, then the '5' and be made to look like a '9'.

Combination plates are plates with two figures on them [83]. One of them is a demonstration figure, and the other is a disappearing/vanishing figure [83]. The demonstration figure is more subtle than the disappearing/vanishing figure, to prevent individuals with normal colour vision from only spotting the demonstration figure. The subject with defective colour vision will only pick out the demonstration figure [83].

Diagnostic/classification plates are used to differentiate protan defects from deutan defects [83]. The plate will have two disappearing/vanishing figures; one will be a disappearing/vanishing figure for a subject with a protan defect, and the other a disappearing/vanishing figure for a subject with a deutan defect [83]. The subjects, in this case, with normal colour vision, a mild anomalous defect, or a tritan defect will see both numbers [10, 83].

Quantitative plates are a series of plates with an increasing colour difference and thus help grade a defect [10, 83]. The later in the series a subject identifies a figure, the more severe their colour defect is [10].

In the hidden plates the spots or patches used to make up the plate appear different, and so no figure is seen. As the figure is made of colours that lie on one confusion line, and the background made of colours on a different confusion line, a subject with defective colour vision will see the figure [10, 83].

The first PIC plates produced were as early as 1876 by Dr J. Stilling [10], however the most frequently used test for screening red-green colour vision deficiencies is the Ishihara test [96]. The other commonly used PIC plate test available is the Hardy, Rand, and Ritter (HRR) plates [45, 83].

1.7.2.1 Ishihara Plates

The Ishihara PIC plates were first published in 1917 by Dr S. Ishihara. There have been numerous editions; the first 15 editions (until 1962) were ranked numerically, thereafter they were identified by the year of publication [10]. Currently there are two

versions of the test in popular use: the full 38-plate test, and from 1989 an abridged 24-plate test [83]. In both versions the figure to be identified is a number, and the subject has a viewing time of approximately four seconds per plate. The books also contain pathway plates for non-verbal subjects which involves tracing a winding line between an 'X' on one side of the plate to an 'X' on the other, however, this part of the test significantly increases screening time and is not recommended [10]. There is also a children's version of the test in which the figure to be identified is a letter rather than a number [83].

Plate 1 is the demonstration plate, 2-9 are transformation plates, 10-17 are vanishing plates (see Figure 1.25), 18-21 are hidden plates, and 22-25 are classification plates. The hidden plates (18-21) show poor sensitivity and specificity and can be omitted [10, 19]. The classification plates should be used with caution, especially when testing anomalous trichromats [108], as in 30-40% of cases the test fails to differentiate protans from deutans as both numerals can be seen [19, 45]. In the case where both numerals are seen, then the subject should be asked which numeral is clearer (protans favour the numeral on the right, and deutans the one on the left) [10]. If relying on a subject only seeing one digit, then as little as 47% of protanomalous trichromats, and 57% of deuteranomalous trichromats were correctly identified [108].

The Ishihara test can only be used for red-green defects; however, it is regarded as the 'gold standard' for rapid identification of congenital red-green colour vision deficiencies [83, 106]. Due to the serif design of the numerals used, only ~55% of subjects with normal colour vision get a perfect score [10]. For the 38-plate test three or more errors on plates 2-17 indicates a red-green colour vision defect [19, 45], and although not designed for grading, 3-7 errors indicates a slight defect [10]. However, based on three errors in plates 2-17, both the sensitivity and specificity are high at 97-99% and 94% respectively [108, 109]. If using a threshold of four errors, then the sensitivity is reduced to 94%, although the specificity increases to 98%, and 100% when compared to the Nagel anomaloscope [106]. In order to perform the Ishihara test an individual needs to have a visual acuity of at least $\frac{6}{18}$ [85]. For the 38-plate Edition Birch recommends using plates 1-17, and if more than three errors are made plates 22-25 [10].

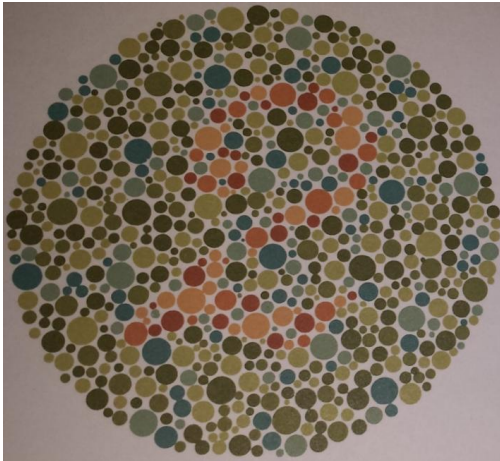


Figure 1.25 Ishihara Plate: vanishing plate (K. Mistry).

1.7.2.2 Hardy, Rand, and Ritter Plates

Originally produced by American Optical, HRR PIC colour vision plates were first printed in 1954 [10] and published in 1955 [83]. They originally tested for protan, deutan, tritan, and tetratan (a proposed yellow photopigment) defects, however, the tetratan plates were later removed [106]. They were reprinted by Richmond in 1996, and then by Waggoner in 2006 [83]. It uses shapes (circle, cross, triangle) [10, 45] rather than numerals, which can make the test easier to do for young children [45]. Unlike the Ishihara test, the HRR test can be used to investigate tritan defects [45, 83, 85].

The test consists of 24 vanishing plates: 1-4 are demonstration plates, 5-8 are screening plates to identify red-green (protan and deutan) defects, 9-10 are screening plates to identify blue (tritan) defects, 11-14 are grading and classifying plates for identifying slight protan and deutan deficiencies, 15-18 are grading and classifying plates for identifying moderate protan and deutan deficiencies, 19-20 are grading and classifying plates for identifying severe protan and deutan deficiencies, 21-22 are grading and classifying plates for identifying moderate tritan deficiencies, and 23-24 are grading and classifying plates for identifying severe tritan deficiencies [10]. If test plates 5-10 are correctly identified, then the test is stopped, and the subject classified as having normal colour vision [10]. For plates 5-8 there is a sensitivity of 90% and a specificity of 72% based on one error [10], which is not quite as high as the Ishihara test. When based on two or more errors for plates 5-8 the specificity increases to 96% [45]. For the subjects who fail the plates 5-8 (red-green

defects) 86-95% of the subjects were correctly classified as either protan or deutan [10, 45]. Care must be taken when examining subjects over the age of 55, as there is an increased risk of false-positive tritan errors [106]. Unfortunately due to the changes in manufacturer, there is some variability in the quality across the editions [10]. The threshold visual acuity of $\frac{6}{60}$ for HRR test is a little lower than the Ishihara test [85]. The HRR complements the Ishihara test well [10].

1.7.3 Arrangement Tests

There are two main arrangement tests: the Farnsworth-Munsell 100 Hue test (FM100), and the Farnsworth Dichotomous test for colour blindness (D15); and other less commonly used arrangement tests include the Farnsworth Dichotomous B20, Lanthony D15, Roth 28 Hue test, Desaturated D15 [10, 45, 83]. They require the subject to arrange coloured samples, enclosed in plastic caps, in order of hue starting from a reference cap [10, 83]. Both the FM100 and the D15 were devised by Farnsworth in the 1940s primarily for vocational use [10].

1.7.3.1 Farnsworth-Munsell 100 Hue Test

The FM100 involves the arrangement of 85 caps into four boxes [106]. Each cap subtends 1.5° at 50 cm [110]. Originally there were 100 caps, but 15 were removed when Farnsworth found the perceptual steps between certain hues were too small [83]. Unfortunately the perceptual steps between each cap are not equal; in particular the third box, which contains the blue-green caps, has smaller hue differences between each cap thus resulting in higher errors in this region [106]. Each box has two reference caps (also known as end caps), and all the other caps in that particular box need to be arranged in order of hue between the reference caps [110].

The purpose of this test is to measure a subject's hue discrimination ability at a constant value and chroma [10, 110]. An error score is calculated for each cap, and the results are plotted on a polar graph [83, 85]. Farnsworth's method of calculating an error score involves summing the difference between the cap in question and the caps either side, this means that for caps placed in the correct order the error score is '2' [111, 112]. A total error score (TES) is calculated as the sum of all the error scores minus 2 for each cap (i.e. 170) [111]. The TES can give a skewed distribution;

a nearly normal distribution can be obtained by taking the square root of the TES ($\sqrt{\text{TES}}$) [87, 113].

There is an alternative scoring method proposed by Kinnear which calculates the error for the position rather than the cap [112].

$$\begin{array}{ll} \text{Farnsworth method} & E(a_n) = |a_n - a_{n-1}| + |a_n - a_{n+1}| \\ \text{Kinnear method} & E(n) = |a_n - a_{n-1}| + |a_n - a_{n+1}| \end{array} \quad [112]$$

The Kinnear method is thought to be easier when the error scores are being calculated manually, however, neither method has been shown to be superior [83].

Unlike the PIC plate tests or the anomaloscopes, the FM100 does not concentrate testing around the confusion lines of the congenital defects, and therefore can be used to investigate acquired colour vision defects [83, 114]. In addition it can be useful in monitoring a defect over time [85, 113]. Confusion axes occur due to a pair of regions on the plot that have higher error scores and therefore poorer hue discrimination. These regions are on opposite sides of the polar plots, and the line that runs through the peaks of these regions describes the confusion axis [110]. For congenital colour vision defects the distortion in the chromaticity plane can be seen as isochromatic lines that are at a tangent to the specific defect on the circle of hues (see Figure 1.26) [110]. The protan, deutan, and tritan confusion lines can be seen when looking at the cap locations on the UCS (see Figure 1.27).



Figure 1.26 The FM100 plot with confusion axes for protan defects P , deutan defects D , and tritan defects T (courtesy of Oxford Eye Hospital)

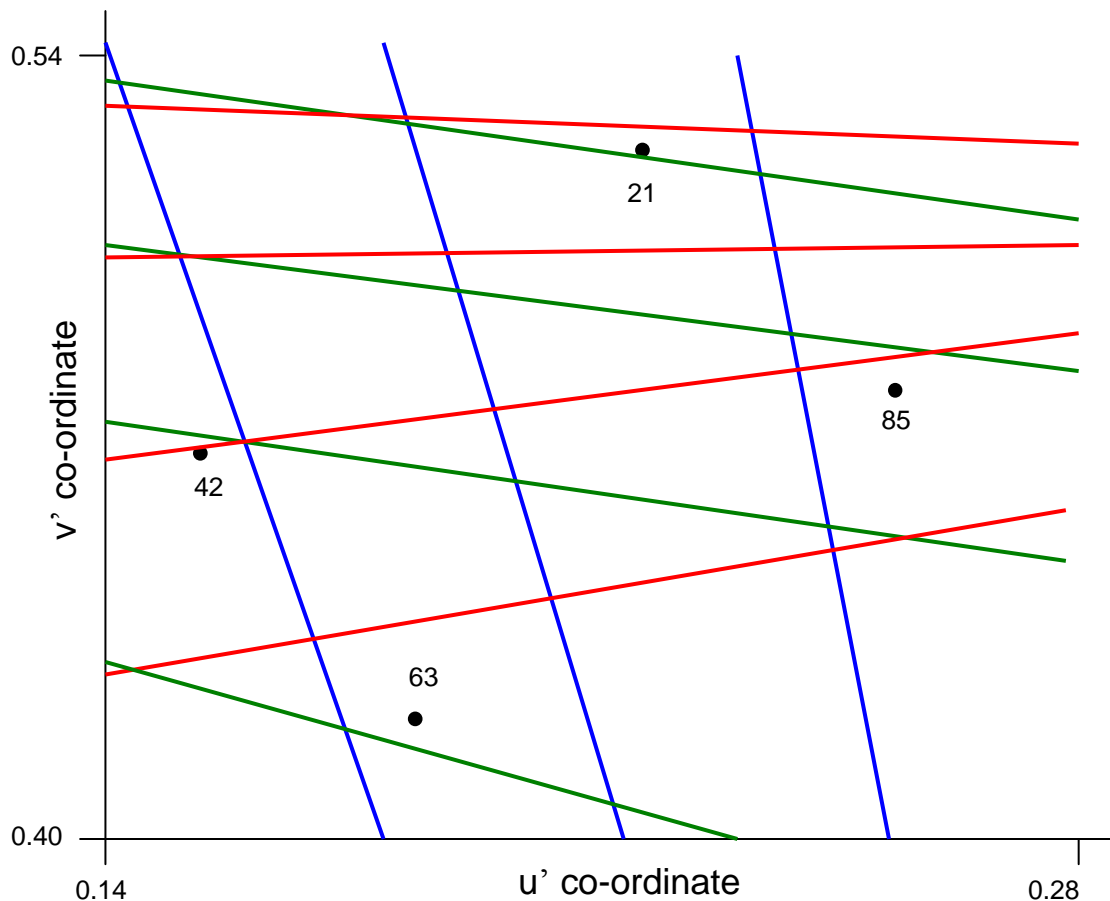


Figure 1.27 The positions of the FM100 cap in UCS, the filled in circles are the end caps, the blue lines refer to the tritan confusion axis, the red to the protan axis and the green to the deutan axis (adapted from Dain 2004) [83] (K. Mistry).

However, there is 'learning effect' (an improved result on repetition of the test) with the FM100 test [114, 115], which with appropriate training can reduce subsequent error scores by up to 30% from the first test [110], and so care has to be taken when considering this test for monitoring a condition [10]. The results are also affected by age, macular pigment density, and illumination [83, 87, 113]. Kinnear and Sahraie found that subjects over 40 had higher error scores especially in the blue-yellow region [113], and there is an increased risk of false-positive tritan defect in subjects over 55 [106]. Another issue is the time taken to the test; it has been suggested that the test takes 10-15 minutes to complete [45]. From personal experience this figure can be considerably longer especially in subjects with a colour vision defect.

The learning effect and test duration make the FM100 unsuitable for screening in a primary care setting [10, 45]. The D15 is more suited to use in primary care.

1.7.3.2 Farnsworth Dichotomous Test for Colour Blindness

The D15 was developed by Farnsworth in 1947 as a vocational test [10, 116]. It consists of one reference cap and 15 caps which need sorting into an order such that the colours progressively change (very much like the FM100 but with only one end cap) [19, 117]. The caps form an incomplete hue circle consisting of Munsell value 5 and chroma 4 [106]. The caps for the D15 can be selected out of the FM100 [83], and thus at 50 cm each cap subtends 1.5° [106]. It is a dichotomous test as it was designed to give a 'pass' or 'fail' verdict [117]. Those subjects that have 'passed' the test are classified as having normal colour vision, or only a mild deficiency [19, 45]. Those that have failed the test are deemed to have a moderate to severe colour vision defect [19, 45].

There are a number of ways judging the results of a D15, such as counting the number of transpositions [19], or a scoring method as adopted by the FM100 [83], however, what is widely used is counting the number of diametric crossings [45, 116]. Using a pass criterion of a complete circle i.e. all the caps in their correct places, Birch found that 1.5% of red-green dichromats and 63% of red-green anomalous trichromats passed; if one diametric crossing was allowed, then that pass rate went up to 3% and 73%, and if 2 diametric crossings were allowed then it was 6% and 80% [84, 116]. A coefficient of reliability for test-retest reliability for pass/fail was found to be high at between 0.96-1.0 [45]. The orientation of the crossings can be used to classify the defect as being tritan, deutan, or protan (see Figure 1.28) [19, 116].

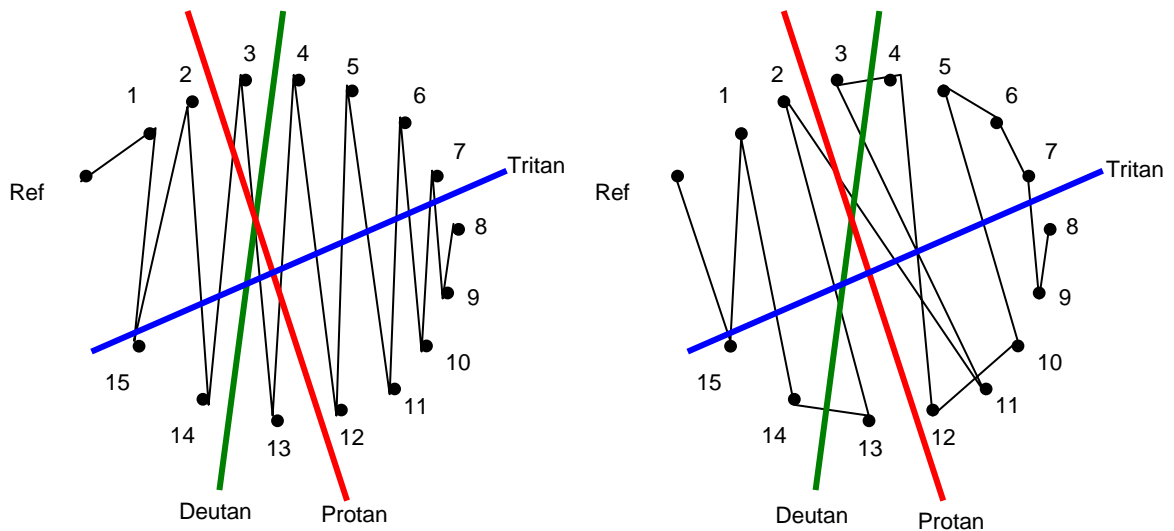


Figure 1.28 D15 plots; deutan defect (left), protan defect (right), adapted from Formankiewicz 2009 [84] (K. Mistry).

1.7.4 The City University Test

The City University Test (CUT) 2nd Edition (discontinued) is based on the hues found on the D15 [117]. It is not a matching test, but a forced choice test [83]. The subject is shown a page on which there is a reference coloured spot in the centre, and four coloured spots around it [83, 118]. The subject is asked to identify which of the four surrounding spots is most similar in colour to the centre (reference) spot [83, 118]. The spot identified will not be the same colour as the reference spot. Of the four surrounding spots, one lies on the tritan confusion line, one on the deutan confusion line, one on the protan confusion line, and one is the next colour in the sequence of D15 hues [117, 118]. The test can be used to identify moderate and severe defects and to classify them as protan, deutan, or tritan [10]. It is not suitable for screening [10], but the number of errors made can be used to grade a defect [84]. The test is carried out at 35 cm, and the subject has three seconds with each page [19].

As the CUT is for identifying moderate-severe defects, a single error is significant [117]. A study carried out by Birch in 1997 using subjects with red-green defects found that 98% of the dichromats failed the CUT; 26.7% of protanomalous, and 44.4% of deuteranomalous subjects failed the CUT [117]. When compared to the D15 the CUT is less sensitive to protan defects [10, 118]. The CUT is useful when used in conjunction with the Ishihara plates as it detects tritan defects and can be used to grade red-green defects [117]. When it comes to classification of red-green

defects the results vary from page-to-page [117]. The 3rd Edition of the CUT was published in 1998 [10]. It has additional pages designed for screening in which the subject is presented with a vertical line of three colour dots and has to identify the colour which is most different from the other two [10]. The 3rd edition has not been validated [106].

1.7.5 Lantern Tests

Although not used routinely in optometric practice, lantern tests are sometimes the occupational colour vision test of choice when it comes to the aviation, maritime, and railway industries [10, 83]. The first lantern test produced was the Edridge-Green Lantern in 1891 [10, 81]. They are used to determine whether a person has adequate colour discrimination to perform a task safely, and the lights used often represent signal lights [10]. Lantern tests involve naming the colour that is seen [10, 83]. The tests are often conducted in the dark, and a subject is presented with one or two lights at a distance (usually 6 m), and then asked to name them [10, 84]. Combinations of red, green, yellow, and white lights are used depending on which lantern test is employed [10, 83]. There are a number of lantern tests available, but the most common are described below.

1.7.5.1 Holmes-Wright Lantern

Developed in 1982, there are two variants: Type A which employs pairs of lights separated vertically, and Type B which shows pairs of lights separated horizontally [10]. The colours chosen are red, green, and white [10], which correspond to signal colours approved by the CIE [81]. Type A is used by the UK armed services, and the British Civil Aviation Authority [10, 119]. The test can be conducted in 'normal room illumination' (200 lux) or in the dark, at a distance of 6 m [10, 119]. After a demonstration of the colours (red, green, and white lights), the test consists of nine pairs of colours each shown three times for approximately 5 seconds [10]. Whereas the Type B is used by British Maritime and Coastguard Agency, and is only conducted on appeal [10]. The Type B test is performed in complete darkness after an adaptation period of 8 minutes [10].

1.7.5.2 Farnsworth Lantern

The Farnsworth lantern (FLANT) test was originally developed by Farnsworth for the US navy [83]; however, it is the test of choice for the US armed service, US coastguard, and Federal Aviation Authority [10]. The coloured lights employed by this test are red, yellow-green, and yellow-white [81]. These colours have chromaticity coordinates within the common Pseudoisochromatic zones for protan and deutan defects [81]. The test is conducted in a normally lit room at a distance of 8 ft, and the subject is shown 9 pairs of lights [10]. If any errors are made then the test is repeated a further two times, and the error scores averaged [10]. Passing the D15 is a poor predictor for passing the Farnsworth Lantern as the D15 is an easier test [83]. The Farnsworth Lantern is no longer available and has been replaced by the Optec 900 (Stereo Optical Company) [83].

1.8 Lamps

1.8.1 History of Lamps

As shown by Newton's experiment, sunlight is made of a mixture of different wavelengths [4, 5, 120], and as diurnal animals, our eyes have evolved to function under this illumination. However, in situations where there is no access to sunlight an artificial source needs to be found. For centuries this source was from a flame (e.g. candles, oil lamps, gas lamps), and then from the heating of different chemicals (e.g. quicklime, thorium) [6, 121]. The manipulation of electricity heralded a new age in artificial lighting. Early experiments involved creating an electrical arc between two closely placed carbon rods [6]. A number of scientists throughout the world were working on passing a current through a material to make it glow, but it was not until Swan and Edison in the late 19th century independently arrived at commercially viable solutions [6, 121]. Swan used carbon filament in his incandescent light bulb, although the modern equivalent uses tungsten [6]. The late 19th century was also when discharge tubes were invented. These were initially tubes filled with mercury vapour which glowed when an electric current was passed through it [6]. By the 1930's other gasses and vapours were being used in discharge lamps making them more practical [6, 121]. In 1907 Round noticed electroluminescence in the form of a yellow glow emitted from crystals of silicon carbide; however, it was not until 1962

and the observations of the gallium arsenide diode junction, did work on developing light-emitting diodes (LED) significantly increase [1, 121].

1.8.2 Black Bodies, Colour Temperature, and Correlated Colour Temperature

Electromagnetic waves are emitted by all bodies regardless of temperature above absolute zero [3]. Kirchhoff, in 1859, had shown that a 'perfectly black body' is one that absorbs all incident radiation such that none is reflected or absorbed, and subsequently a perfect black body makes the best radiator. The colour of a black body is dependant only on its temperature. As the temperature rises every wavelength emitted increases, with the shorter wavelengths increasing faster [4]. The result is that as a black body gets hotter, it gets brighter, and the colour becomes less red, through white, and more blue. Initially the body will look black as the wavelengths radiated are longer than the infrared part of the spectrum, and therefore not visible. The black body locus can be plotted in CIE colour space (see Figure 1.29). Wien, in 1963, showed that although all the wavelengths increase the peak wavelength λ_{max} (in metres) for a given temperature T (in Kelvin) is described by Wien's Displacement Law [2]:

$$\lambda_{max} \cdot T = \text{constant}$$

The constant in this case is 2.9×10^{-3} m.K (Wien's displacement constant) [4].



Figure 1.29 The black body locus plotted on CIE Colour Space (PAR, Public Domain).

To help further describe lamps and their function, it would be useful to introduce two terms at this stage: colour temperature (CT), and correlated colour temperature (CCT), both of are expressed in the unit Kelvin (K) [122].

The colour temperature of a light source is the temperature of a black body that best matches the light source's colour. As explained by Wien's Displacement Law (i.e. peak wavelength is inversely proportional to the temperature of a black body) and can be seen in Figure 1.29, the lower CTs are in the red area, and the higher CTs are in the blue area of CIE Colour Space. Metals such as tungsten approximate to the black body [6, 18], and so the colour of such a material changes in this fashion as the temperature increases (see Figure 1.30).



Figure 1.30 Radiation emitted from heated metals (such as tungsten) (Darth Kule, Public Domain)

When referring to a light source that is not incandescent, then the temperature of that source doesn't get as hot as the colour would indicate; in such a scenario CCT is used instead of CT. As these are not black bodies, they do not always sit on the black body locus, and are shown by the straight lines cutting across to the locus on Figure 1.29.

1.8.3 Incandescent Lamps

Incandescent lamps use the filament through which an electrical current is passed. As the filament heats up it starts to glow, and the spectrum emitted is continuous [2].

1.8.3.1 General Lighting Service Lamps

General Lighting Service lamps (GLS) use a tungsten filament, usually curled, through which an electric current is passed, causing the filament temperature to increase to approximately 2800 K [6]. As seen by Wien's Displacement Law, this leads to the peak wavelength being 1036 nm, which is in the infrared region (see Figure 1.1 and Figure 1.30). This is the reason why GLS lamps get hot. The tungsten filament is surrounded by a mixture of gases (argon and nitrogen) which prevents arcing across the filament, and reduces the rate at which the tungsten evaporates [6]. The outer glass envelope can be clear glass, etched to diffuse light, or coloured. With the clear envelope the colour of this lamp will be yellow (see Figure 1.29). GLS lamps are examples of Standard Illuminant A [18].

1.8.3.2 Tungsten-halogen Lamps

Tungsten-halogen lamps (THLs) use a quartz envelope rather than a glass one. This allows the lamp to be made smaller, run at a higher temperature (typically 2900-3450 K), and have a higher pressure of gas in the envelope [6]. The halogens added to the gas within the envelope combine with the evaporated tungsten to prevent it from depositing on the inner surface of the envelope, therefore allowing the tungsten to return to the filament [6]. Using Wien's Displacement Law again, it can be seen that the peak wavelength is 840-1000 nm. The peak is moving closer to the visible region of the electromagnetic spectrum (see Figure 1.1 and Figure 1.30). As can be seen on Figure 1.29, the colour of the THL is closer to white on the black body locus than a GLS lamp due to its higher CT.

1.8.4 Discharge Lamps

Discharge lamps consist of a glass tube filled with a gas through which an electrical current is passed [5, 6]. In 1913 Bohr combined the work of Balmer, Rutherford, Planck, and Einstein to describe the orbit of an electron around the proton of a hydrogen atom, and arrived at [3]:

$$E_i - E_f = h.f$$

Where E_i is the energy of the electron in its initial (the excited state), E_f is the energy of the electron in final state (the lower orbit), h is Planck's constant, and f is the frequency of the electromagnetic wave emitted.

When the electrons orbiting the atoms that constitute the gas are excited they occupy a higher level of orbit [3, 6]. This excitation is due to the collisions between electrons and ions [2]. When the electrons return to their normal orbit photons are emitted [5, 6]. The electrons can orbit only at specified levels and not in between [1, 3]. Optical line spectra are the specific frequencies (and wavelengths) that are emitted when causing the electron to jump down from a higher shell to a lower shell for a particular element [1]. Not all of the quanta are emitted as light; for a low level electron that has been elevated to a high shell and then dropped back down, the amount of energy released is greater and so according to Planck's quantum theory the frequency of electromagnetic radiation emitted is higher (and the wavelength shorter) which can be in the ultraviolet or even X-ray regions of the spectrum (see Figure 1.1) [1].

This means that the colour of light produced from a discharge tube depends on the frequencies (or wavelengths) that are emitted, which in turn is dependent on the gas in the tube [5]. Because the lamp does not behave like a black body, the colour is described in terms of CCT [6, 18]. Unlike the continuous spectra seen with incandescent sources, discharge lamps have discrete spectra [2].

Examples would include the noble gasses; neon, which appears red-orange and is used in signage, and xenon, which appears blue-grey, and is used in some car headlamps.

1.8.4.1 Fluorescent Lamps

Fluorescent lamps are discharge lamps using low pressure mercury [18]. They produce emissions at 254 nm and 185 nm, both of which are in the ultraviolet region of the electromagnetic spectrum. In order to convert this into light, the inner surface of the envelope is coated with phosphors. The phosphors absorb the ultraviolet radiation, and then emit longer wavelengths. The choice of phosphors determines the characteristics of the light emitted. White light can be created by the correct combination of narrowband tri-phosphors (red, green, and blue). Lamps with similar colours can have different SPDs due to the choice of phosphors employed [6, 18, 122]. Fluorescent lamps fall into a further two categories: hot cathode lamps, and cold cathode lamps. Hot cathode lamps establish an arc by preheating the electrodes, whereas cold cathode lamps use a higher voltage [6].

1.8.4.2 Mercury Vapour Lamps

Mercury vapour lamps use high pressure mercury in an inner envelope and nitrogen, with or without argon, in an outer envelope. The outer glass envelope has a phosphor coating and filters out the ultraviolet radiation. The phosphor coating helps 'correct' the colour of the lamp from a blue/green bias to white. Mercury blended lamps contain a tungsten filament, which due to its lower CT, adds 'warmth' to the colour of the lamp [6].

1.8.4.3 Metal Halide Lamps

Metal halide lamps are discharge lamps where different metals halides (metals combined with either bromine or iodine) are added to mercury vapour to change the colour output. Examples include dysprosium (broadband blue-green), indium (narrowband blue), lithium (narrowband red), scandium (broadband blue-green), sodium (narrowband yellow), thallium (narrowband green), and tin (broadband orange-red) [6].

1.8.4.4 Sodium Vapour Lamps

Low pressure sodium lamps have an output wavelength of 589 nm, and thus produces monochromatic yellow light [6]. As this is very close to the peak sensitivity of the human eye (555 nm) the lamp has a very high efficacy (lumens per watt), and due to it being monochromatic, the light does not disperse when travelling through different media [6]. For this reason they are often seen lighting large sections of the motorway network. The downside of monochromatic light is that colour rendering is impossible.

High pressure sodium lamps emit a broader band in the yellow region of the spectrum, although this reduces the efficacy of the lamp, it increases its colour rendering properties [6].

1.8.5 Light-Emitting Diodes

Light-Emitting Diodes (LEDs) utilise the properties of p-n junctions; the p-type material is full of 'holes', and the n-type material is full of electrons. When an electron fills a hole a quantum of electromagnetic energy is released. For the semi-conductor gallium arsenide the part of the electromagnetic spectrum emitted is light. LEDs can be described as solar cells that operate in reverse.

Early LEDs emitted yellow light through to infrared radiation, the problem lay in designing an LED that would emit blue light. The blue LEDs made before the 1990s had a relatively short life, and low output efficiency. A significant improvement in blue LED technology was achieved by Nichia Chemical Industries in the mid-1990s using gallium nitride [121].

The development of a blue LED was particularly important in the production of 'white' LEDs. There are two ways in which this can be achieved. Firstly, blue LEDs can be phosphor coated to produce white light in a similar to way employed by fluorescent lamps. The second method is to use an array of coloured LEDs in such a way that the addition of light results in white light. This mixture is usually achieved using red + green + blue, but can also be achieved with red + green + blue + yellow [21, 121, 123, 124].

LEDs have a number of advantages over the sources described above: they have a very high luminous efficacy, produce very little heat, are robust (unlike the filaments), are quoted by manufacturers as having an extensive lamp life (~50,000 hours compared to 1000-2000 hours for a GLS lamp), they operate at extra-low voltages (<50 V), they are compact, and they have instantaneous full luminous output (unlike discharge lamps which need to 'warm up') with superb re-strike characteristics [121]. However, LEDs have narrow bandwidths, 20-50 nm, SPDs which can be almost monochromatic [121], and this can lead to difficulties when colour rendering especially when cluster LED are used to produce white light [124]. Also, due to extra-low voltage operation, a driver is required to make LEDs suitable for mains (230 V) voltage.

1.8.6 Sources of Illumination for Colour Discrimination

Where illumination can be controlled there are recommendations for enabling good colour discrimination. Shoppers can often be seen taking their prospective purchases to a window to better judge the colours in hand. Therefore, as colour perception is influenced by the source of illumination, then choosing the correct illumination for colour vision testing is paramount.

When it comes to the testing of colour vision in the optometric and medical professions, the illumination recommended is Standard Illuminant C [18, 125]. Standard Illuminant C has a CCT (correlated colour temperature) of 6774 K [126]. This is the illumination source recommended for the PIC plates such as the Ishihara test and HRR plates, as well as for arrangement tests such as the FM100 and D15 [10, 45, 111]. However, the Ishihara seems to fair well under incorrect sources of illumination [127]. Farnsworth recommended an illuminance of 25 foot candles (270 lux) or greater for the FM100 [111]. Mantyajarvi used illumination of 1000 lux for the FM100, although some studies use an illumination between 1000 and 1500 lux [128], and Hardy et al used an illumination source of 1700 lux for their study on the FM100 [114].

Standard Illuminant C is no longer in general use and so Standard Illuminant D₆₅ (CCT of 6500 K) has also been recommended for colour vision testing [18, 45, 125]. Standard Illuminant D₆₅ is the equivalent of daylight on a cloudy day, also referred to as *north sky* [18, 125] when the clouds are high in the sky [129]. Farnsworth, for the

FM100, recommended north sky, lightly-moderately overcast [111]. Daylight through a window can vary depending of the time of day, weather conditions, and the season [10]. In addition to the daylight variation, the testing area may not have a window, or the tests may be conducted after sunset; therefore an artificial source needs to be available. Historically the MacBeth easel lamp has been the lamp of choice despite its CCT being a little high (6800-7500 K) relative to Standard Illuminant D₆₅ [124, 125, 129]. Unfortunately the MacBeth easel lamp has been discontinued and so an alternative needs to be found [10].

A number of studies have looked at alternatives to the MacBeth easel lamp [6] using fluorescent tubes and LEDs; however, these studies published their results on short arrangement tests and PIC plates instead of the more sensitive and precise FM100 which allows scores to be graded [130].

Using illuminant A, which has a colour temperature (CT) of 2800-2900 K [130-132] e.g. GLS lamps, can cause deuteranomalous subjects to make fewer errors, and for protanomalous subjects to show a rotation in their axis of confusion on the FM100 [133]. However, a GLS lamp can be made to replicate illuminant C when used in conjunction with a pair of Kodak Wratten filters (types 78B and 80B) [6, 131]. The lighting within optometric practices is in the main part provided by THLs and compact fluorescent lamps (CFLs) [126, 133]. Each has its advantages: THLs provide a warm and welcoming colour with a CT of around 2900-3450 K [45, 127], but will not be ideal for colour vision testing, whereas CFLs can be made to produce a much higher CCT (depending on the phosphors used they can be 6500 K). However, CFLs require approximately 10 minutes to reach a steady lumen output and colour temperature [6]. These problems may be solved by using LEDs which are now readily available for domestic lighting.

It should be remembered that lamps with identical CCTs may exhibit different spectral properties. The colour rendering index (CRI) grades how the illumination source distorts colours. A CRI of 100, e.g. from Artificial Daylight, is excellent at colour reproduction, whereas a CRI of less than 50 is very poor e.g. some sodium lamps [10]. Lamps used for colour vision testing need to have a CRI >90 [10]. The CRI was first introduced by CIE in 1965, with a revision made in 1974, and the final version published in 1995 [21]. The CRI is calculated using differences in reflected light off test samples using a reference illuminant, with that reflected by the illuminant under investigation [21]. There are a number of shortcomings to the CRI relating to

the visual non-uniformity in the red region, and the chromatic adaption transforms used, which results in some believing that the CRI is outdated. However, the CRI is still used by the lighting industry [21, 122, 123]. An example of this oddity is that an incandescent source, which often has a CT under 3000 K, can have a very high CRI, and yet not be recommended for colour vision testing [122].

1.9 Smoking

It is well documented that smoking can be harmful to the human body: it can lead to stroke, eye disease, cancers (mouth, throat, oesophagus, larynx, lung, pancreas, bladder, cervix), coronary heart disease, chronic obstructive pulmonary disease, ulcers, peripheral artery disease, and low birth-weight babies (summarised in Table 1.8) [134-144].

Smoking		Secondhand Smoke Exposure	
Cancers	Chronic Disease	Children	Adults
Oropharynx	Stroke	Middle ear disease	Nasal irritation
Larynx	Blindness	Respiratory symptoms	Lung cancer
Oesophagus	Cataract	Impaired lung function	Coronary heart disease
Trachea	Periodontitis	Lower respiratory illness	Reproductive effects in women: low birth weight
Bronchus	Aortic aneurysm	Sudden infant death syndrome	
Lungs	Coronary heart disease		
Acute myeloid leukaemia	Pneumonia		
Stomach	Atherosclerotic peripheral disease		
Pancreas	Pulmonary disease		
Kidney	Hip fractures		
Ureter	Reproductive effect in women		
Cervix			
Bladder			

Table 1.8 Summary of health consequences associated with smoking and secondhand smoke exposure [143]

According to a government white paper produced in 1996 on the effects of smoking tobacco, there are over 12,000 smoking related deaths per year [135, 136]. The rate of smoking in the UK peaked in the 1950s and 1960s, and although there was a downward trend, the number of smokers increased in 1996 to 13 million people (equating to 28% of over 16 year olds in England, 32% in Wales, 32% in Scotland, and 29% in Northern Ireland) [135, 136]. Smoking has been found to be highly addictive; and 82% of smokers take up the habit in their teenage years with many smoking throughout their rest of their lives [135]. A later inquiry in 2010 on 'smoking and health' by the All Party Parliamentary Group estimated nearly 9 million smokers in England alone [134]. The prevalence of cigarette smoking in Great Britain had declined from 55% in 1974 to just over 20% in 2010 [134]. They reported over 80,000 deaths from smoking, and possibly up to 10,000 deaths from secondhand smoke [134]. It was estimated in 2004 that 603,000 deaths worldwide were due to secondhand smoke [145]. In the U.S. there are an estimated 443,000 deaths each year due to cigarette-smoking [143].

Cigarette smoke contains in excess of 7,000 chemicals, of which 69 are known to be carcinogens [143]. One of the reasons for why smoking causes damage to tissues is due to the production of free-radicals [138, 143]. Free-radicals are unstable and react with the nearest substance that will stabilise them, which can cause damage to that tissue [138]. Although the cigarette filter can absorb up to 99.9% of the particulate matter greater than 0.1 μm , free-radicals can pass through it [138]. The free-radicals can be formed in three main ways: combustion (burning of the cigarette), the tar in the cigarette, and the oxidation of nitrous oxide to the more reactive nitrous dioxide [138].

The relationship between smoking and cardiovascular disease has been shown to be non-linear [143, 146]. The relationship is linear between 10-15 cigarettes per day, and plateaus after 20 cigarettes per day [146]. The proposed mechanism involves increased plasma fibrinogen, reduced high-density lipoprotein cholesterol, increased carboxyhaemoglobin, and increased platelet stickiness and aggregation [143, 146]. This leads to endothelial damage to the arteries, increased risk of thrombosis, arterogenic chronic inflammation, and atherogenic lipid profile [143].

A report produced by Action on Smoking and Health regarded smoking as the most important preventable risk factor for peripheral arterial disease (PAD) [141]. They

reported that smoking doubles the risk of developing PAD [141]. PAD results in a reduced blood flow to the organ or tissue supplied by the affected artery [141]. PAD secondary to smoking occurs due to three main factors. Firstly, smoking can cause an abnormal vasodilator response in the arteries due to the release of adrenaline and noradrenaline, caused by the absorption of inhaled nicotine, which causes blood vessels to constrict [141]. Secondly, the carbon monoxide has a greater affinity than oxygen to haemoglobin, resulting in carboxyhaemoglobin instead of oxyhaemoglobin [141, 147]. In non-smokers <2% of their haemoglobin is bound to carbon monoxide, however, this proportion can be as high as 15% in smokers [147]. Thirdly, tobacco leads to atherosclerosis. The endothelial cells on blood vessel walls are directly damaged by chemicals in tobacco which enhances the transfer of low density lipoproteins across arterial walls [141].

As cigarette smoke is inhaled into the lungs, the link between smoking and non-malignant pulmonary disease is easily hypothesised. About 60% of the particles inhaled when smoking passed through the upper respiratory pathway and are deposited in the lungs [143]. Smoking has been linked with chronic obstructive pulmonary disease, emphysema, chronic bronchitis, and asthma [143].

There are three common ways in which smoking can cause cancer via a loss of normal growth control mechanisms. Firstly, the uptake of carcinogens can bind to the receptors activating protein kinase A and B. Secondly, the carcinogens can activate DNA adducts which result in miscoding mutations in oncogenes and tumour suppressor genes. Thirdly, the uptake of carcinogens and tumour promoters can result in tumour suppressor gene inactivation. Smoking has been shown to cause cancers of the lungs, oral cavity, pharynx, larynx oesophagus kidney, liver, uterine cervix, stomach, bladder, pancreas, nasal cavity and paranasal sinuses. It was estimated that smoking was the cause of 405,112 cancer deaths in China in 2005 [143, 144].

1.9.1 Ocular Pathology Secondary to Smoking

When considering ocular pathology, the role of smoking in the development of age-related macular degeneration (ARMD) was first considered in 1978. However, it has been over the past 25 years that the area has been more thoroughly explored [136]. There are two types of ARMD: dry, and wet [23, 25].

Dry ARMD, also known as atrophic ARMD, accounts for 80-90% of diagnosed ARMDs, and is characterised by drusen in the macula (seen as yellow deposits), and areas of RPE atrophy [23, 25, 90]. The condition is progressive, and there is currently no treatment available to reverse the damage caused [23, 25, 90]. The damage to the RPE is caused in part by oxidative stress, i.e. the production of highly reactive oxygen species that react with the RPE [23, 25]. As the RPE is critical to maintaining the health of the photoreceptors, damage to the RPE results in photoreceptor degeneration [25].

Wet ARMD, also known as exudative ARMD, accounts for 10-15% of diagnosed ARMDs [23, 25]. It is characterised by the presence of a choroidal neovascularisation (CNV) due to the increased production of vaso-endothelial growth factors (VEGF) in the choroid [23, 25]. The production of VEGF by the RPE has a protective function on the RPE, Müller cells, and neuronal cells of the retina [25]. However, one possible cause of CNV is the combination of damage to Bruch's membrane (the basement membrane for the RPE [29]) and an elevation in the production of VEGF [25]. Bruch's Membrane gets thicker with age due to structural changes and the accumulation of waste materials (drusen) [23]. One of the causes of the increased production of VEGF is the oxidative damage to the RPE [25].

A statistical analysis of smoking and ARMD has shown a link between smoking and both dry ARMD and wet ARMD, and that current smokers are more likely to develop ARMD compared to ex-smokers [136, 137, 148]. The mechanism for this link may be due to the increased free-radicals (which increase lipid peroxidation and oxidative damage), a reduction in choroidal blood flow, (which increases hypoxia, ischaemia, and microinfarctions), and decrease in macular pigment [136, 148].

Other eye related consequences of smoking include formation of cataracts, raised intraocular pressure, optic neuropathies (such as tobacco amblyopia, and non-arteritic anterior ischaemic optic neuropathy), retinal vasculopathy (such as emboli, thromboses, resulting in vascular occlusions), and Graves ophthalmopathy (thyroid eye disease) [136, 142, 149, 150].

1.9.2 Colour Vision and Smoking

As smoking can result in macular disease, cataract, and optic nerve disease [136, 137, 140, 148], it has the potential to cause colour vision defects [10, 87]. Studies investigating smoking and colour vision have used the Roth 28-Hue desaturated arrangement test, and the desaturated D15 test, which are short arrangement tests [149, 150]. Using the Roth 28-Hue Erb et al found that those subjects who smoked more than 20 cigarettes per day had significantly higher error scores, without any significant axis of confusion [149]. Whereas Bimler and Kirkland using the D15 and desaturated D15 found a red-green defect amongst smokers [150]. This would suggest that smokers have reduced colour vision; however, the axis of the defect is not certain.

Erb et al speculated the cause of reduced colour vision could be due to the toxic effect of smoking on the RPE [149]. As stated in section 1.3.1, the RPE is responsible for maintaining the photoreceptor outer segments, regulating nutrient/waste product flow, and forms an integral part of the blood-retina barrier [23, 24], therefore as toxins are accumulated in the blood they may affect all three cone types, resulting a general increase in error scores. Erb et al noted the reduction in retina's electrophysiological function as a potential sign of retinal toxicity. They hypothesised that other causes for increased error scores may relate to the vascular abnormalities such as reduced retinal blood flow, especially as smokers have been found to have decreased blood fluidity (a measure of blood viscosity and the state of the blood cells). The resulting vascular changes and increased carboxyhaemoglobin could lead to hypoxic changes [149, 151].

Bimler and Krikland found a significant reduction in sensitivity along the red-green axis [150]. They hypothesised that if this were due to photoreceptor damage, then it should be along the blue-yellow axis as the S-cone was more fragile. There are fewer S-cones in the retina [40], and thus damage to them could impair their function before the more plentiful M- and L- cones. Subsequently the conclusion they reached was that smoking caused damage to the optic nerve. They were unsure to whether the effects seen were acute or chronic in nature. Bimler and Krikland suggested that the damage to the optic nerve, resulted in a red-green defect [150].

1.10 Aims of the Study

Many optometry practices are situated within shopping centres, and clinic times are after sunset, and therefore reliance on natural light, or *north sky*, for colour vision testing is not always possible. Thus an artificial source needs to be found which is easy to install, and economically viable for an optometric practice not specialising in colour vision testing. A lamp costing hundreds of pounds may not be a practical for a practice to fit in every consulting room. Unfortunately as the MacBeth Easel Lamp has been discontinued, optometrists face a dilemma in finding an alternative. With the array of 'daylight lamps' available, an optometrist needs guidance on which lamp to choose, especially as CRI may not be a reliable indicator for performance. Colour discrimination can be very important to patients who have hobbies such as painting, craftwork, model-making, and optometrists are often asked to give advice to patients on lighting within the home. The first part of this study looks to find an economically viable alternative to the MacBeth Easel lamp, which can be used for both colour vision testing, and for other tasks requiring good colour discrimination.

Previous studies have explored the effects of smoking on colour vision using the less sensitive D15 and Roth 28-Hue tests. The second part of this study aims to compare subjects who smoke with subjects who don't smoke to explore the effects of smoking on colour discrimination using the FM100 with illumination from the 'daylight lamps' used in the first part of the study.

When advising patients on lighting to be used around the home it may be important to take into account the colour discrimination abilities of the other householders. The third part of the study aims to explore the colour discrimination of subjects with CCVDs using the 'daylight lamps' being assessed above.

2. RESEARCH OBJECTIVES

2.1 Part 1 Normal/Control Subjects

Previous studies have looked at the use of Daylight simulators on colour vision; however, they have either used fluorescent tubes only, or have used the less sensitive D15 test rather than the more detailed FM100 [125]. Due to the issues with availability of the MacBeth easel lamp, a cost-effective alternative needs to be found that can be easily applied to everyday clinical practice. A budget of £10 per lamp would not be prohibitive to either optometric practices or patients. The first part of this study compares two available 'daylight' lamps with the type of lighting that can be readily found in optometric practices, shops, and homes: tungsten-halogen. Specific aims were:

- 2.1.1. Can a cheap and readily available daylight source be found for colour vision testing?
- 2.1.2. Do any of these illumination sources perform differently with respect to the areas of the spectrum where errors are made?

Hypotheses:

- All the lamps chosen will cost less than £10, making them all economically viable.
- As all the lamps chosen will have good colour rendering indices, the expected TESs should be within the normal range.
- As THLs have a lower CT there will be greater reflectance from the red area of the spectrum thus affecting the isoluminant nature of the FM100. The result will be reduced sensitivity in the red area, and potentially at the blue area if the CT is too low.
- A CFL should perform well across the whole range.
- There is some uncertainty of the performance of the LED, however, due to the increased output in the blue part of the spectrum, there may be an increase in errors in the yellow-blue part of the FM100.

2.2 Part 2 Smoker/Test Subjects

Smoking has been shown to be toxic to the eye, and some of the related ocular conditions can produce colour vision defects [10]. However, the previous studies investigating this used short arrangement test such as D15 and Roth 28 (and their desaturated variants) as opposed to the more detailed FM100 [149, 150]. The aims of this part of the research were:

2.2.1. Does smoking affect colour vision?

2.2.2. Is the colour vision of smokers affected in the same way as non-smokers under different sources of illumination?

2.2.3. Do smokers have higher errors in certain parts of the spectrum compared to non-smokers?

Hypotheses:

- As previous studies have shown some deterioration in colour discrimination in subjects that have smoked, there is expected to be an increase in TES in the Smoker/Test group.
- The Smoker/Test group is likely to be affected in the same way as the Normal/Control under each of the lamps.
- Due to the retinal toxicity that caused by cigarette smoking, and the increased detriment to the S-cone during retinal damage, a tritan-type defect would be expected before a red-green defect. This may result in the slightly lower TESs with the LED due to its increased blue output.

2.3 Part 3 Case Study Subjects

The most common CCVD is deuteranomalous trichromacy; it affects 5% of the males [10, 19, 45, 152]. Therefore, there is a high likelihood that an optometrist would be asked to give advice on lighting to a patient who is a deuteranomalous trichromat. The aims of this part of the research were:

2.3.1. How do deuteranomalous trichromats compare with normal trichromats under each light source?

2.3.2. Is there light source recommended for deuteranomalous trichromats to use?

Hypotheses:

- The greater output of the THL at longer wavelengths is likely to cause an increase in TESs, and more specifically at the red-yellow part of the FM100.
- The CFL and LED should produce similar TES.

3. METHODS

Ethical approval for research was granted by Aston University.

3.1 Materials

The study involved the exploration of colour vision under three different sources of illumination. The requirements for the illumination sources were:

1. They needed to have good colour rendering properties in terms of a high colour rendering index and are capable of meeting the illuminance levels required of colour vision testing
2. They needed to be easily available.
3. They needed to be inexpensive.
4. They needed to be easily maintained.

The reason for such criteria was for the acquisition of meaningful data from the study, and also to provide an option for the illumination source for colour vision testing which would be practical for optometric practices and hospital departments to use.

3.1.1 The Lamps

The three lamps chosen were all under £10 per lamp. They were all MR16s with GU10 cap. The GU10 has an inbuilt transformer which allows the lamp to take mains voltage. The alternative is an MR16 with a GU5.3 cap; however, an additional step-down transformer would need to be used.

Lamp A

The first lamp chosen (A) was the *EcoHalo Twist* (Philips Lighting, Guilford, UK) (see Figure 3.1). This is a tungsten halogen lamp (THL) with a colour temperature (CT) of 2800 K (warm white) but a colour rendering index (CRI) of 100. This is the sort of lamp that would be found in shops and homes. This lamp was chosen to provide a link to the '*real world*' as this is the type of illumination a subject would experience at home or when examining items in a shop. With such a high CRI one would expect error scores to be low in individuals with normal colour perception.



Figure 3.1 Lamp A (THL) (K. Mistry)

As seen by the spectral power distribution (SPD) for the THL (Figure 3.2) the output of the lamp is lowest at the shorter wavelengths (violet end of the spectrum), and shows a steady increase as the wavelength increases, and is greatest in the red (and infrared) part of the spectrum. Due to this SPD, the light was a 'warmer' appearance than Standard Illuminant D_{65} , and therefore a CT of only 2800 K. Due to the large difference in the output in the longer wavelengths, the expected colour discrimination difficulties were expected in the red and orange colours.

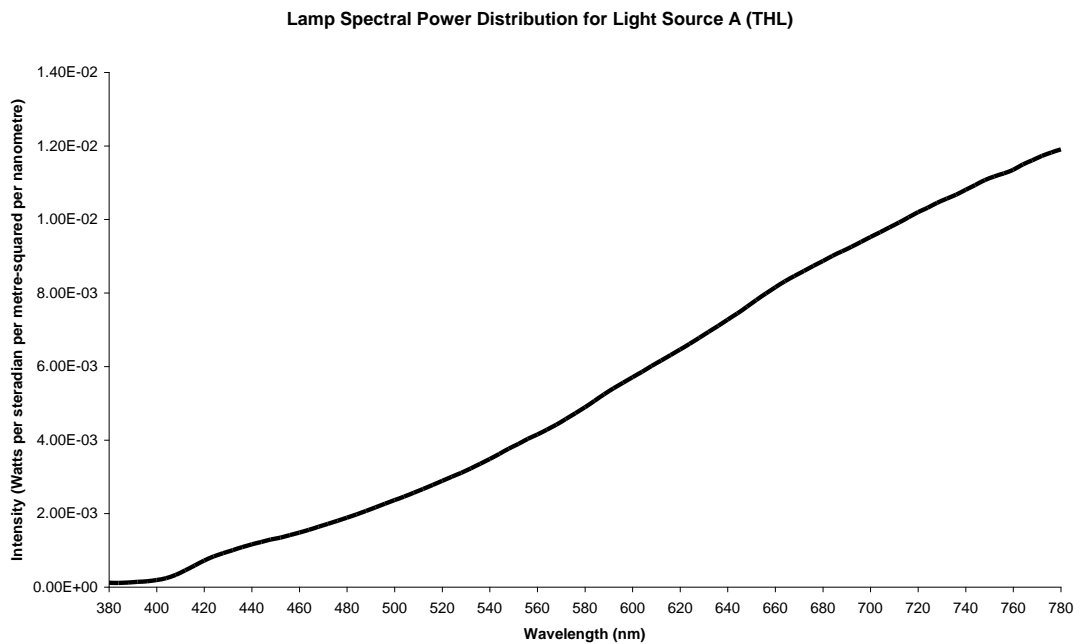


Figure 3.2 Spectral power distribution for the THL (K. Mistry).

Lamp B

The second lamp chosen (B) was the *KCF07ALU/GU10-865* (Kosnic UK Ltd, Newbury, UK) which is a daylight compact fluorescent lamp (CFL) (see Figure 3.3). It has a correlated colour temperature (CCT) of 6500 K and a CRI specified by the manufacturer as >80.



Figure 3.3 Lamp B (CFL) (K. Mistry).

The SPD of the lamp (see Figure 3.4) shows a series of peaks coinciding with the phosphors. The largest peak occurs at 544 nm (green), there are two slightly smaller peaks at 612 nm (orange) and 436 nm (violet), and two peaks which are smaller still at 488 nm (blue) and 580 nm (yellow). The additive nature of coloured lights gives the appearance of a 'cool' white light in a similar way to Newton's third experiment [120].

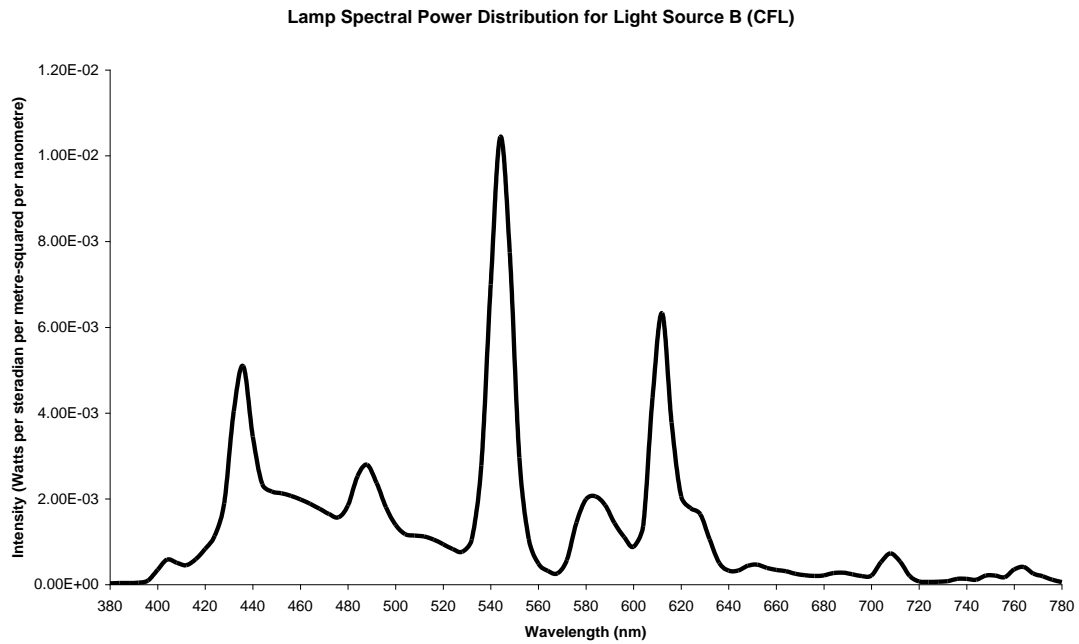


Figure 3.4 Spectral power distribution for the CFL (K. Mistry).

Lamp C

The third lamp chosen (C) was the *GU103X2WA4B-60* (*Deal Guardian Ltd, Innishannon, Ireland*), a light-emitting diode (LED) (see Figure 3.5). It has a CCT of 6500 K, which is the same as the daylight CCT, but no quoted CRI.



Figure 3.5 Lamp C (LED) (K. Mistry).

Although having a similar colour (cool white) and CCT as the CFL, the LED has a very different SPD (see Figure 3.6). The SPD shows a substantial peak at 448 nm (violet), but is followed by a substantial trough at 484 nm (blue), and then a much smoother curve than the CFL, that has gentle rise up to 548 nm (green) after which is gradually decreases. There is an expected reduction in colour discrimination for the violet and purple colours. The differences between the SPDs of the CFL and LED re-enforces that not all white lights are the same.

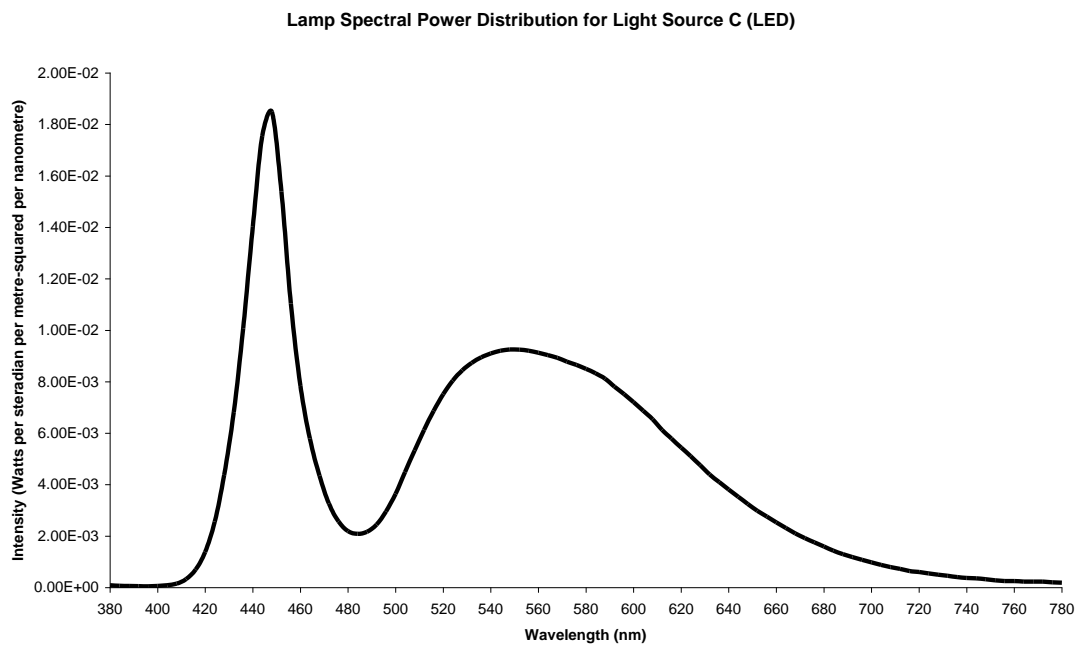


Figure 3.6 Spectral power distribution for the LED (K. Mistry).

3.1.2 Examination Box

An examination box was created in two parts. The first part housed the illumination sources (see Figure 3.7). Its outer dimensions were 0.64 m x 0.19 m x 0.41 m (width x height x depth). In order to get a sufficient spread of light two THLs, three CFLs, and two LEDs were used.

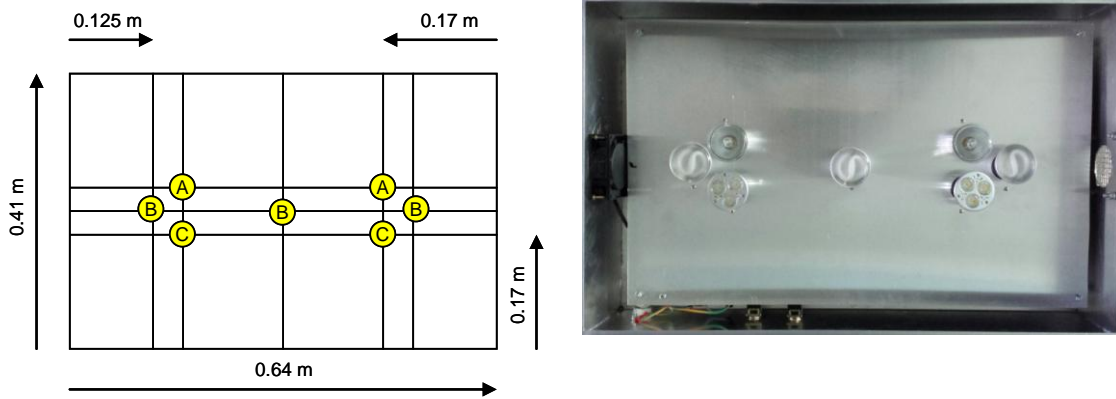


Figure 3.7 The layout of the lamps (K. Mistry).

Using Cartesian x-y notation with the origin being the bottom-left corner of the box, then A (0.17, 0.24) and (0.47, 0.24); B (0.125, 0.205), (0.320, 0.205), and (0.515, 0.205); and C (0.17, 0.17) and (0.47, 0.17): where A is the THL, B is the CFL, and C is the LED. The circuit diagram for the illumination system can be seen in Figure 3.8.

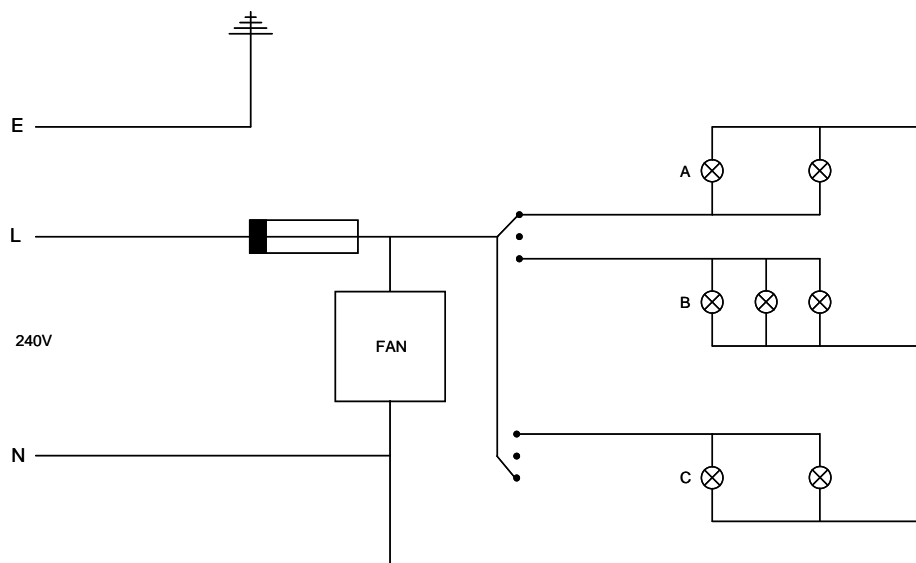


Figure 3.8 Circuit diagram for the for the illumination system (K. Mistry).

The second part of the examination box consisted of three walls and a base. All the inner surfaces were painted mat black. The dimensions were 0.64 m x 0.33 m x 0.41 m on the outside, 0.59 m x 0.31 m x 0.39 m on the inside.

The first part sat on top of the second part such that the illumination sources were placed 0.35 m from the testing surface and the lamps recessed ensuring that the subjects were unaware to which lamps are in operation. The complete examination box can be seen in Figure 3.9.



Figure 3.9 The Complete examination box (K. Mistry).

3.1.3 Illumination Outputs of the Lamps

The requirement for the Farnsworth Munsell 100 Hue Test (FM100) stated by Farnsworth is 25 foot candles (270 lux) or greater, however it was also important to have an even spread of light. Some authors suggest 600 lux is required for the testing of colour vision [84], whereas others have used illumination up to 1700 lux [114, 128].

With the lamps fitted, the illuminance spread at the examination surface can be seen in Figure 3.10. The maximum difference in log units for the illumination across the three sources was 0.71 Lux.

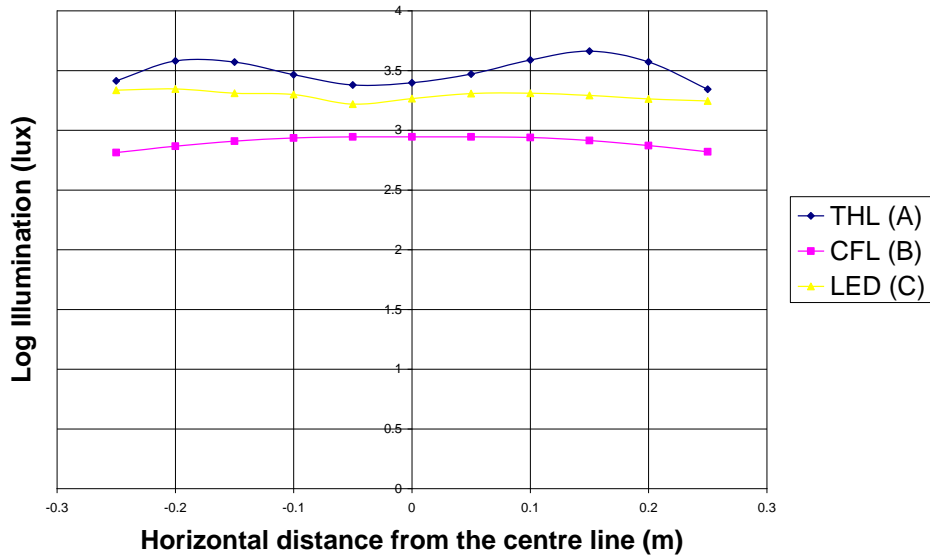


Figure 3.10 The illumination from the each light source across the testing surface.

Screening was conducted using a 38-plate Ishihara PIC test, which has been shown to be a test that is robust [127], and is considered as the ‘gold standard’ for rapid identification of red-green CCVD [83].

3.2 Subjects

Due to the variation in FM100 error scores with age, subjects chosen were aged between 20 and 39 years old [113]. Subjects were recruited from patients seen in optometric practice, as well as colleagues within the hospital. As the testing equipment was portable, the tests were conducted at a location convenient for the subject. A number of subjects attended clinical environments (Milton Keynes General Hospital, Lesley Arkin Optometrists, and Heron Opticians). Those that were not able to attend one of these locations participated at their own residences. Consent was attained from each subject before the collection of any data. There were no expenses or payments for participation in the study.

Previous studies using FM100 have yielded significant variation in TESs amongst the normal population; for example Dain et al in their study on TES with iris colour and pupil size had mean TES of 20.0-28.4, whereas Zahiruddin et al had a mean TES of 76.17 in their study on booth illumination [7, 153]. Therefore determining a size of effect needs to factor in the variation in TES. Using Cohen’s definitions of effect size

for t-test d (0.8 = large, 0.5 = medium, and 0.2 = small), the results from the Dain et al and Zahirudin et al, and the equations below, the large, medium, and small effect sizes were calculated:

$$d = \frac{x_{\square_1} - x_{\square_2}}{S}$$

Where d is the effect size, x_{\square_1} is the mean of the first group, x_{\square_2} is the mean of the mean of the second group, and S is the combined standard deviation [154].

To calculate S the following equation needs to be employed:

$$S^2 = \frac{(n_1 - 1)S_1^2 + (n_2 - 1)S_2^2}{n_1 + n_2}$$

Where n_1 is the number of subjects in first study, n_2 is the number of subjects in second study, S_1 is the standard deviation in the first study, and S_2 is the standard deviation in the second study [154].

Thus for the TESs in the Normal/Control group a large effect size is 32.1, a medium effect size is 20.1, and a small effect size is 8.0.

Using G Power 3.1.7 to calculate the sample size for a large effect and statistical power of 0.8, the number of subjects required was 12 for a dependant or paired t-test (13 if using the non-parametric Wilcoxon signed-rank test) and was for an independent or two-sample t-test 21 (22 if using the non-parametric Mann-Witney test) [155, 156].

Excluded from the study were subjects that smoked and failed the Ishihara PIC test, as determining the effect of smoking of colour vision beyond their CCVD would not be possible within the design of this study. Also excluded were subjects that had any ocular pathology, or were taking medications which had a known effect on colour vision. No vulnerable adults or visually impaired subjects were recruited. Any potential subjects not between the ages of 20 and 39 years old were also excluded due to significant variation in error scores outside of this age range [113].

Subjects were advised to wear their spectacle corrections. Tinted lenses were not allowed as they may alter colour perception. All tests were conducted binocularly to create the environment that the subject was likely to encounter in their day-to-day lives, and to minimise the burden on the subjects.

3.3 Procedure

Each subject was given a consent form to read and sign before the study started. Once they were happy to proceed, a quick ocular and medical history was taken from the subject (which included a list of medications, and a smoking history where relevant). Screening was conducted using a *1988 38-plate edition Ishihara PIC test (H. K. Lewis & Co. Ltd, London)*. Due to the robustness of the test [127], it was conducted at a distance of 60-75 cm, under natural daylight where possible, and normal room lighting using THLs when daylight was not accessible. Each subject identified the demonstration plate, the transformation plates, the vanishing plates, the hidden plates, and the classification plates (plates 1-25). Any subject with more than 4 errors was classified as having defective colour vision. Where the results of the Ishihara PIC test were inconclusive the diagnosis was refined using the City University Test (2nd Edition). The subjects were categorised into one of three groups:

1. Non-smoking subjects who passed the Ishihara PIC test (Normal/Control Group).
2. Smoking subjects who passed the Ishihara PIC test (Smoker/Test Group).
3. Non-smoking subjects who failed the Ishihara PIC test (Defective/Case study).

In order to minimise the effect from learning, and to remove any bias resulting from the order in which lamps were used, a set of six protocols were devised (see Table 3.1). Each protocol consisted of four FM100 tests such that each light source was tested once, and then the first lamp used was repeated and averaged. The tests were conducted binocularly due to the demands of the test. The tests were conducted over two sessions within the space of eight weeks.

Protocol	Visit 1	Visit 2
1	A, B	C, A
2	B, C	A, B
3	C, A	B, C
4	C, B	A, C
5	B, A	C, B
6	A, C	B, A

Table 3.1 The Protocols: A = THL, B = CFL, C = LED

The FM100 was conducted as instructed in the “The Farnsworth-Munsell 100- Hue Test for the Examination of Color Discrimination Manual”[111]. The subject was sat at the examination box, the room curtains or blinds drawn, and the room lights were extinguished. Thus the only source of illumination in the room was the test illumination in the examination box. This was to ensure that there was no ambient lighting influencing the test conditions. Whilst showing the first box to the subject (caps 85-21) the following instructions for the FM100 were explained to the subject:

“As you can see the colours of the caps vary in between the two fixed caps. The object of the test is to arrange the caps in order according to colour. You can arrange them outside of the box first and then place them in, or place them directly into the box. Do not turn the caps over. There is no time limit for the test. If you have any questions please feel free to ask.”

Once the subject was happy with the arrangement in a box it was swapped for the next box until all four boxes had been completed. The order of the caps in each box were written down and later inputted into a spreadsheet to calculate error scores using the Farnsworth method. On completion, the light source was switched, and the subject given a minimum of ten minutes before repeating the test (under the new light source). This was done to give the subject a break (thus minimising fatigue), to enable the subjects adapted to the change in light source, and to allow the lamps to reach a steady operating output (critical for CFL). The subject was not informed of which light source was which until completion of all four FM100 (all four boxes under four light sources – see Table 3.1).

4. RESULTS

The data was analysed using SPSS version 21.

4.1 Subjects

A total of 42 subjects were seen. 36 passed the Ishihara PIC test, and were subdivided into 18 non-smokers (Normal/Control), and 18 smokers (Smoker/Test). None of the subjects were taking medications which were known to cause colour vision defects. Of the subjects that passed the screening test there were 17 males and 19 females; with a mean age of 27.9 ± 4.4 years. The Normal group consisted of 5 males and 13 females, with a mean age of 26.8 ± 4.1 years; whereas the Smoker group had 12 males and 6 females, with a mean age of 29.1 ± 4.4 years. There was no significant difference between the ages of the subjects in the two groups ($p = 0.133$).

Pack years were calculated by multiplying the number of cigarettes smoked per day by the years the subject has been smoking, and then dividing that by 20 (i.e. the number of cigarettes in a pack). For the groups that smoked, the mean pack years was 7.9 ± 4.7 years.

The details are summarised in Table 4.1.

		Normal	Smoker	Total
Gender	Male	5	12	17
	Female	13	6	19
	Total	18	18	36
Age (years)	Mean \pm SD	26.8 \pm 4.3	29.1 \pm 4.4	27.9 \pm 4.4
	Min	20	21	20
	Max	34	37	37
Pack Years	Mean \pm SD	0	7.9 \pm 4.7	3.9 \pm 5.2
	Min	0	1.25	0
	Max	0	22	22

Table 4.1 The distribution of subjects that passed the screening test

Six subjects failed the Ishihara test and were classified as having defective colour vision, and entered the 'Case Study' group. In this group there were five males and one female; and the mean age was 31.7 ± 5.2 years old (see Table 4.2). All the subjects in this group were diagnosed as being deuteranomalous trichromats.

		Defective
Gender	Male	5
	Female	1
	Total	6
Age (years)	Mean \pm SD	31.7 ± 5.2
	Min	22
	Max	36

Table 4.2 The distribution of subjects that failed the screening test

4.2 Total Error Scores

4.2.1 Normal/Control Subjects

The 18 subjects who did not smoke and passed the screening test were equally distributed across the six protocols (three doing each protocol). Using the Kruskal-Wallis test the protocols did not show bias for any of the light sources: THL $H(5) = 3.36$, $p = 0.642$, CFL $H(5) = 8.17$, $p = 0.147$, and LED $H(5) = 4.56$, $p = 0.473$.

4.2.1.1 Light Source A – THL

As can be seen from the protocol list (see Table 3.1), subjects that performed protocols 1 and 6 had to repeat the FM100 under the THL. The mean value for total error score (TES) was 50.6 ± 35.0 . The minimum TES was 4 and the maximum TES was 120. Using the Shapiro-Wilk test for normality, the results were normally distributed ($p = 0.238$). The test for skewness gave a slight positive result of $+0.106$ due to the high frequency of scores below 20. The distribution of the TES and Q-Q plots can be seen in Figure 4.1A and Figure 4.1B.

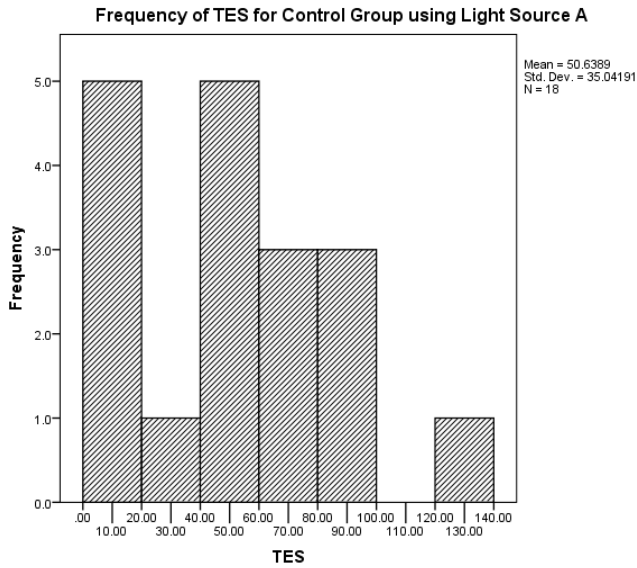


Figure 4.1A The distribution of TES for Normal/Control group using light source A

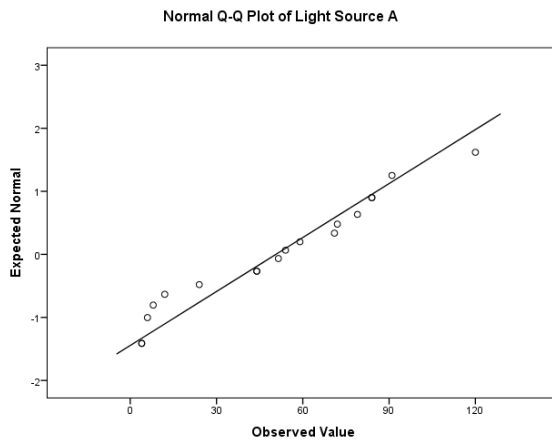


Figure 4.1B The Q-Q plot for Normal/Control group using light source A

4.2.1.2 Light Source B – CFL

Protocols 2 and 5 resulted in repeat testing under the CFL (see Table 3.1). The mean TES was 36.2 ± 35.9 . The minimum TES was 0, and the maximum TES was 136. Using the Shapiro-Wilk test for normality, the results were not normally distributed ($p = 0.019$), and there was a positive skew (+1.348). The distribution of the TES and Q-Q plots can be seen in Figure 4.2A and Figure 4.2B.

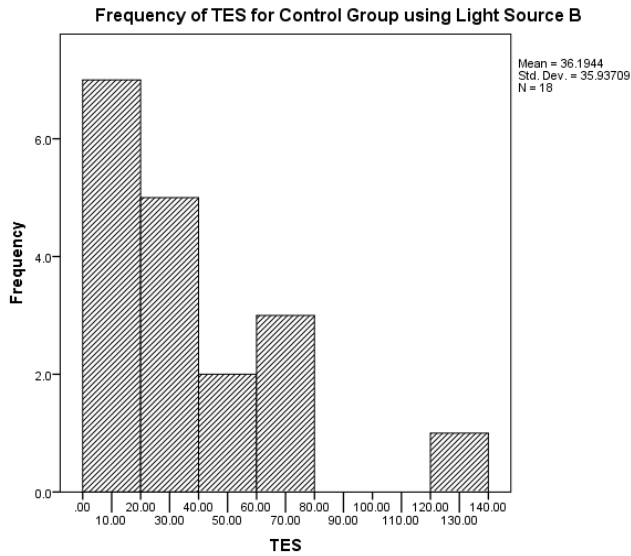


Figure 4.2A The distribution of TES for Normal/Control group using light source B

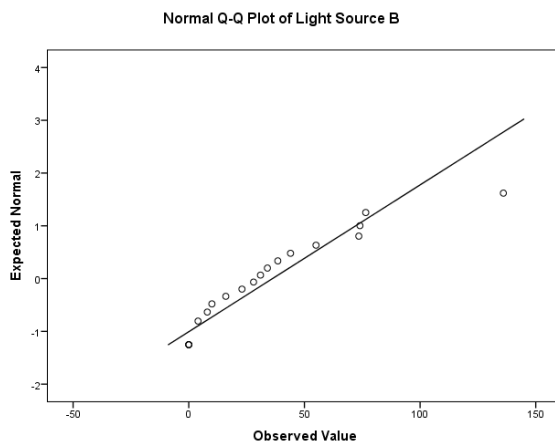


Figure 4.2B The Q-Q plot for Normal/Control group using light source B

4.2.1.3 Light Source C – LED

Testing under the LEDs was repeated for protocols 3 and 4. The mean TES was 43.8 ± 34.0 . The minimum TES was 0 and the maximum TES was 106.5. Using the Shapiro-Wilk test for normality, the results were normally distributed ($p = 0.102$). There was also a positive skew (+0.521). The distribution of the TES and Q-Q plots can be seen in Figure 4.3A and Figure 4.3B.

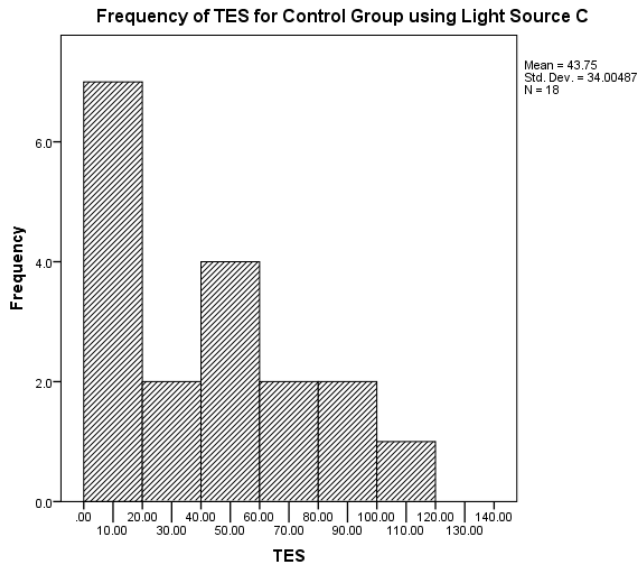


Figure 4.3A The distribution of TES for Normal/Control group using light source C

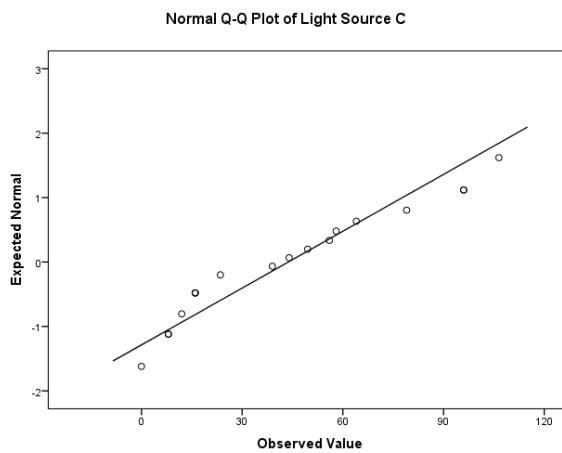


Figure 4.3B The Q-Q plot for Normal/Control group using light source C

4.2.2 Smoker/Test Subjects

As with the Normal/Control group, the subjects that were in the Smoker/Test group were equally split between the 6 protocols. Using the Kruskal-Wallis test the protocols did not show bias for any of the light sources: THL $H(5) = 8.84$, $p = 0.116$, CFL $H(5) = 6.68$, $p = 0.246$, and LED $H(5) = 10.3$, $p = 0.068$.

4.2.2.1 Light Source A – THL

Under the illumination of light source A (THL), the mean TES for the Smoker group was 50.6 ± 43.0 , with a minimum TES of 0 and a maximum TES of 154. The histogram shows a positive skew (+0.844), however, using the Shapiro-Wilk test for normality, the results were normally distributed ($p = 0.140$). The distribution of the TES and Q-Q plots can be seen in Figure 4.4A and Figure 4.4B.

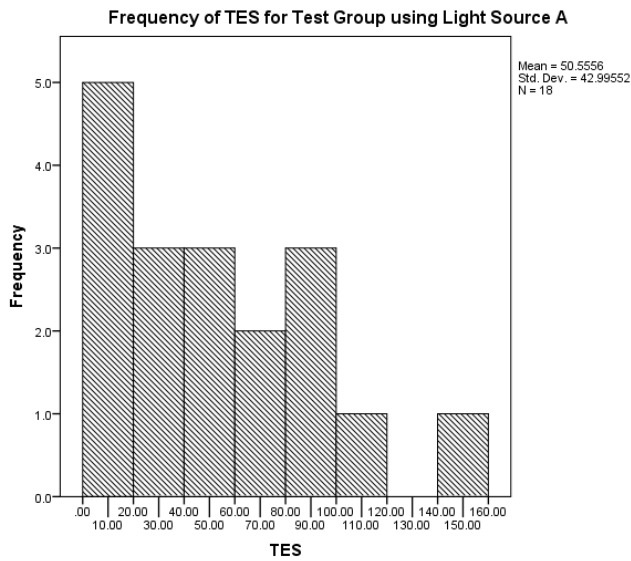


Figure 4.4A The distribution of TES for Smoker/Test group using light source A

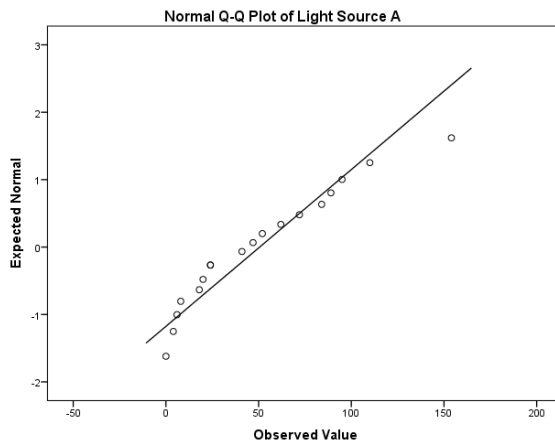


Figure 4.4B The Q-Q plot for Smoker/Test group using light source A

4.2.2.2 Light Source B – CFL

The mean TES using light source B was 44.7 ± 36.6 , with a minimum TES of 0 and a maximum TES of 102. The Shapiro-Wilk test for normality shows that the data was not normally distributed ($p = 0.034$), and again there was a positive skew (+0.382). The distribution of the TES and Q-Q plots can be seen in Figure 4.5A and Figure 4.5B.

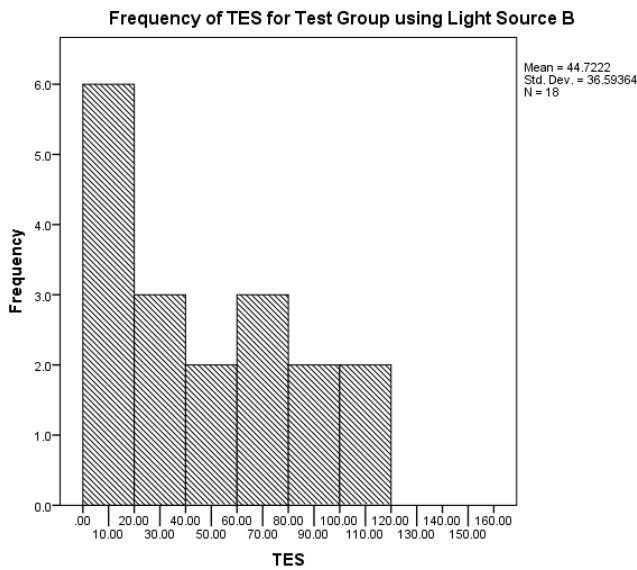


Figure 4.5A The distribution of TES for Smoker/Test group using light source B

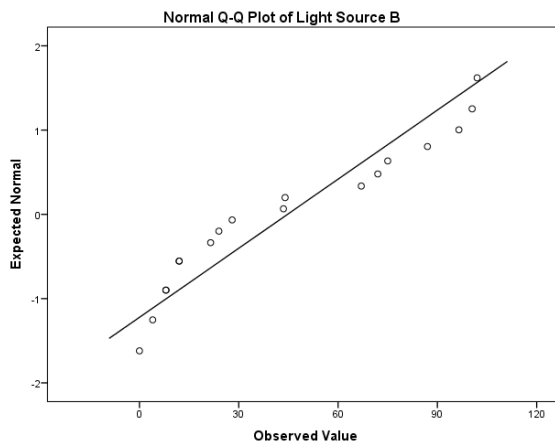


Figure 4.5B The Q-Q plot for Smoker/Test group using light source B

4.2.2.3 Light Source C – LED

Using lights source the C the mean TES for the Smoker/Test group was 49.4 ± 36.9 , with a minimum TES of 0, and a maximum TES of 114.5. The Shapiro-Wilk test for normality show that the data were normally distributed ($p = 0.283$), however there was a slight positive skew ($+0.170$). The distribution of the TES and Q-Q plots can be seen in Figure 4.6A and Figure 4.6B.

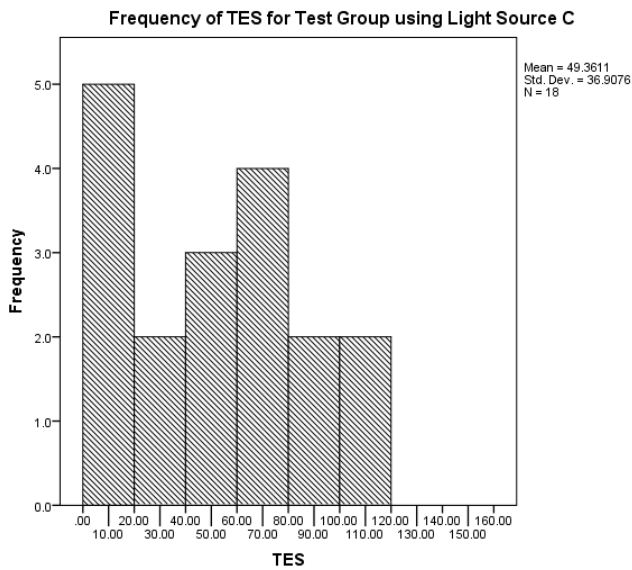


Figure 4.6A The distribution of TES for Smoker/Test group using light source C

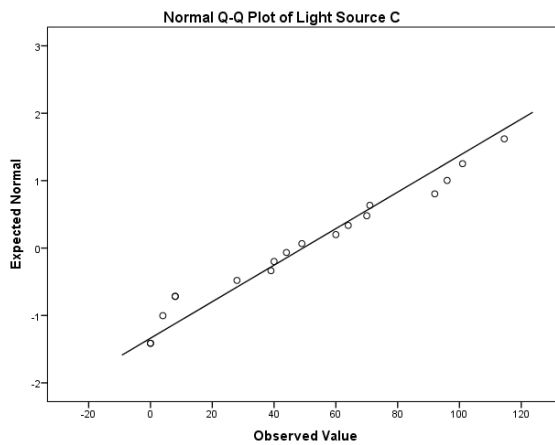


Figure 4.6B The Q-Q plot for Smoker/Test group using light source C

4.2.3 Summary of the Total Error Score Results

The mean TESs and standard deviations for the Normal/Control group for the three light sources can be seen in Figure 4.7A and for the Smoker/Test group in Figure 4.7B. The results have been summarised in Table 4.3.

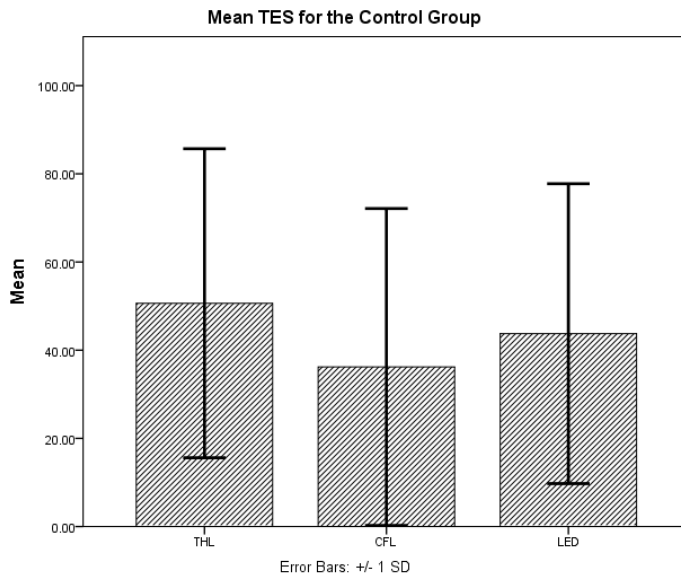


Figure 4.7A The mean TES and standard deviations for the Normal/Control group for the three light sources

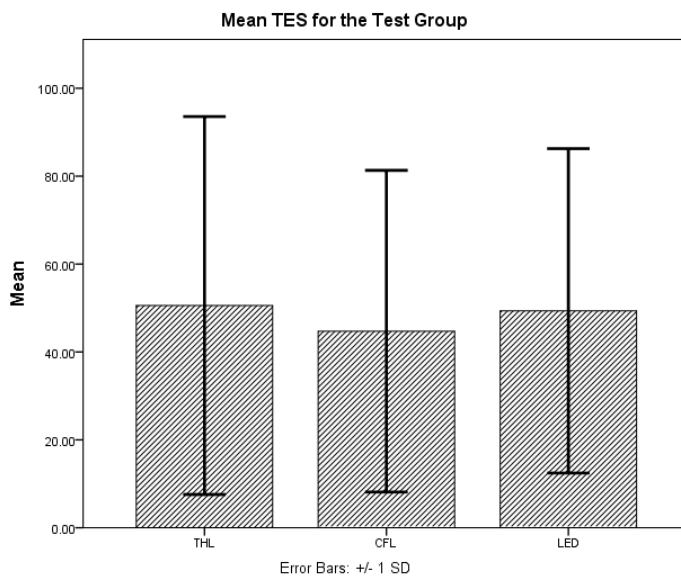


Figure 4.7B The mean TES and standard deviations for the Smoker/Test group for the three light sources

Group	Light Source	n	Mean \pm SD	Median	Min	Max
Normal/Control	THL (A)	18	50.6 \pm 35.0	52.8	4	120
Normal/Control	CFL (B)	18	36.2 \pm 35.9	29.5	0	136
Normal/Control	LED (C)	18	43.8 \pm 34.0	41.5	0	106.5
Smoker/Test	THL (A)	18	50.6 \pm 43.0	44.0	0	154
Smoker/Test	CFL (B)	18	44.7 \pm 36.6	35.8	0	102
Smoker/Test	LED (C)	18	49.4 \pm 36.9	46.6	0	114.5

Table 4.3 Summary of the TES results for the Normal/Control group and Smoker/Test group.

4.2.4 Analysis of Total Error Scores

As can be seen from the data collected there were three questions that needed to be asked with respect to TESs:

1. Was there a difference between the light sources for the Normal/Control group?
2. Was there a difference between the light sources for Smoker/Test group?
3. Was there a difference between the Normal/Control and Smoker/Test groups?

4.2.4.1 Total Error Scores for the Normal/Control Group

Conducting a Friedman's test showed a significant difference in the results between the light sources for the Normal/Control group ($\chi^2(2) = 8.15, p = 0.017$).

In order to examine the differences between the light sources further, three related-samples Wilcoxon signed-rank tests were performed. The results show that there was a significant difference between the THL and the CFL ($z = -2.38, p = 0.017$), but not between the THL and LED ($z = -0.427, p = 0.670$), and the CFL and LED ($z = -1.82, p = 0.068$). As three comparisons are being made, the likelihood of a Type 1 error has increased [157]. The test had enough statistical power (0.8) when looking for a large change (0.5) [155, 156].

4.2.4.2 Total Error Scores for the Smoker/Test Group

A Friedman's test showed no significant difference in the results between the light sources for the Smoker/Test group ($\chi^2(2) = 0.088$, $p = 0.957$).

4.2.4.3 Normal/Control Group Total Error Scores versus Smoker/Test Group Total Error Scores

When comparing the Normal/Control group with the Smoker/Test group using Mann-Witney tests, there was found to be no significant difference for any of the three light sources: THL ($U = 157.5$, $z = -0.134$, $p = 0.887$), CFL ($U = 138$, $z = -0.760$, $p = 0.447$), and LED ($U = 152.5$, $z = -0.301$, $p = 0.763$).

4.2.4.4 Decision Tree Analyses of Total Error Scores

The statistical power of the analyses carried out in sections 4.2.4.1-4.2.4.3 was only 0.76 rather than the desired 0.8 due to the shortfall in the subjects available [155]. In order to increase the statistical power of the analyses, and to reduce the likelihood of a type 1 error (i.e. rejection of the null hypothesis) from running multiple analyses, the results of the groups were pooled and Decision Tree Analyses were conducted. A Decision Tree Analysis (DTA) works by classifying the data into groups, or predicting the values of dependant (target) variables based on the values of independent (predictor) variables. As a result a DTA allows the identification of homogeneous groups with high or low risk. There are a number of considerations about the data that take place. Firstly, the variables need to be classified as nominal (categories with no intrinsic ranking – e.g. Control, and Test; THL, CFL, and LED), ordinal (categories with some intrinsic ranking), or scale (categories with a meaningful metric – e.g. TES; pack years). Secondly, the frequencies are weighted to the nearest integer. The growing method chosen was Chi-squared Automatic Interaction Detection (CHAID). CHAID chooses the independent variable that has the strongest interaction with the dependant variable at each step. CHAID merges independent variables that are not significantly different to the dependant variable. The chart produced allowed identification of the independent variables in order of significance.

A DTA was conducted using the TES as the dependant variable, and the 'Light source' and 'Group' as the independent variables (see Table 4.4).

Specifications	Growing Method	CHAID
	Dependent Variable	TES
	Independent Variables	Light, Group
	Validation	None
	Maximum Tree Depth	5
	Minimum Cases in Parent Node	2
	Minimum Cases in Child Node	1

Results	Independent Variables Included	No Independent Variable Included
	Number of Nodes	1
	Number of Terminal Nodes	1
	Depth	0

Table 4.4 The DTA results for TES using the light source and group as independent variables

The DTA showed that neither the 'Light source' nor the 'Group' produced any significant effects

The added advantage of DTAs over individual analyses is the exploration of independent variables that are continuous. Therefore, for this study a threshold for when pack years becomes a significant variable was explored. Alternative approaches of grouping smokers were employed by Bimler and Kirkland (who had the categories non-smokers, and smokers), and Erb et al (who had non-smokers, smokers consuming fewer than 20 cigarettes per day, and smokers consuming 20 or more cigarettes per day) [149, 150]. Both these methods cannot identify the threshold at which smoking may be significant unlike the DTA.

The DTA was conducted again, however, the variable 'Group' was replaced by 'Pack years' (see Table 4.5):

Specifications	Growing Method	CHAID
	Dependent Variable	TES
	Independent Variables	Light, Pack Years
	Validation	None
	Maximum Tree Depth	5
	Minimum Cases in Parent Node	2
	Minimum Cases in Child Node	1

Results	Independent Variables Included	Pack Years
	Number of Nodes	3
	Number of Terminal Nodes	2
	Depth	1

Table 4.5 The DTA results for TES using the light source and pack years as independent variables

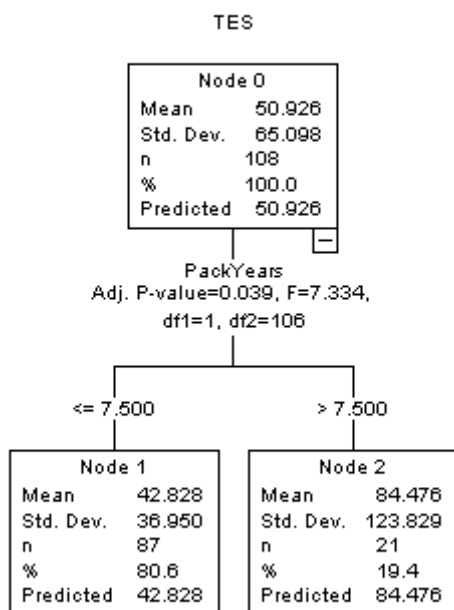
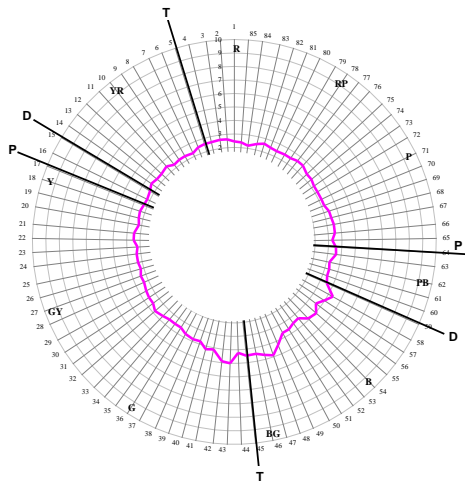


Figure 4.8 The DTA for TES using the light source and pack years as independent variables

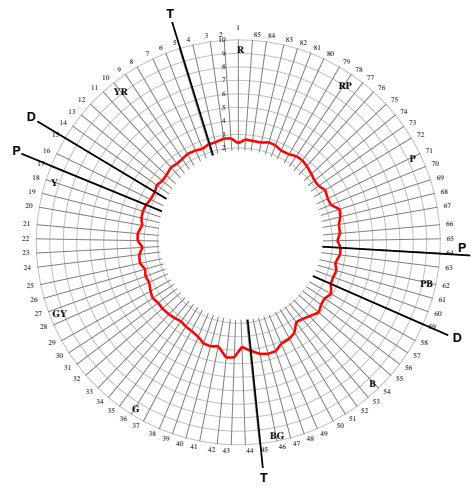
It can be seen by this DTA that there was a significant increase in the TES seen when pack years exceeded 7.5 (see Figure 4.8).

4.3 FM100 Plots

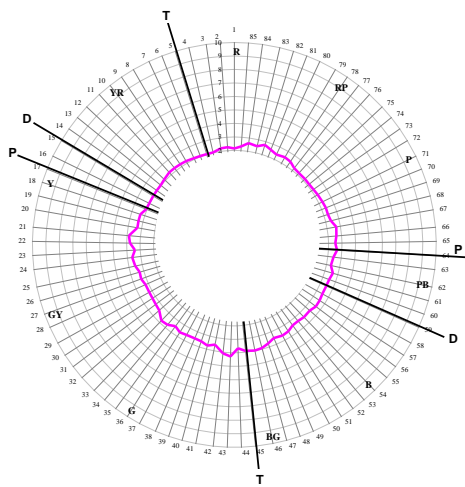
Traditionally FM100 results are plotted on polar charts; the 85th cap is plotted at 12 o'clock, followed by the 1st, and then sequentially in an anti-clockwise manner. The results can be seen in Figure 4.9 A-F. The FM100 charts display the colours red *R*, red/yellow *YR*, yellow *Y*, yellow/green *GY*, green *G*, green/blue *BG*, blue *B*, blue/purple *PB*, purple *P*, and purple/red *RP*. As well as the 'axes of confusion' for tritan defects as *T*, for deutan defects as *D*, and protan defects as *P*. Note that the deutan axis does not run through green, but is the diameter of the plot that is parallel to the tangent of green. Similarly the protan axis does not run through red, but is the diameter of the plot that is parallel to the tangent of red. The same is not true about the tritan axis, however the pathway for the tritan system is different to the deutan and protan pathways.



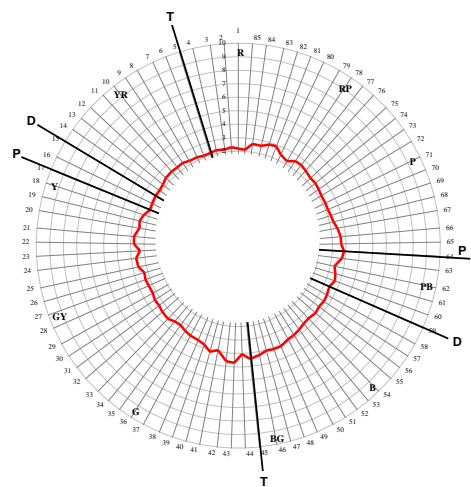
A



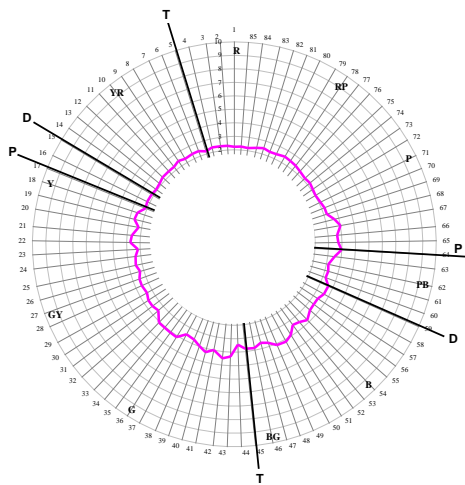
D



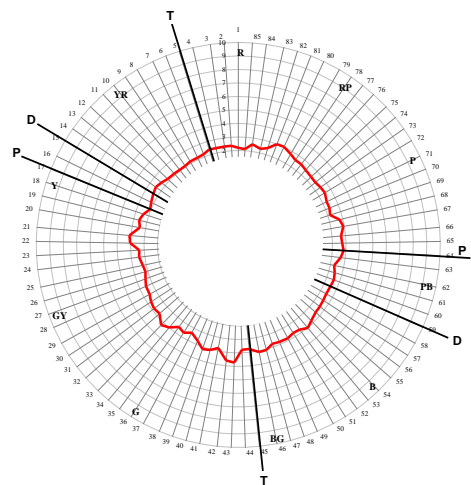
B



E



C



F

Figure 4.9 A-F. The FM100 plots (A - Control group with light source A, B - Control group with light source B, C - Control group with light source C, D - Test group with light source A, E - Test group with light source B, F - Test group with light source C)

The FM100 plots in Figure 4.9 A-F incorporate the mean cap error scores (CES). The minimum cap error score was 2. The TES is the sum of the CES minus 170 (i.e. the total number of caps multiplied by two). The range for CES can be seen in Table 4.6.

Group	Lamp	Individual CES			Mean CES		
		Min	Max	Range	Min	Max	Range
Normal/Control	THL	2	9	7	2.19	4.05	1.86
Normal/Control	CFL	2	7.5	5.5	2.03	3.28	1.25
Normal/Control	LED	2	10	8	2.03	3.50	1.47
Smoker/Test	THL	2	11	9	2.11	3.58	1.47
Smoker/Test	CFL	2	8	6	2.08	3.69	1.61
Smoker/Test	LED	2	9.5	7.5	2.06	3.72	1.66

Table 4.6 The CES for each Group and Light source

4.4 Colour Bands

The next area requiring exploration was the effect of the light sources on the discrimination of different colours. The FM100 caps were separated out into colour bands [83] (see Table 4.7):

Colour	Caps
Red-Red/Yellow	1-9
Red/Yellow-Yellow	10-17
Yellow-Yellow/Green	18-26
Yellow/Green-Green	27-35
Green-Green/Blue	36-45
Green/Blue-Blue	46-53
Blue-Blue/Purple	54-60
Blue/Purple-Purple	61-70
Purple-Purple/Red	71-77
Purple/Red-Red	78-85

Table 4.7 Colour bands

The questions to be asked of the data were:

1. Was there any difference between the light sources for discrimination of different colours for the Normal/Control group?
2. Was there any difference between the light sources for discrimination of different colours for the Smoker/Test group?
3. Did these chromatic errors vary because of smoking?

4.4.1 Colour Band Error Scores

As there were a different number of caps in each colour band, an average error score was calculated. The colour band error scores (CBES) can be seen in Table 4.8 and Table 4.9.

4.4.1.1 Colour Band Error Scores for the Normal/Control Group

Colour Band	Mean Score \pm SD		
	THL	CFL	LED
Red-Red/Yellow	2.48 \pm 0.55	2.13 \pm 0.22	2.33 \pm 0.34
Red/Yellow-Yellow	2.35 \pm 0.45	2.09 \pm 0.15	2.19 \pm 0.23
Yellow-Yellow/Green	2.31 \pm 0.44	2.49 \pm 0.51	2.45 \pm 0.51
Yellow/Green-Green	2.53 \pm 0.49	2.41 \pm 0.51	2.70 \pm 0.72
Green-Green/Blue	3.18 \pm 0.79	2.74 \pm 0.69	2.96 \pm 0.63
Green/Blue-Blue	3.05 \pm 0.88	2.63 \pm 0.67	2.78 \pm 0.81
Blue-Blue/Purple	2.82 \pm 0.64	2.49 \pm 0.61	2.50 \pm 0.58
Blue-/Purple-Purple	2.40 \pm 0.38	2.48 \pm 0.50	2.54 \pm 0.56
Purple-Purple/Red	2.37 \pm 0.54	2.19 \pm 0.39	2.19 \pm 0.33
Purple/Red-Red	2.43 \pm 0.45	2.51 \pm 0.81	2.36 \pm 0.52

Table 4.8 Mean Error Scores in each colour band for the Normal/Control group

4.4.1.2 Colour Band Error Scores for the Smoker/Test Group

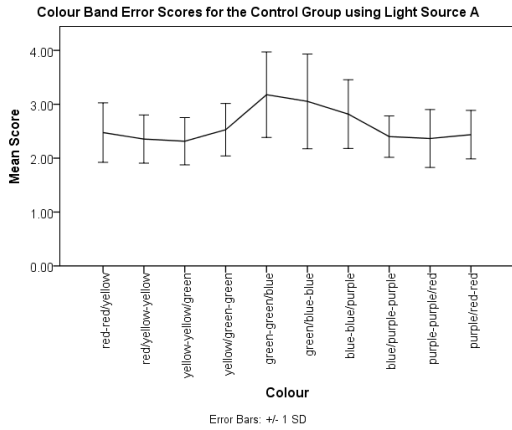
Colour Band	Mean Score \pm SD		
	THL	CFL	LED
Red-Red/Yellow	2.55 \pm 0.59	2.23 \pm 0.31	2.24 \pm 0.29
Red/Yellow-Yellow	2.33 \pm 0.41	2.23 \pm 0.36	2.22 \pm 0.29
Yellow-Yellow/Green	2.36 \pm 0.42	2.52 \pm 0.40	2.52 \pm 0.52
Yellow/Green-Green	2.39 \pm 0.50	2.35 \pm 0.44	2.71 \pm 0.62
Green-Green/Blue	2.90 \pm 0.88	3.02 \pm 0.99	2.96 \pm 0.74
Green/Blue-Blue	3.04 \pm 1.13	2.93 \pm 0.91	2.88 \pm 0.68
Blue-Blue/Purple	2.68 \pm 0.65	2.54 \pm 0.54	2.58 \pm 0.55
Blue-/Purple-Purple	2.58 \pm 0.77	2.48 \pm 0.41	2.58 \pm 0.52
Purple-Purple/Red	2.46 \pm 0.53	2.35 \pm 0.50	2.44 \pm 0.43
Purple/Red-Red	2.62 \pm 0.65	2.53 \pm 0.63	2.60 \pm 0.78

Table 4.9 Mean Error Scores in each colour band for the Smoker/Test group

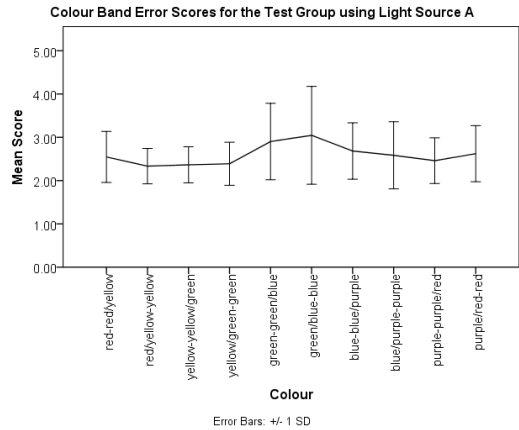
4.4.1.3 Normal/Control Group Colour Band Error Scores versus Smoker/Test Group Colour Band Error Scores

The general trend showed a slight peak in the green-green/blue part of the spectrum. The exception was the Smoker/Test group using light source A which peaked in the green/blue-blue part of the spectrum. However the error bars (\pm one standard deviation) showed a notable overlap of results (see Figure 4.10 A-F)

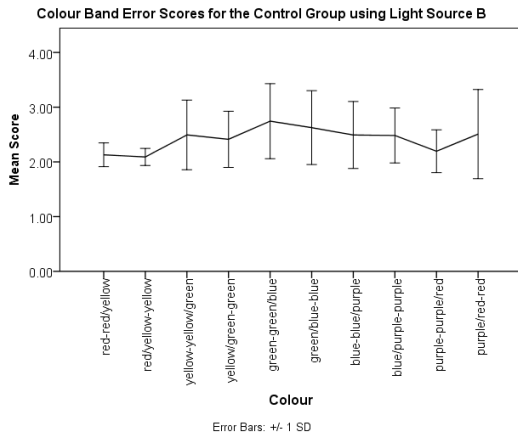
A)



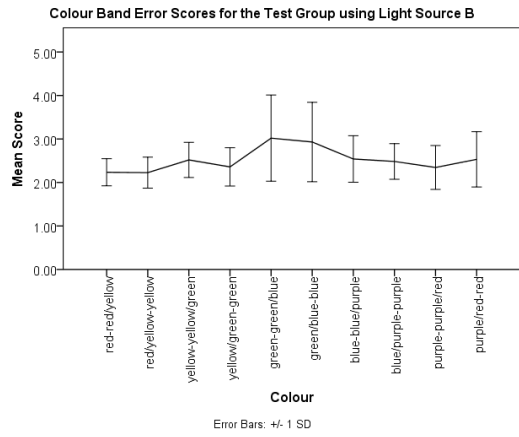
D)



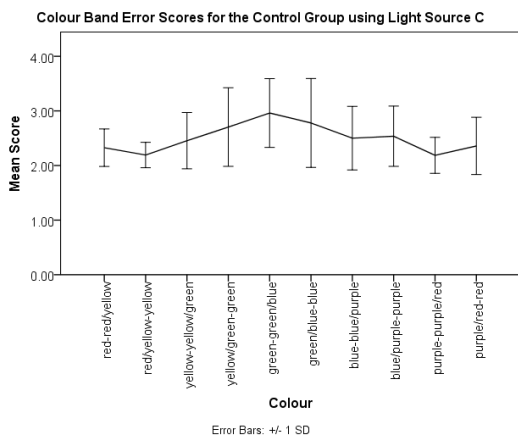
B)



E)



C)



F)

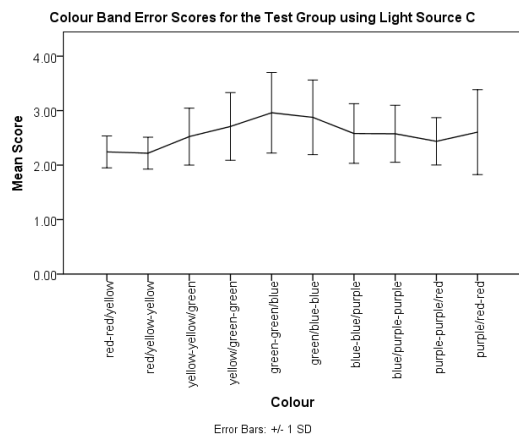


Figure 4.10 Mean Error Scores in each colour band: A = control group with light source A, B = control group with light source B, C = control group with light source C, D = test group with light source A, E = test group with light source B, and F = test group with light source C.

4.4.1.4 Decision Tree Analysis of Colour Band Error Scores

As pack years has been shown to be a significant variable with TESs, DTAs were conducted to see if that was the case for each colour band.

Specifications	Growing Method	CHAID
	Dependent Variable	Score
	Independent Variables	Pack Years, Light
	Validation	None
	Maximum Tree Depth	5
	Minimum Cases in Parent Node	2
	Minimum Cases in Child Node	1

Significant variables were found in only the following colour bands:

Red-Red/Yellow

Results	Independent Variables Included	Light, Pack Years
	Number of Nodes	8
	Number of Terminal Nodes	5
	Depth	3

Table 4.10 The DTA results for the red-red/yellow CBES using the light source and pack years as independent variables

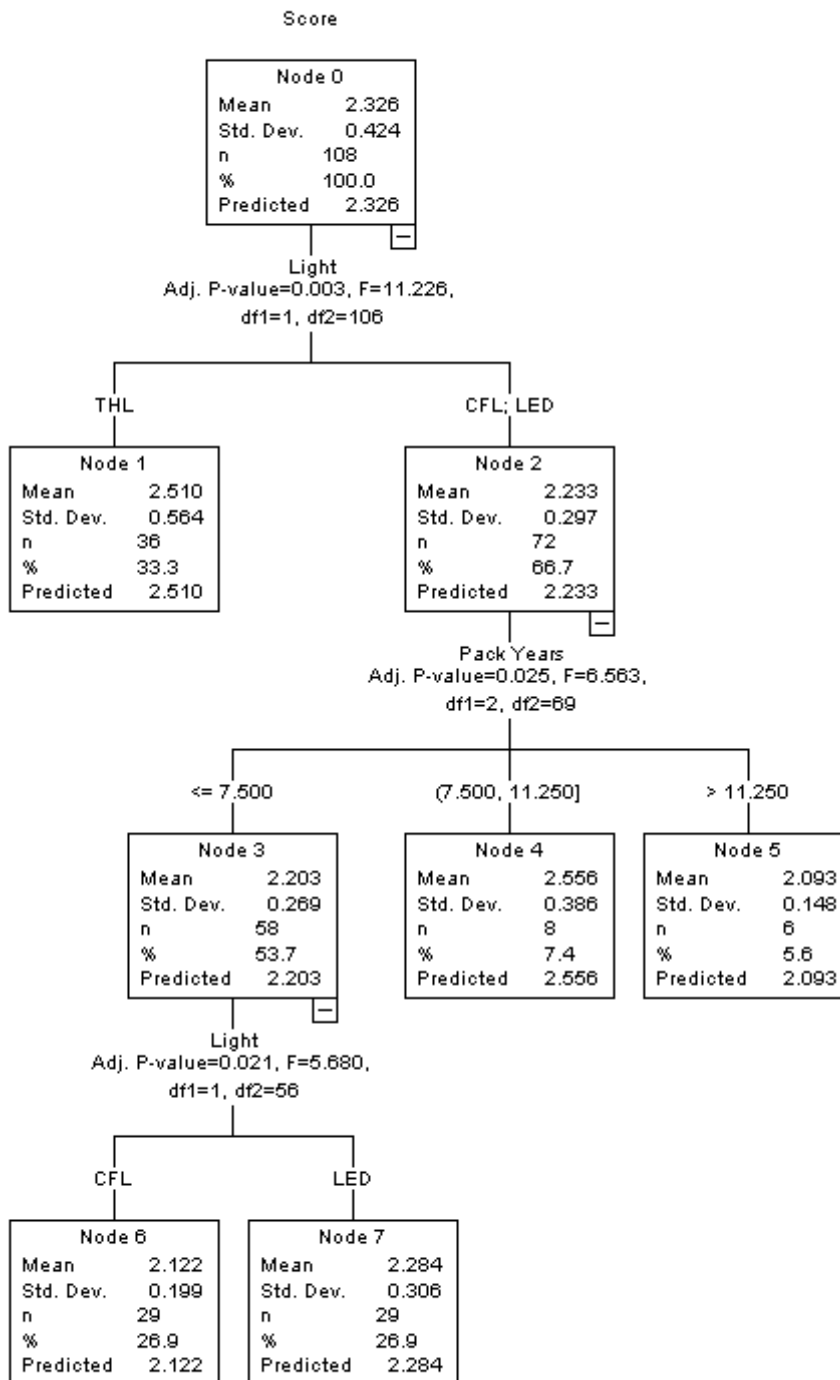


Figure 4.11 The DTA for red-red/yellow CBES using the light source and pack years as independent variables

There most significant variable was the light source; the THL had a significantly higher error than the CFL and the LED (see Table 4.10 and Figure 4.11). There was a further division of the CFL and LED into three 'Pack years' branches, where the

error scores seemed lowest with the highest pack year followed by the lowest. Finally the ≤ 7.5 'Pack years' branch split further into CFL and LED (with LED having the higher error score). Therefore, for the red-red/yellow colour band: THL had the highest error scores; subjects that had ≤ 7.5 pack years showed a further difference between CFL and LED (with CFL having lower error scores).

Red/Yellow-Yellow

Results	Independent Variables Included	Light
	Number of Nodes	3
	Number of Terminal Nodes	2
	Depth	1

Table 4.11 The DTA results for the red/yellow-yellow CBES using the light source and pack years as independent variables

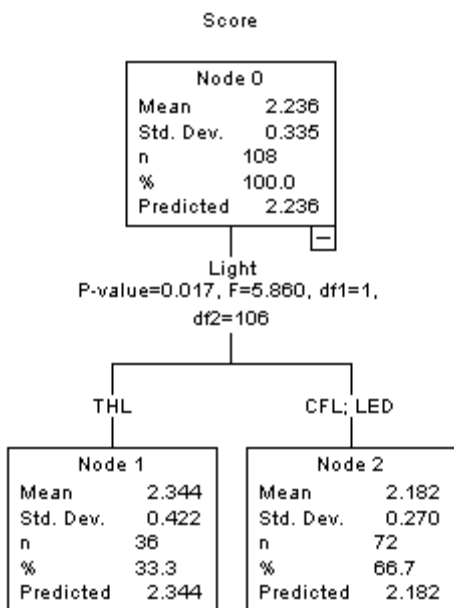


Figure 4.12 The DTA for red/yellow-yellow CBES using the light source and pack years as independent variables

Again there was a significant difference in error scores between THL, and CFL and LED light sources. The THL resulted in a higher error score (see Table 4.11 and Figure 4.12).

Yellow/Green-Green

Results	Independent Variables Included	Light
	Number of Nodes	3
	Number of Terminal Nodes	2
	Depth	1

Table 4.12 The DTA results for the yellow/green-green CBES using the light source and pack years as independent variables

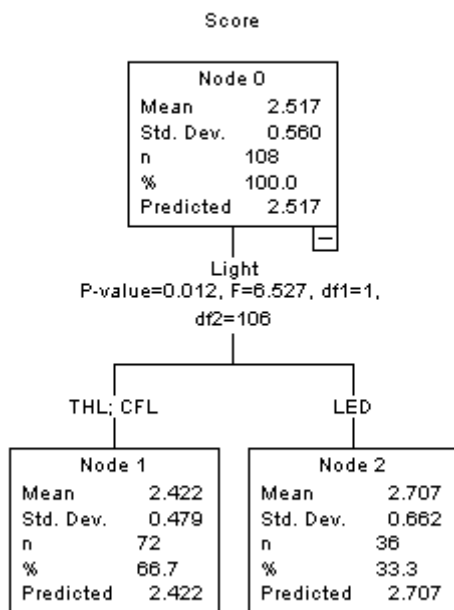


Figure 4.13 The DTA for yellow/green-green CBES using the light source and pack years as independent variables

For this colour band the significant variable was the light source again, however the distinction was between the LED (highest error score) and a branch combining the THL and CFL (see Table 4.12 and Figure 4.13).

Green-Green/Blue

Results	Independent Variables Included	Pack Years
	Number of Nodes	3
	Number of Terminal Nodes	2
	Depth	1

Table 4.13 The DTA results for the green-green/blue CBES using the light source and pack years as independent variables

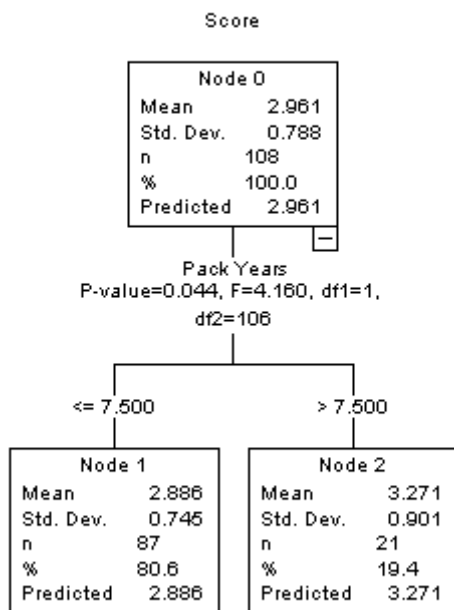


Figure 4.14 The DTA for green-green/blue CBES using the light source and pack years as independent variables

Here the significant variable was pack years. The lower error score was found in the group with ≤ 7.5 pack years (see Table 4.13 and Figure 4.14).

Purple-Purple/Red

Results	Independent Variables Included	Pack Years
	Number of Nodes	3
	Number of Terminal Nodes	2
	Depth	1

Table 4.14 The DTA results for the purple-purple/red CBES using the light source and pack years as independent variables

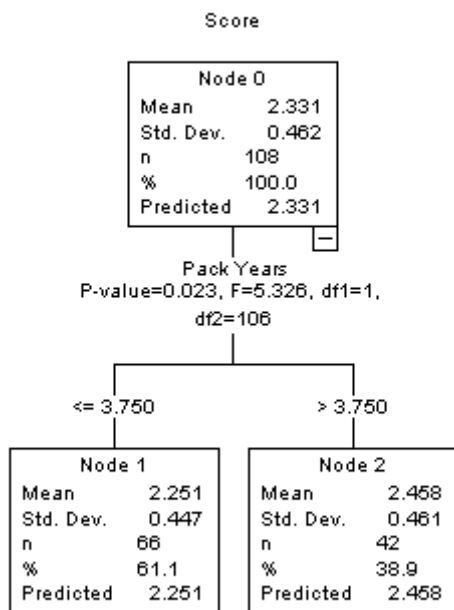


Figure 4.15 The DTA for purple-purple/red CBES using the light source and pack years as independent variables

The significant variable found was pack years, with ≤ 3.75 pack years having a lower error score compared with > 3.75 pack years (see Table 4.14 and Figure 4.15).

4.4.1.5 Summary of Decision Tree Analyses of Colour Band Error Scores

Test	Significant Difference	Factor	Group with Min Error Score	Group with Max Error Score
TES	✓	Pack years	≤7.5	>7.5
Red-Red/Yellow	✓	Light source, Pack years	CFL/LED + >11.25	CFL/LED + 7.5-11.25
Red/Yellow-Yellow	✓	Light source	CFL/LED	THL
Yellow-Yellow/Green	×			
Yellow/Green-Green	✓	Light source	THL/CFL	LED
Green-Green/Blue	✓	Pack years	≤7.5	>7.5
Green/Blue-Blue	×			
Blue-Blue/Purple	×			
Blue/Purple-Purple	×			
Purple-Purple/Red	✓	Pack years	≤3.75	>3.75
Purple/Red-Red	×			

Table 4.15 Summary of the DTA using TES and Mean Error Scores in the colour bands

4.4.2 Alternative Colour Band Analysis

Another method for analysing the colour bands was to count the number occasions the cap error score was greater than four (FCES4). As with CBES, an average was calculated in each colour band. The aim of this method was to remove any bias created by solitary high error scores (see Table 4.16 and Table 4.17).

4.4.2.1 Colour Band Frequency of Cap Error Scores greater than four for the Normal/Control Group

Colour Band	Mean FCES4 \pm SD		
	THL	CFL	LED
Red-Red/Yellow	0.06 \pm 0.10	0.00 \pm 0.00	0.04 \pm 0.11
Red/Yellow-Yellow	0.06 \pm 0.11	0.00 \pm 0.00	0.00 \pm 0.00
Yellow-Yellow/Green	0.05 \pm 0.11	0.08 \pm 0.15	0.10 \pm 0.20
Yellow/Green-Green	0.09 \pm 0.18	0.07 \pm 0.17	0.13 \pm 0.21
Green-Green/Blue	0.30 \pm 0.23	0.16 \pm 0.20	0.21 \pm 0.20
Green/Blue-Blue	0.25 \pm 0.28	0.14 \pm 0.22	0.18 \pm 0.25
Blue-Blue/Purple	0.14 \pm 0.24	0.09 \pm 0.20	0.10 \pm 0.16
Blue-/Purple-Purple	0.04 \pm 0.10	0.06 \pm 0.10	0.10 \pm 0.17
Purple-Purple/Red	0.04 \pm 0.12	0.02 \pm 0.07	0.02 \pm 0.10
Purple/Red-Red	0.07 \pm 0.12	0.11 \pm 0.23	0.07 \pm 0.15

Table 4.16 Frequency of Cap Error Scores greater than four in each colour band for the Normal/Control group

4.4.2.2 Colour Band Frequency of Cap Error Scores greater than four for the Smoker/Test Group

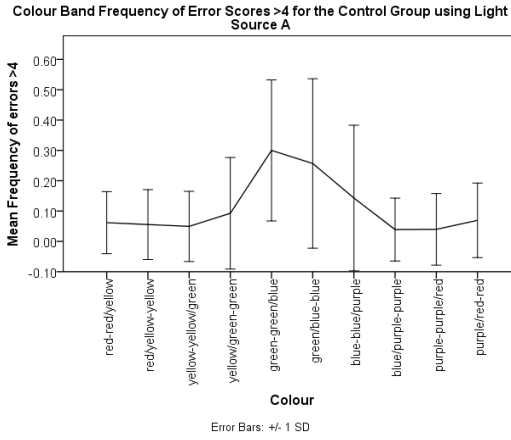
Colour Band	Mean FCES4 \pm SD		
	THL	CFL	LED
Red-Red/Yellow	0.09 \pm 0.16	0.01 \pm 0.03	0.01 \pm 0.03
Red/Yellow-Yellow	0.04 \pm 0.15	0.01 \pm 0.06	0.01 \pm 0.06
Yellow-Yellow/Green	0.09 \pm 0.18	0.09 \pm 0.13	0.07 \pm 0.13
Yellow/Green-Green	0.07 \pm 0.15	0.04 \pm 0.11	0.14 \pm 0.17
Green-Green/Blue	0.20 \pm 0.27	0.26 \pm 0.29	0.20 \pm 0.22
Green/Blue-Blue	0.27 \pm 0.33	0.23 \pm 0.28	0.21 \pm 0.23
Blue-Blue/Purple	0.14 \pm 0.22	0.07 \pm 0.14	0.08 \pm 0.10
Blue-/Purple-Purple	0.08 \pm 0.16	0.06 \pm 0.11	0.10 \pm 0.15
Purple-Purple/Red	0.06 \pm 0.15	0.04 \pm 0.08	0.03 \pm 0.08
Purple/Red-Red	0.12 \pm 0.18	0.08 \pm 0.17	0.10 \pm 0.16

Table 4.17 Frequency of Cap Error Scores greater than four in each colour band for the Smoker/Test group

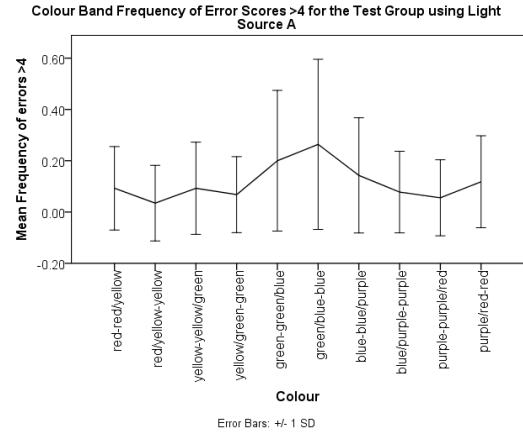
4.4.2.3 Normal/Control Group Colour Band Frequency of Cap Error Scores greater than four versus Smoker/Test Group Colour Band Frequency of Cap Error Scores greater than four

The FCES4s were highest for green-green/blue for the all groups except the Smoker/Test groups under light sources A and C. This showed similar results to that seen when using CBESs i.e. a peak in the green-green/blue to green/blue-blue part of the spectrum, with significant standard deviations and thus overlaps between the results for each colour band (see Figure 4.16 A-F).

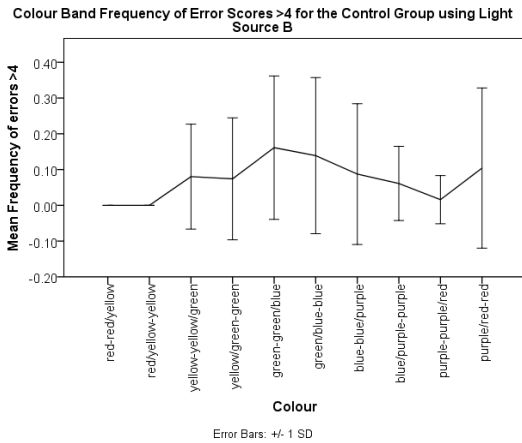
A)



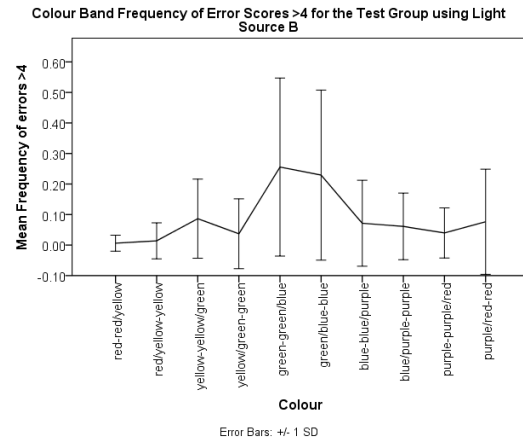
D)



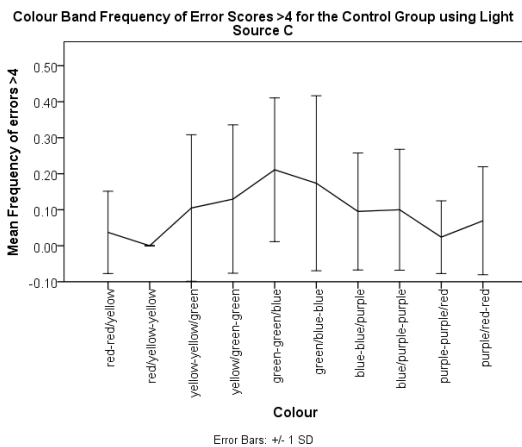
B)



E)



C)



F)

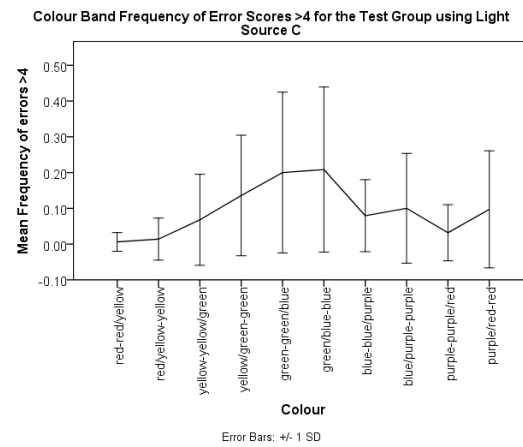


Figure 4.16 Frequency of Cap Error Scores greater than four in each colour band: A = control group with light source A, B = control group with light source B, C = control group with light source C, D = test group with light source A, E = test group with light source B, and F = test group with light source C.

4.4.2.4 Decision Tree Analysis of Colour Band Frequency of Cap Error Scores greater than four

As with CBES, DTAs for FCES4 were conducted:

Specifications	Growing Method	CHAID
	Dependent Variable	Frequency of errors greater than four
	Independent Variables	Pack Years, Light
	Validation	None
	Maximum Tree Depth	5
	Minimum Cases in Parent Node	2
	Minimum Cases in Child Node	1

Significant variables were found in only the following colour bands:

Red-Red/Yellow

Results	Independent Variables Included	Light
	Number of Nodes	3
	Number of Terminal Nodes	2
	Depth	1

Table 4.18 The DTA results for the red-red/yellow FCES4 using the light source and pack years as independent variables

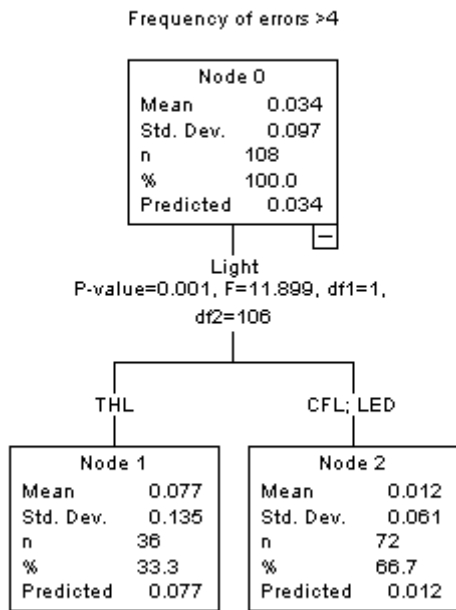


Figure 4.17 The DTA for red-red/yellow FCES4 using the light source and pack years as independent variables

The significant variable for this colour band was the light source, with a greater FCES4 found for the THL, and no significant difference between the CFL and LED (see Table 4.18 and Figure 4.17).

Red/Yellow-Yellow

Results	Independent Variables Included	Light
	Number of Nodes	3
	Number of Terminal Nodes	2
	Depth	1

Table 4.19 The DTA results for the red/yellow-yellow FCES4 using the light source and pack years as independent variables

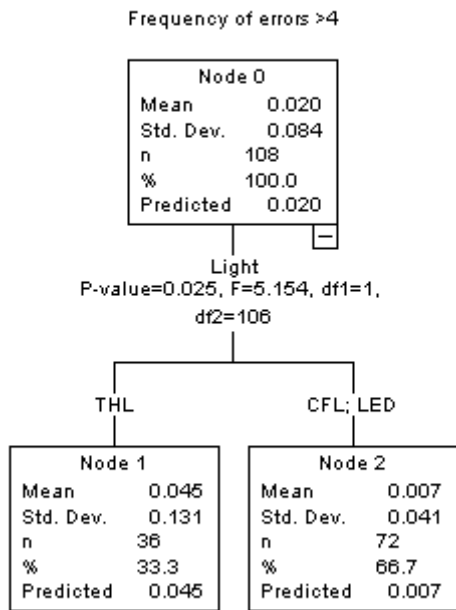


Figure 4.18 The DTA for red/yellow-yellow FCES4 using the light source and pack years as independent variables

As with the red-red/yellow colour band, for the red/yellow-yellow colour band the significant variable was the light source. Again THLs resulted in a greater FCES4 (see Table 4.19 and Figure 4.18).

Green-Green/Blue

Results	Independent Variables Included	Pack Years
	Number of Nodes	3
	Number of Terminal Nodes	2
	Depth	1

Table 4.20 The DTA results for the green-green/blue FCES4 using the light source and pack years as independent variables

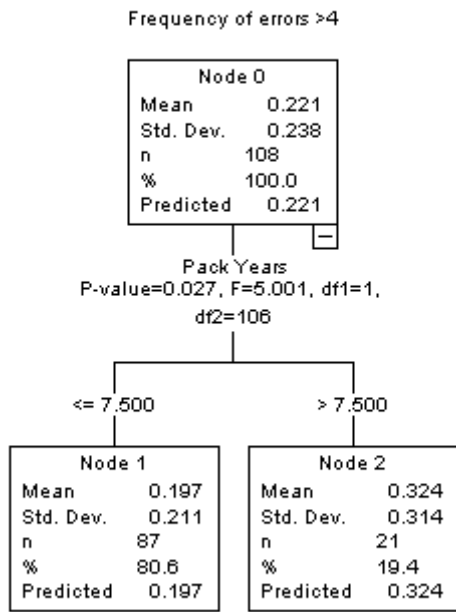


Figure 4.19 The DTA for green-green/blue FCES4 using the light source and pack years as independent variables

Here the significant variable was the pack years, subjects with >7.5 pack years had a higher FCES4 in the green-green/blue section of the spectrum (see Table 4.20 and Figure 4.19).

4.4.2.5 Summary of Decision Tree Analyses of Colour Band Frequency of Cap Error Scores greater than four

Test	Significant Difference	Factor	Group with Min Frequency	Group with Max Frequency
Red-Red/Yellow	✓	Light source	CFL/LED	THL
Red/Yellow-Yellow	✓	Light source	CFL/LED	THL
Yellow-Yellow/Green	×			
Yellow/Green-Green	×			
Green-Green/Blue	✓	Pack years	≤7.5	>7.5
Green/Blue-Blue	×			
Blue-Blue/Purple	×			
Blue/Purple-Purple	×			
Purple-Purple/Red	×			
Purple/Red-Red	×			

Table 4.21 Summary of the DTA using the Frequency of Cap Error Scores greater than four in the colour bands

4.4.3 Correlation between Mean Error Scores and Frequency of Cap Error Scores greater than four

(Spearman Rho coefficient, Probability) sig. 0.05			
	THL	CFL	LED
Control	✓ (0.82, 0.00)	✓ (0.74, 0.00)	✓ (0.80, 0.00)
Test	✓ (0.80, 0.00)	✓ (0.77, 0.00)	✓ (0.83, 0.00)

Table 4.22 Correlation between the CBES and FCES4 for the Normal/Control group and Smoker/Test group

There was good correlation between the two methods of determining errors for both the Control group and the Test group (see Table 4.22).

4.4.4 Correlation between Pack Years and Colour Vision

To further investigate the influence of smoking on colour vision the correlation between pack years and error score, and correlation pack years and Frequency of error scores greater than four were determined. If smoking did have a significant influence then a correlation would be seen.

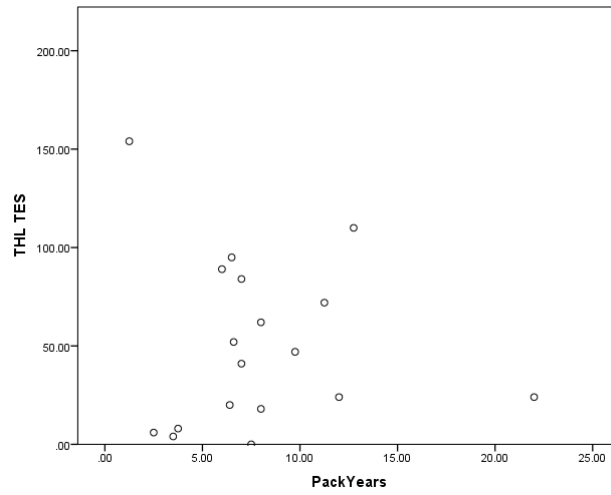
4.4.4.1 Correlation between Error Scores and Pack Years

A scatter graph of TES versus pack years for the Test group was plotted to look for a correlation between these two variables (see Figure 4.20 A-C). There does not appear to be any correlation between TES and pack years.

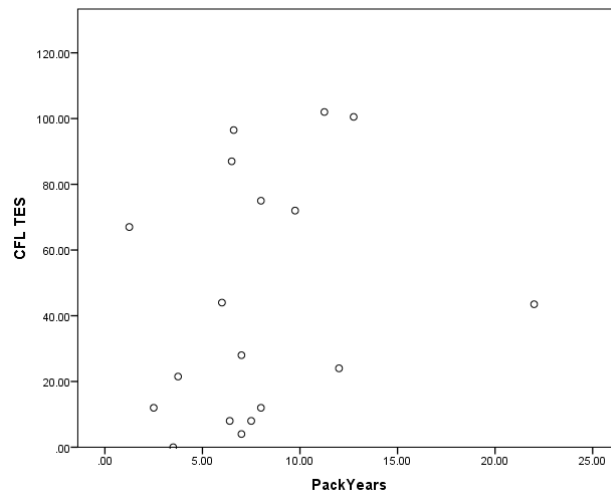
	(Spearman Rho coefficient, Probability) sig. 0.05		
	THL	CFL	LED
TES	* (0.00, 0.99)	* (0.21, 0.22)	* (0.17, 0.32)
Red-Red/Yellow	* (0.12, 0.49)	* (0.27, 0.11)	* (-0.14, 0.40)
Red/Yellow-Yellow	* (0.06, 0.75)	* (0.23, 0.19)	* (0.09, 0.59)
Yellow-Yellow/Green	* (0.09, 0.62)	* (0.28, 0.10)	* (0.15, 0.37)
Yellow/Green-Green	* (-0.08, 0.66)	* (0.02, 0.92)	* (0.13, 0.46)
Green-Green/Blue	* (-0.18, 0.31)	* (0.19, 0.27)	* (0.10, 0.57)
Green/Blue-Blue	* (-0.10, 0.55)	* (0.29, 0.08)	* (0.13, 0.44)
Blue-Blue/Purple	* (-0.05, 0.77)	* (0.20, 0.24)	* (0.14, 0.42)
Blue/Purple-Purple	* (0.07, 0.69)	* (0.08, 0.65)	* (0.12, 0.47)
Purple-Purple/Red	* (0.16, 0.34)	* (0.18, 0.29)	✓ (0.34, 0.04)
Purple/Red-Red	* (0.08, 0.65)	* (0.14, 0.41)	* (0.08, 0.65)

Table 4.23 Correlation coefficients and probabilities for pack years with Error Scores

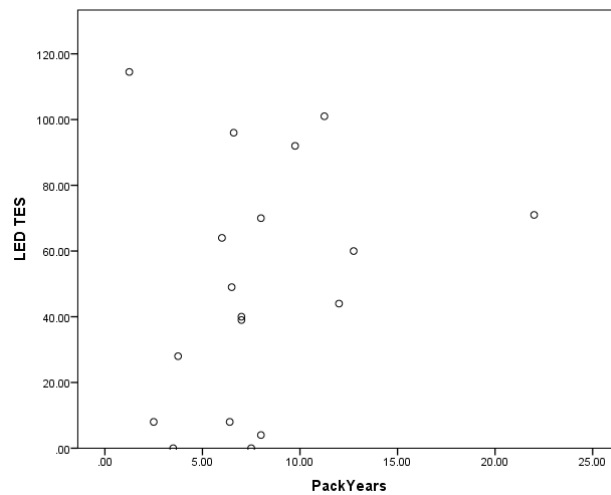
It can be seen that there was no correlation between TES and pack years. When using the CBESs in each for each light source, only the purple-purple/red colour band under the LED showed correlation with pack years (see Table 4.23).



A



B



C

Figure 4.20 A-C: Scatter plots of TES versus pack years (A - for light source A, B - for light source B, and C - for light source C). No correlation was found.

4.4.4.2 Correlation between Frequency of Cap Error Scores greater than four and Pack Years

(Spearman Rho coefficient, Probability) sig. 0.05			
	THL	CFL	LED
Red-Red/Yellow	* (0.09, 0.60)	* (0.24, 0.17)	* (0.06, 0.74)
Red/Yellow-Yellow	* (-0.28, 0.09)	* (0.01, 0.96)	* (0.24, 0.17)
Yellow-Yellow/Green	* (-0.02, 0.93)	* (0.13, 0.46)	* (0.03, 0.86)
Yellow/Green-Green	* (0.09, 0.62)	* (-0.11, 0.52)	* (0.13, 0.44)
Green-Green/Blue	* (-0.21, 0.21)	* (0.18, 0.30)	* (0.04, 0.80)
Green/Blue-Blue	* (-0.06, 0.73)	* (0.19, 0.28)	* (0.11, 0.52)
Blue-Blue/Purple	* (-0.01, 0.97)	* (0.03, 0.86)	* (0.06, 0.72)
Blue/Purple-Purple	* (0.02, 0.92)	* (0.00, 0.98)	* (0.01, 0.98)
Purple-Purple/Red	* (0.09, 0.60)	✓ (0.34, 0.04)	* (0.14, 0.42)
Purple/Red-Red	* (0.15, 0.38)	* (0.01, 0.98)	* (0.11, 0.54)

Table 4.24 Correlation coefficients and probabilities for pack years with Frequency of Cap Error Scores greater than four

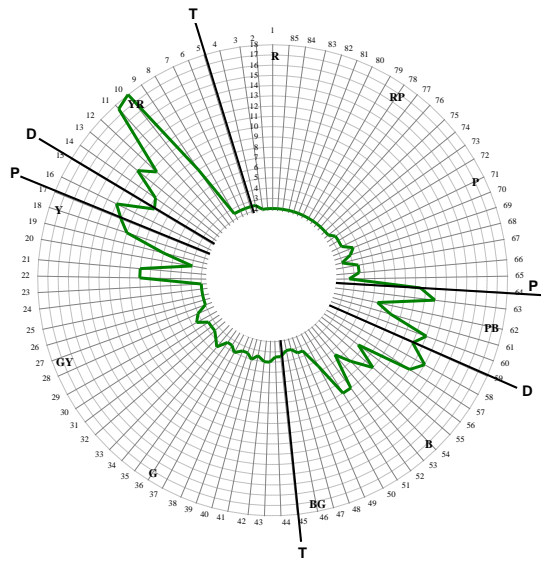
As with the CBESs, the only correlation for FCES4 was seen in the purple-purple/red area of the spectrum, however this time it exists only with the CFL (see Table 4.24).

4.5 Case Study Group – Colour Vision Defects

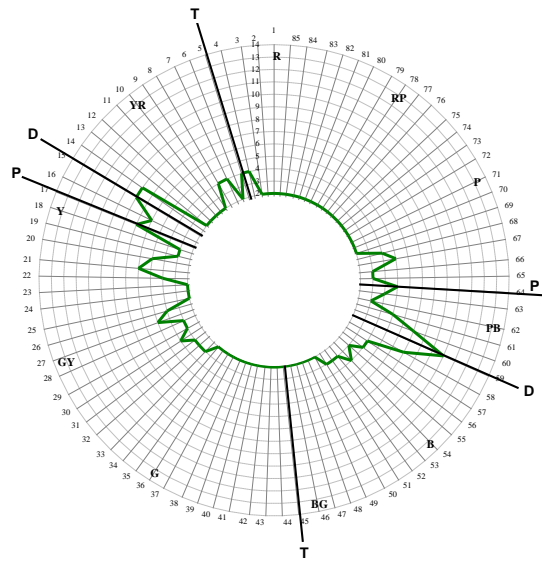
During the screening process six subjects failed the Ishihara PIC test, and were placed in a Case Study group. The highest score was 11, and the lowest was 1 (out of 25). Of these six subjects, five of them were male. All six subjects appeared to be deuteranomalous trichromats using the plates 22-25. Three of the subjects in this group were only able to see the left-hand digit on these plates, one saw only the left-hand digit on two of these plates, and two subjects commented that the left-hand number as significantly easier to see despite indentifying all four numbers correctly. This group had a mean age of 31.7 ± 5.2 (min. 22, max. 36).

4.5.1 Case Study Subjects' FM100 Plots

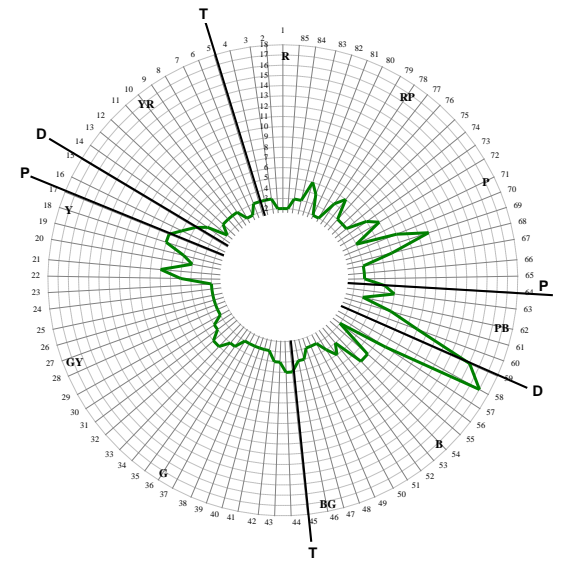
As colour defective individuals can have such a large variation in FM100 plots, the plots for each subject have been shown in Figure 4.21 A-C.



A

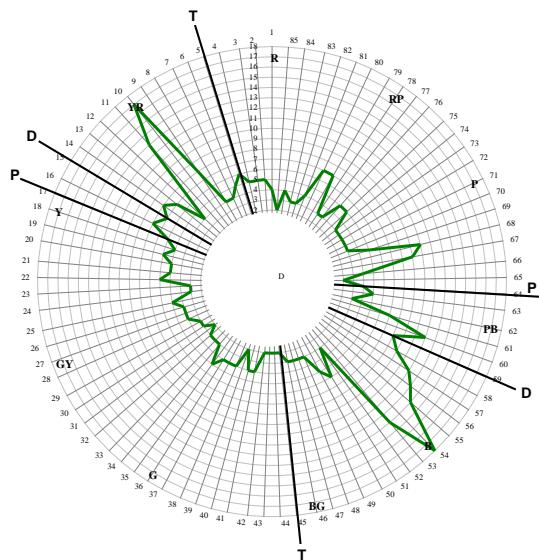


B

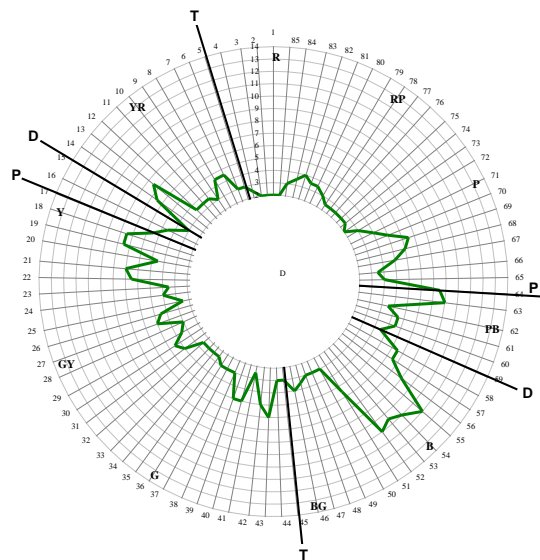


C

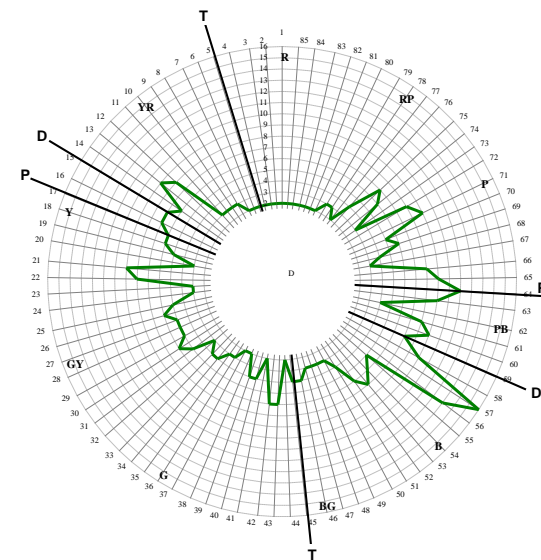
Figure 4.21 A-C – The FM100 plots for Subject 1 in the Case Study group (A - with light source A, B - with light source B, C - with light source C)



A

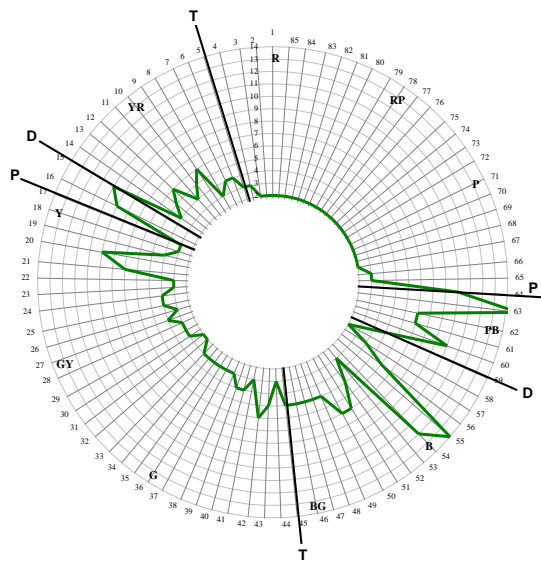


B

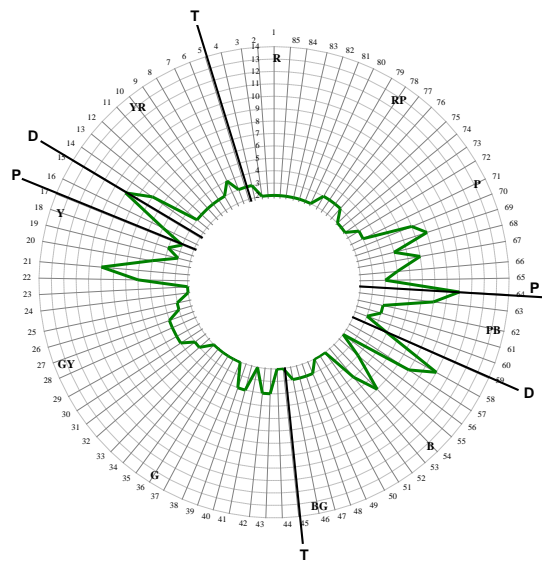


C

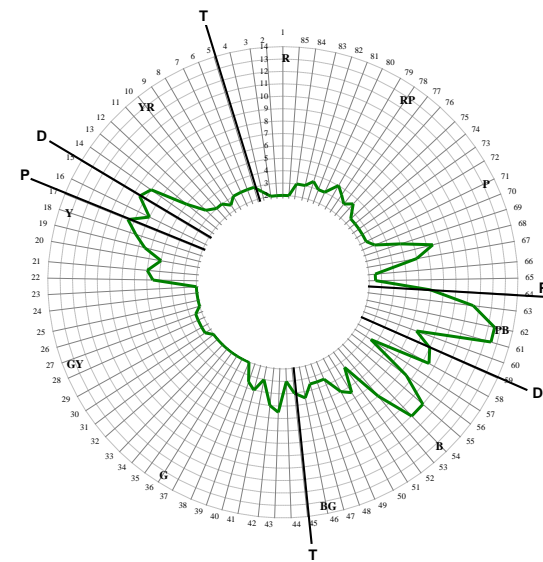
Figure 4.22 A-C – The FM100 plots for Subject 2 in the Case Study group (A - with light source A, B - with light source B, C - with light source C)



A

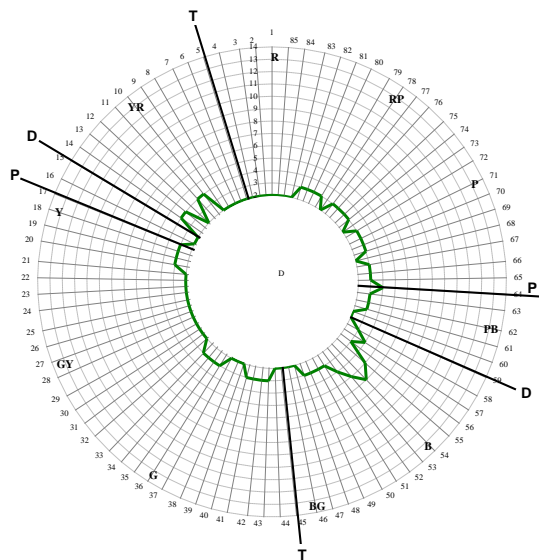


B

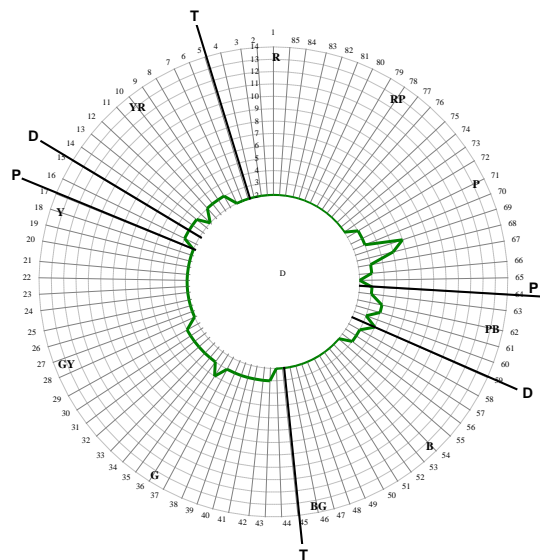


C

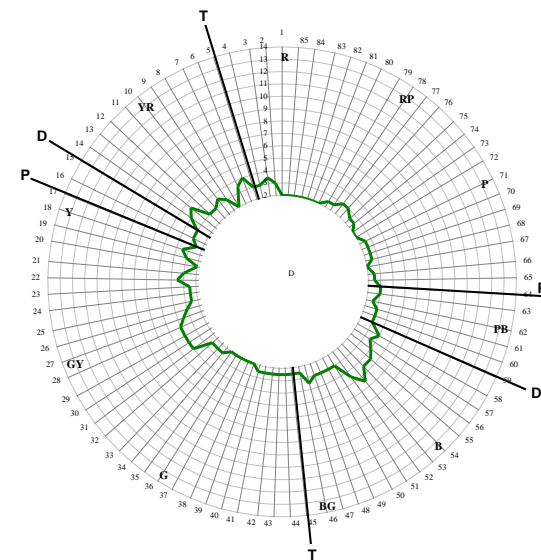
Figure 4.23 A-C – The FM100 plots for Subject 3 in the Case Study group (A - with light source A, B - with light source B, C - with light source C)



A

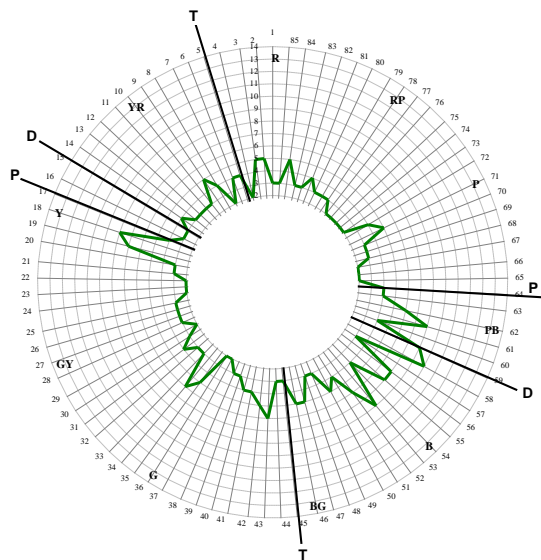


B

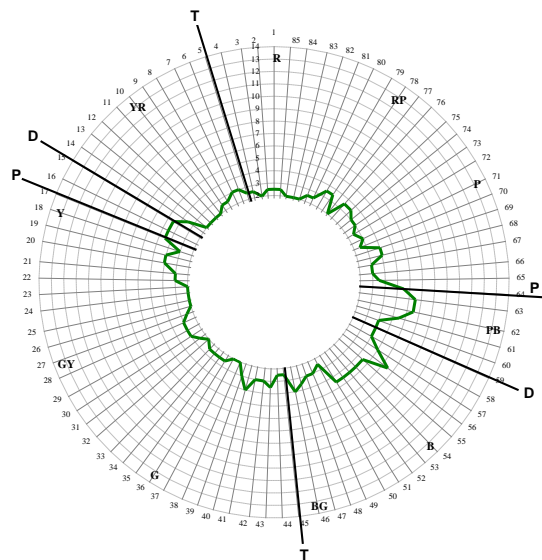


C

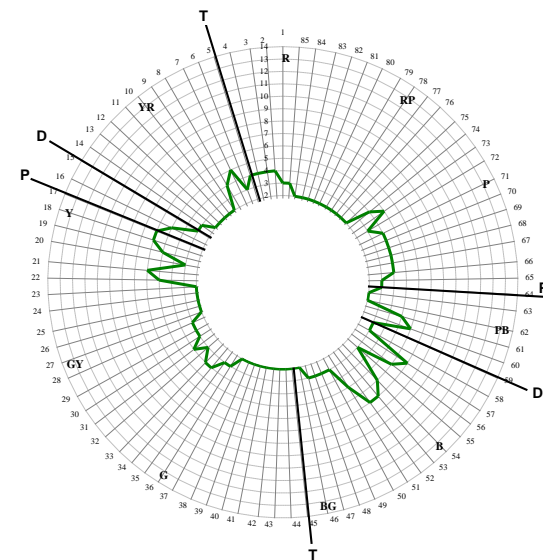
Figure 4.24 A-C – The FM100 plots for Subject 4 in the Case Study group (A - with light source A, B - with light source B, C - with light source C)



A

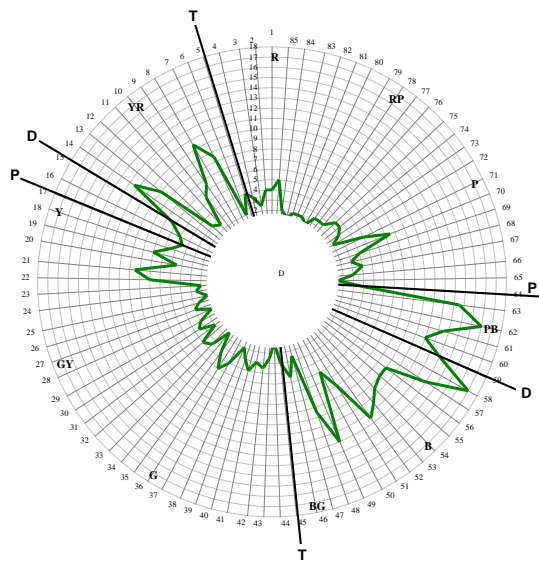


B

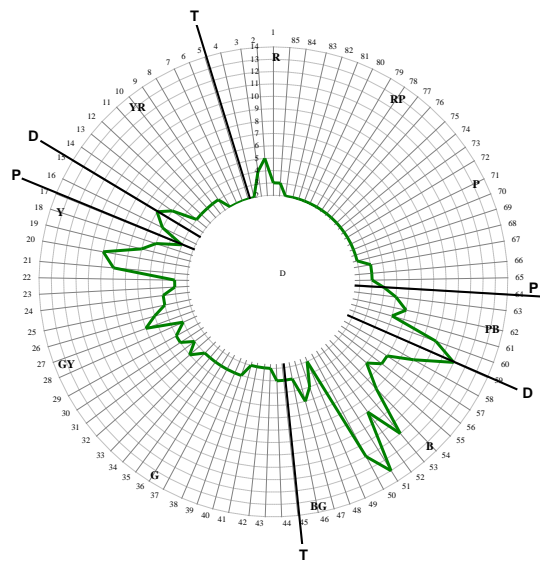


C

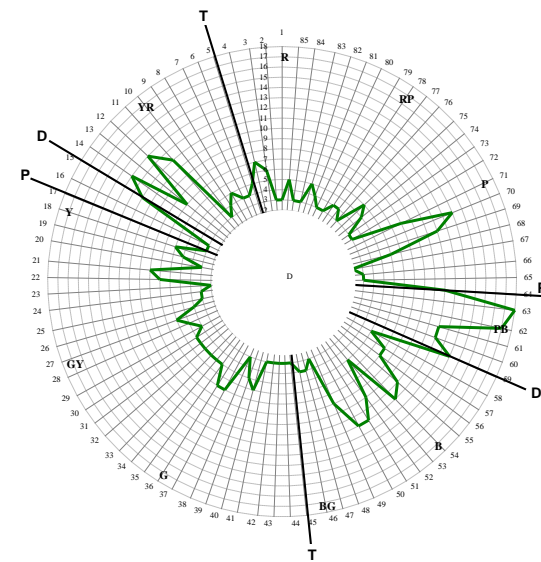
Figure 4.25 A-C – The FM100 plots for Subject 5 in the Case Study group (A - with light source A, B - with light source B, C - with light source C)



A



B



C

Figure 4.26 A-C – The FM100 plots for Subject 6 in the Case Study group (A - with light source A, B - with light source B, C - with light source C)

4.5.2 Case Study Group TES Results

The TES results can be seen in Table 4.25 and Figure 4.27.

Group	Light Source	n	TES \pm SD	Min	Max
Defective/Case Study	THL (A)	6	197 \pm 82.8	60	279
Defective/Case Study	CFL (B)	6	127 \pm 56.3	48	205
Defective/Case Study	LED (C)	6	160 \pm 60.0	76	244

Table 4.25 The TES results for the Case Study group

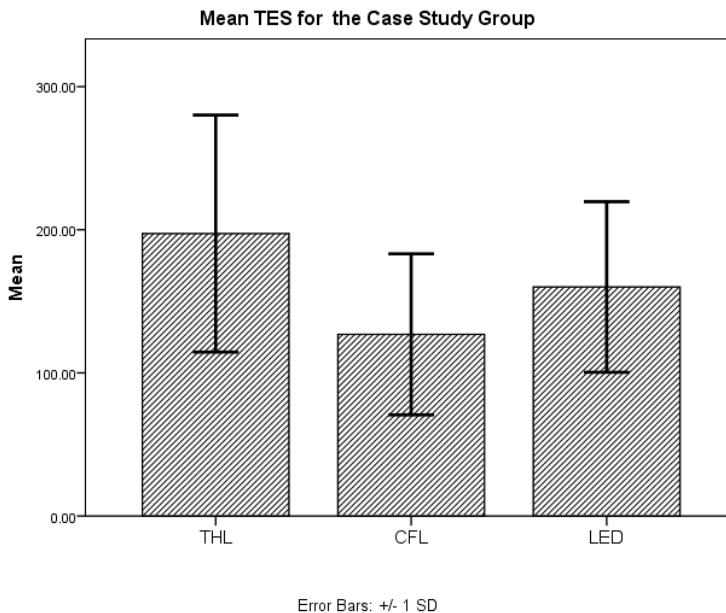


Figure 4.27 The mean TES and standard deviations for the Case Study group for the three light sources

Conducting a Friedman's test showed that there was a significant difference between the light sources for the Defective/Case Study group ($\chi^2(2) = 9.33, p = 0.009$).

The related-samples Wilcoxon signed-rank tests, revealed a significant difference between the THL and CFL ($z = -2.20, p = 0.028$), and the CFL and LED ($z = -2.20, p = 0.028$), but not the THL and LED ($z = -1.57, p = 0.116$). This means that the Case Study subjects displayed better colour discrimination using the CFL than when using

either the THL or the LED, and that there was no significant difference in the TESs of when using the THL compared to the LED.

4.5.3 Case Study Group FM100 Plots

The FM100 plots can be seen in Figure 4.28 A-C. For comparison the plots for the Control group were also plotted.

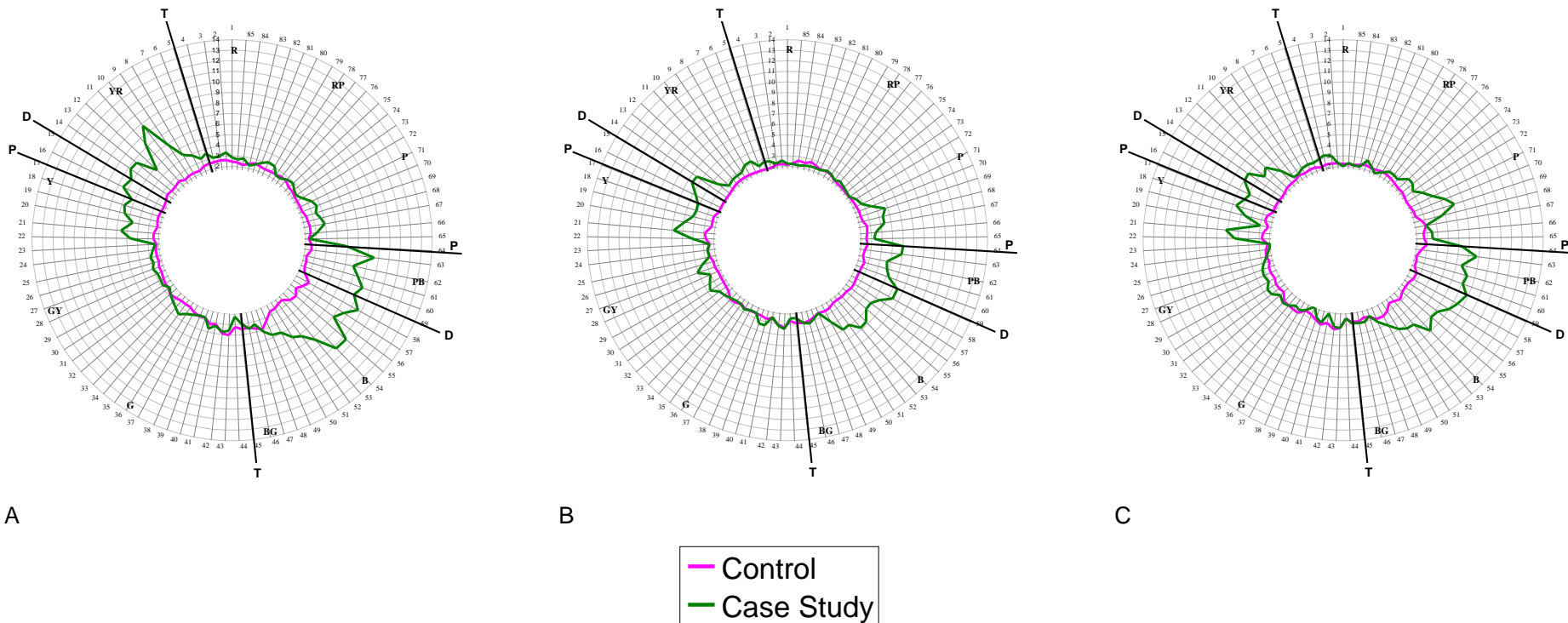
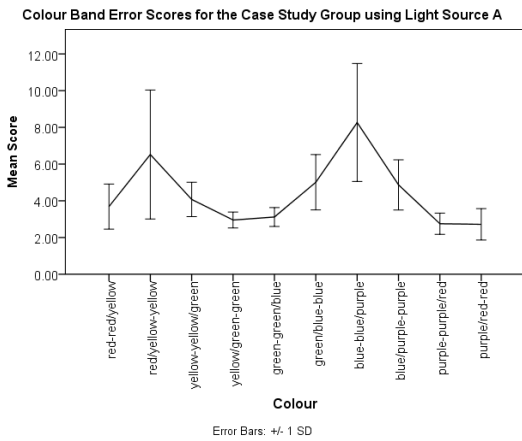


Figure 4.28 A-C – The FM100 plots for the Control group and Case Study group (A - with light source A, B - with light source B, C - with light source C)

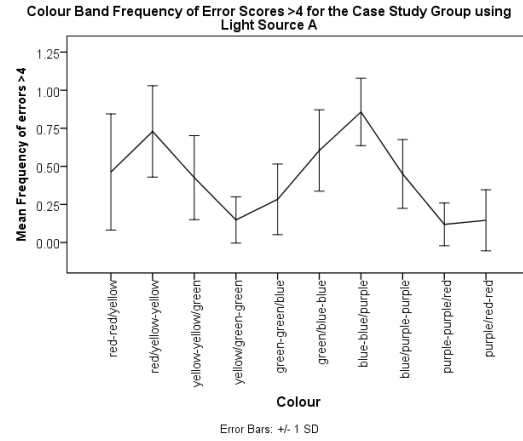
4.5.4 Case Study Group Colour Band Analyses

After splitting the error scores into colour bands, it can be seen that the Case Study group produce greatest errors in the blue-blue/purple, followed by the red/yellow-yellow regions of the spectrum (see Figure 4.29 A-C). This is pattern is confirmed when analysing the colour bands for caps where the error score is greater than four (see Figure 4.29 D-E). The peak errors in the colour bands coincide with the deutan axis of confusion.

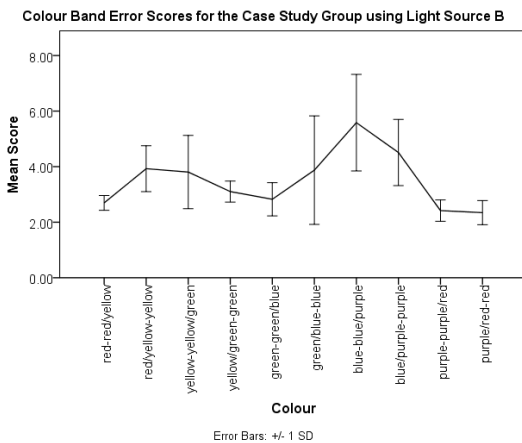
A)



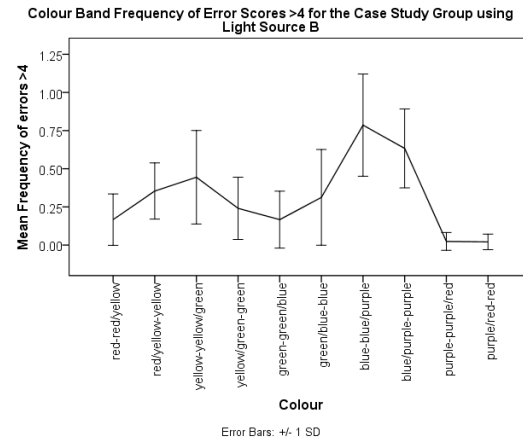
D)



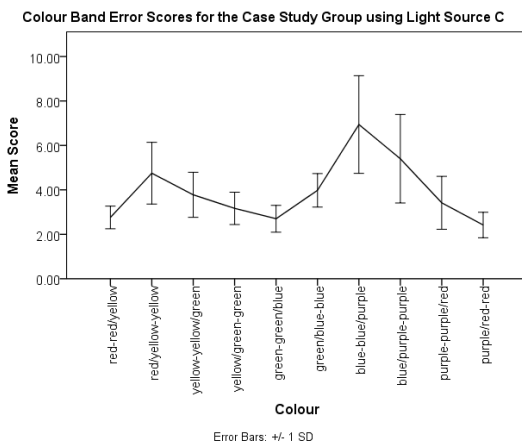
B)



E)



C)



F)

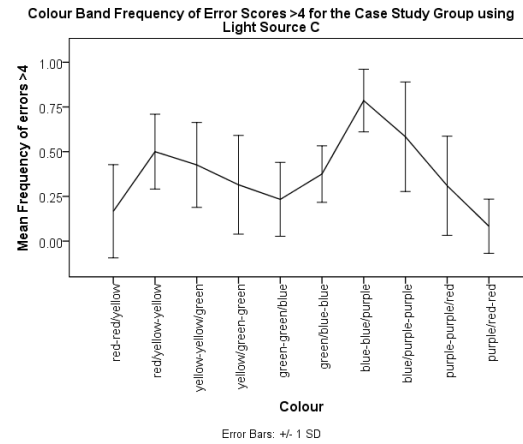


Figure 4.29 Case Study colour band charts: A = Error Score with light source A, B = Error Score with light source B, C = Error Score with light source C, D = Frequency of error scores greater than four with light source A, E = Frequency of error scores greater than four with light source B, and F = Frequency of error scores greater than four with light source C

To see if there was a difference between the light sources for each of the colour bands a series of Friedman's tests were performed.

4.5.4.1 Case Study Colour Band Error Score Analysis

The choice of light source did not result in a significant difference in the CBES for any of the colour bands (see Table 4.26)

Colour Band	Significant Difference	H(2)	p
Red-Red/Yellow	×	4.33	0.115
Red/Yellow-Yellow	×	5.48	0.065
Yellow-Yellow/Green	×	2.65	0.309
Yellow/Green-Green	×	1.65	0.438
Green-Green/Blue	×	3.00	0.220
Green/Blue-Blue	×	0.433	0.155
Blue-Blue/Purple	✓	7.00	0.030
Blue/Purple-Purple	×	1.33	0.513
Purple-Purple/Red	×	5.33	0.069
Purple/Red-Red	×	1.65	0.438

Table 4.26 Summary of the Friedman's tests for the Case study group using Mean Error Scores in the colour bands

A significant difference was found between the light sources in the Blue-Blue/Purple colour band (see Table 4.26). Wilcoxon signed-rank tests found that the CBES was significantly higher with the THL compared to the CFL ($z = -2.20$, $p = 0.028$), but not between the THL and LED ($z = -1.36$, $p = 0.173$), and the CFL and LED ($z = -1.78$, $p = 0.075$).

4.5.4.2 Case Study Colour Band Frequency of Cap Error Score greater than four Analysis

Colour Band	Significant Difference	H(2)	p
Red-Red/Yellow	×	2.67	0.264
Red/Yellow-Yellow	✓	6.09	0.048
Yellow-Yellow/Green	×	0.13	0.939
Yellow/Green-Green	×	1.37	0.504
Green-Green/Blue	×	1.68	0.431
Green/Blue-Blue	×	3.55	0.170
Blue-Blue/Purple	×	1.41	0.494
Blue/Purple-Purple	×	3.52	0.172
Purple-Purple/Red	✓	7.60	0.022
Purple/Red-Red	×	2.00	0.368

Table 4.27 Summary of the Friedman's tests for the Case study group using Frequency of Error Scores greater than four in the colour bands

A significant difference was found between the light sources in the Red/Yellow-Yellow, and Purple-Purple/Red colour bands (see Table 4.27). Wilcoxon signed-rank tests for the Red/Yellow-Yellow colour band found that the FCES4 was significantly higher with the THL compared to the CFL ($z = -2.49$, $p = 0.040$), and the THL and LED ($z = -2.06$, $p = 0.039$), but not the CFL and LED ($z = -1.84$, $p = 0.066$). However, conducting Wilcoxon signed-rank tests for the Purple-Purple/Red colour band did not reveal any significant differences between any of the light sources: THL and CFL ($z = -1.60$, $p = 0.109$), THL and LED ($z = -1.83$, $p = 0.068$), and CFL and LED ($z = -1.84$, $p = 0.066$).

4.5.4.3 Correlation between Mean Error Scores and Frequency of Cap Error Scores greater than four

(Spearman Rho coefficient, Probability) sig. 0.05			
	THL	CFL	LED
Case Study	✓ (0.90, 0.00)	✓ (0.93, 0.00)	✓ (0.93, 0.00)

Table 4.28 Correlation between the CBES and FCES4 for the Case Study group

There is good correlation between the two methods of determining errors for the Case Study group (see Table 4.28).

4.5.5 Case Study Group compared to the Normal/Control Group

The results of for the Case Study group were plotted on the same graph as the Normal/Control group to show how the groups scored for each colour band. As can be seen in Figure 4.30, Figure 4.31, and Figure 4.32, the CBESs appear to be similar in the red-red/yellow, green-green/blue, and purple-purple-red bands; and are most disparate in the red/yellow-yellow, and blue/purple-purple bands.

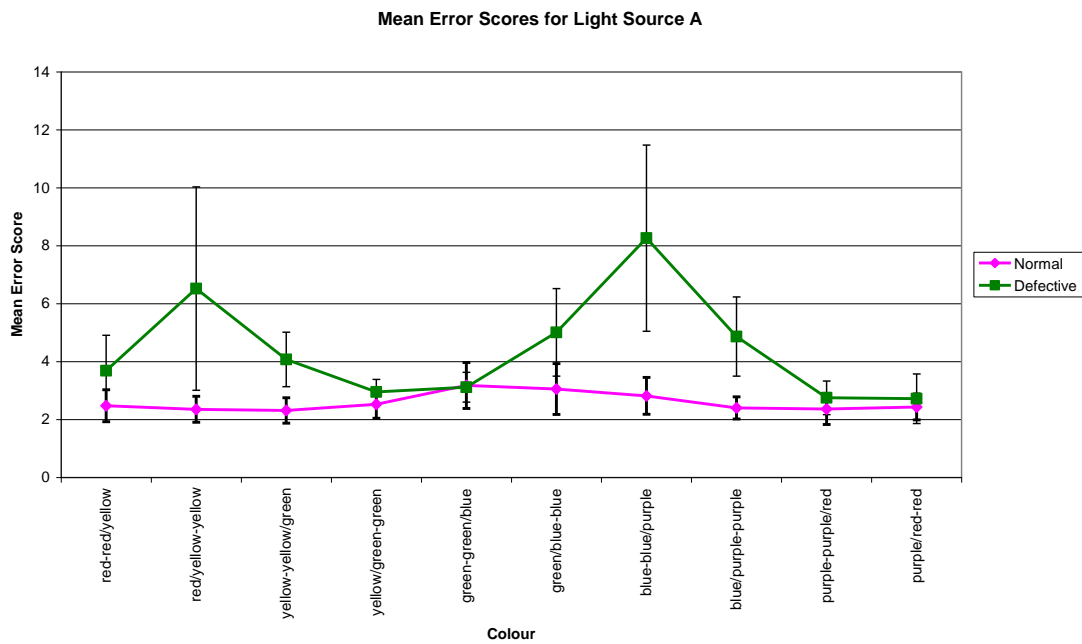


Figure 4.30 Mean error scores for colour bands for subjects in the Control group and the Case Study group when using Light Source A

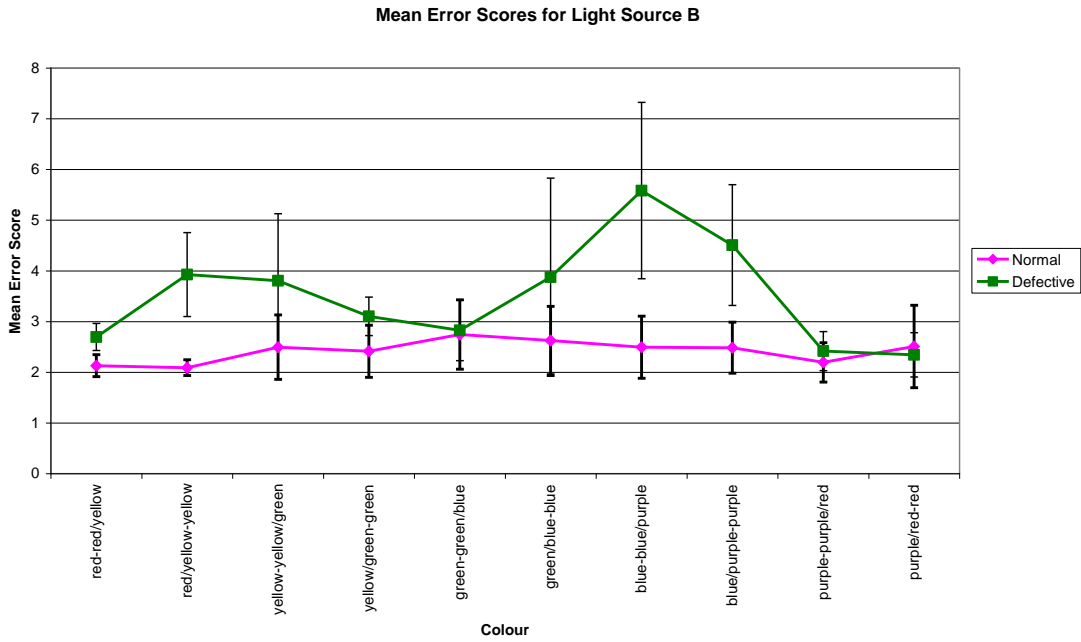


Figure 4.31 Mean error scores for colour bands for subjects in the Control group and the Case Study group when using Light Source B

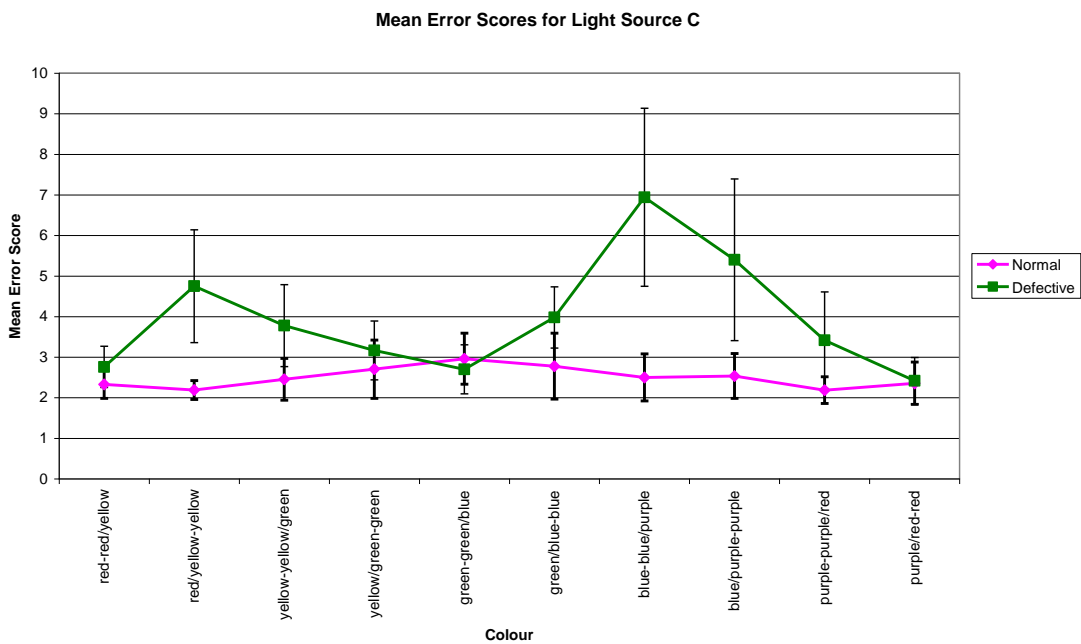


Figure 4.32 Mean error scores for colour bands for subjects in the Control group and the Case Study group when using Light Source C

The results of the two groups were compared using Mann-Witney U tests, and can be seen in Table 4.29, Table 4.30, and Table 4.31.

Test	Significant Difference	U	z	p
Red-Red/Yellow	✓	21.5	-2.21	0.025
Red/Yellow-Yellow	✓	2	-3.56	0.00
Yellow-Yellow/Green	✓	7	-3.25	0.00
Yellow/Green-Green	×	28	-1.74	0.084
Green-Green/Blue	×	52.5	-0.100	0.936
Green/Blue-Blue	✓	9	-3.01	0.001
Blue-Blue/Purple	✓	1	-3.55	0.00
Blue/Purple-Purple	✓	1	-3.56	0.00
Purple-Purple/Red	×	29	-1.71	0.089
Purple/Red-Red	×	46	-0.541	0.608

Table 4.29 Summary of the Mann-Witney U tests comparing scores in each colour band for the Normal/Control group and the Case study group for the THL

Test	Significant Difference	U	z	p
Red-Red/Yellow	✓	6	-3.33	0.00
Red/Yellow-Yellow	✓	0	-3.85	0.00
Yellow-Yellow/Green	✓	22.5	-2.18	0.028
Yellow/Green-Green	✓	15	-2.64	0.006
Green-Green/Blue	×	49.5	-0.302	0.780
Green/Blue-Blue	×	32	-1.49	0.145
Blue-Blue/Purple	✓	4	-3.38	0.00
Blue/Purple-Purple	✓	0	-3.65	0.00
Purple-Purple/Red	×	33	-1.56	0.135
Purple/Red-Red	×	50	-0.285	0.794

Table 4.30 Summary of the Mann-Witney U tests comparing scores in each colour band for the Normal/Control group and the Case study group for the CFL

Test	Significant Difference	U	z	p
Red-Red/Yellow	✓	21.5	-2.20	0.026
Red/Yellow-Yellow	✓	0	-3.70	0.00
Yellow-Yellow/Green	✓	12	-2.84	0.003
Yellow/Green-Green	✓	0	-3.65	0.00
Green-Green/Blue	×	44.5	-0.635	0.546
Green/Blue-Blue	✓	14	-2.69	0.005
Blue-Blue/Purple	✓	1	-3.60	0.00
Blue/Purple-Purple	✓	8	-3.10	0.001
Purple-Purple/Red	✓	5.5	-3.36	0.00
Purple/Red-Red	×	48.5	-0.375	0.728

Table 4.31 Summary of the Mann-Witney U tests comparing scores in each colour band for the Normal/Control group and the Case study group for the LED

As can be seen Table 4.29, Table 4.30, and Table 4.31 there are colour bands where the Case Study subject performed as well as the Normal/Control subjects.

5. DISCUSSION

5.1 Lamps

The SPDs of the lamps were significantly different due to the mechanisms by which the illumination was produced (see Figure 3.2, Figure 3.4, and Figure 3.6). The THL had a continuous SPD as expected by an incandescent source. There was a greater output of light in the red area of the visible spectrum, and this mixed with the other colours in diminishing amounts as the wavelength decreased, and therefore resulted in 'warm white' light with a hint of yellow. The resulting CT was 2800 K. In contrast to this, the SPD of the CFL had peaks due to the phosphors used. There was very little output beyond 640 nm. This light source did not produce a continuous SPD, but more discrete one. The mixture of these peaks resulted in a 'cool white' light, and a CCT of 6500 K, which is the recommended CCT for colour vision testing. The LED SPD was a mixture of the continuous spectrum, like that found with the THL, and a peak, like those found with the CFL. There was a very large peak at 448 nm, and then a trough at 484 nm. The light did not look violet due to the continuous-appearing output between 500-680 nm. Similarly, without the peak at 448 nm, the LED would have looked 'warm white'. As with the CFL, the LED had a CCT of 6500 K.

5.2 Subjects

5.2.1 Age

As age is a significant variable when it comes to FM100 TES [87, 113, 128], it was important that there was no significant difference in the ages taking part in the study between the Control group and the Test group. If there had been, then that could give rise to higher TESs found in the group with older subjects. That was the reason for restricting the age group for the study. The mean age in this study was 27.9 ± 4.4 years. A study by Kinnear and Sahraie did not have an examination group between the ages of 22 and 30, but their results showed a notable reduction in TES between the ages 16 and 39 [113]. Mantyajarvi examined six age groups: 10-19, 20-29, 30-39, 40-49, 50-59, and 60-69 [128], and found the lowest TES in the 20-29 age range, followed by the 30-39 age range. Dain on his study of Daylight Simulators makes no comment on the age of his subjects [125], although in his later work he investigated subjects aged 18-24 [153], Hardy et al used six subjects aged 23-32 [114], Zahirrudin

et al in their control group had subjects with a mean age of 24 ± 7 [7], and Beirne et al split their subjects into two age groups: 20-29, 50-59 [87].

Erb et al examined colour vision in smokers using the Roth 28 Hue test, which uses every third cap from the FM100, and split his study into three groups, whose mean ages were 28.1 ± 10.3 , 28.6 ± 9.6 , and 30 ± 8.4 [149]. Bimler and Kirkland used the Roth 28 and the D15 in their study, and examined subjects aged 18-34 [150].

Thus looking at the studies above, it can be seen that the age range in this study was comparable to the ages tested in studies where age was not the variable being tested.

5.2.2 Pack Years

The calculation of pack years allowed this study to investigate if there was a cumulative effect that smoking had on colour discrimination. However, pack years did not allow a differentiation between the 'dose' of smoking and the 'duration' of smoking, i.e. it could not differentiate a subject that had smoked one pack per day for ten years, from a subject that smoked ten packs per day for one year. Nor did it allow the investigation of any differences which may have occurred due to brand smoked. The subjects in the Smoker/Test group smoked a number of brands, and had switched brands during their time smoking. In addition, many subjects had gone through periods of cessation, although, these were taken into account when calculating their pack years. Unfortunately the restriction on age range also resulted in a restriction to the pack years. The range of pack years in this study was large at 1.25-22 in the Smoker/Test group, but not uniform. The calculation of pack years as a variable allowed this study to investigate the threshold at which smoking became a significant factor in a subject's ability to discriminate colours. Erb et al split their smokers into two groups: those who smoked fewer than 20 cigarettes per day, and those who smoke 20 or more cigarettes per day [149]. Unlike this study, Erb et al did not calculate pack years [149]. Bimler and Kirkland only specified that smokers had to be smoking at least one pack per day for at least one year, beyond this there was no other information in smoking quantities gathered [150].

5.3 Normal/Control Group

Screening with the Ishihara PIC produced some anomalies when those subjects were tested using the FM100. All the subjects in this group scored greater than 21 out of 25, and were deemed to have passed the test. The threshold TES for 'defective colour discrimination' according to Farnsworth is 100; and the maximum normal TES at 95% confidence limit for the age groups tested are shown in Table 5.1. According to Farnsworth's criterion, two of the subjects in the Normal/Control group would have been classed as defective on at least one of the light sources, with one of them averaging higher than 100 across all the three sources. With respect to the 95% confidence limit set by Kinnear and Sahraie [113], five subjects had a TES of >80 for at least one of the light sources, and three of them averaged >80 across the three sources. If using the 95% confidence limit set by Verriest et al [117, 158], only one subject under lay outside this, and that high TES was obtained using the CFL.

Age Range	Normal TES at 95% confidence limit	
	Verriest et al [117, 158]	Kinnear and Sahraie [113]
20-29	107	76-78*
30-39	133	80

Table 5.1 The normal TES at 95% confidence limits for the age ranges in this study. (*Kinnear and Sahraie only tested subjects aged 20, 21, and 22 in this age range)

When testing for normality, the TESs were not normally distributed. The histograms would indicate that there was a positive skew to the data, which concurs with results found by Dain [153]. Some studies have circumvented this problem by taking the square-root of the TES to normalise the data [87, 113, 128, 153]. Dain investigated other transformations performed such as cube roots, fourth roots, and \log_{10} , but these transformations were not universally applicable, and the relationship back to the untransformed data can only be approximated [159]. It was decided that the results were more meaningful if the data were left untransformed, and non-parametric tests were employed.

When comparing the TES of the Control group with the age-matched results for subjects with normal colour vision, it was seen that the results for all three light sources compared favourably. For this study they were: THL 50.6, CFL 36.2, and LED 43.8; which were comparable with Kinnear and Sahraie 44-50 [113], and Mantyajarvi 55.4-60.8 [128]. Whereas lower TES were found by Dain 20-28.4 [153],

and Beirne et al had a TES of 10.3 [87]; A higher TES was found by Zahirrudin et al 70.2 [7].

Statistical analysis on the TES of the Normal/Control group was carried out in two ways: firstly by using a Friedman's test followed by multiple Wilcoxon signed-rank tests, and secondly by using DTAs.

The Friedman's test indicated that there was a difference between the light sources, and multiple Wilcoxon signed-rank tests found that the difference in TES was significant between the THL and the CFL. The THL had the higher TES, and therefore resulted in poorer colour discrimination when compared to the CFL. This was despite the THL having a CRI of 100. However, the THL was the light source whose CT that deviated from the recommended light source (Standard Illuminant D_{65}) by the greatest, and so one would expect it to result in higher TESs.

The LED was not found to be statistically different to either the THL or the CFL with respect to TESs. The CCTs of the LED and the CFL were the same, and despite this the TESs obtained using the LED were not significantly better than the THL.

5.4 Smoker/Test Group

As with the Normal/Control group, the Smoker/Test group also had some disagreement between the Ishihara PIC and the FM100 in classification of normal and defective colour vision. All the subjects in this group passed the Ishihara PIC. Using Farnsworth's threshold of a TES of >100 indicating defective colour discrimination, three of the subjects had defective colour discrimination for at least one of the light sources, and one of them had an average TES of >100 across the three sources. When considering the 95% confidence intervals in Table 5.1, eight subjects lay outside this interval set by Kinnear and Sahraie [113] for at least one of the light sources, and three of them had an average TES across all three light sources >80 . None of the subjects had a TES greater than the 95% confidence interval set by Verriest et al [117, 158].

The mean TESs found in the Smoker/Test group were, at first glance, similar to the results of the Normal/Control group. The means and medians were more tightly grouped than the Normal/Control group. The data fitted a normal distribution for the

THL and LED light sources, but not for the CFL. As with the Normal/Control group, the TESs for the three light sources for the Smoker/Test group were positively skewed. Due to the data not fitting a normal distribution, non-parametric tests were applied to this data.

The same analyses were applied to the Smoker/Test group, and the results showed there was no statistically significant difference between the light sources. As with the Normal/Control group the TESs using the THL were highest (mean and median), and the CFL had the lowest TES (mean and median). However, unlike the Normal/Control group, this difference was not statistically significant. This is because the difference between the mean THL and the CFL was smaller in Smoker/Test group (5.9) compared to the Normal/Control group (14.4).

5.5 Normal/Control versus Smoker/Test

The mean and median TESs were slightly higher in the Smoker/Test group than the Normal/Control group for the CFL and LED. For the THL the means were identical, but the Normal/Control group had a higher median. However, no significant differences in TESs were found. This would suggest that in this study the act of smoking itself did not influence colour discrimination. DTAs were conducted to increase the power of the statistical analyses.

5.6 Decision Tree Analyses on Total Error Scores

The second method of analysing the data was to use DTAs. This facilitated an element of data mining. When using 'Light source' and 'Group' as variables, no significant differences were found. If this is put into the context of the questions posed at the beginning of the study, it would suggest that the three light sources allowed similar levels of colour discrimination, and that non-smokers and smokers had similar levels of colour discrimination. This mostly agrees with the analyses conducted above, and casts some doubt over the result from Friedman's test comparing the light sources for the Normal/Control group.

However, Erb et al showed that smoking itself was not found to be damaging to colour vision when fewer than 20 cigarettes were smoked per day [149]; therefore by

removing 'Group' as a variable and replacing it with 'Pack years' the cumulative of effect of smoking was explored. This time, the number of pack years was a significant variable. This would concur with the findings of Erb et al, that smoking itself did not impair colour discrimination when smoking was below a certain threshold. Above this threshold, colour vision was impaired by smoking [149]. That threshold for damage was only found using a DTA with 'Pack years' as a variable, and not in the individual analyses. In this study that threshold was found to be 7.5 pack years. Unfortunately, this is not directly comparable to the results of Erb et al [149].

5.7 Comparing the colour discrimination for different colours

Traditionally there are three ways in which colour discrimination for different colours can be assessed: firstly by looking at the FM100 plots for peaks in errors, secondly partial error scores, and thirdly by taking the error scores of each box. The first method is qualitative, and relies upon the judgement of the observer. However, it is useful to examine the plots to get an overview of how the test was performed. In cases of severe defects for certain bands e.g. moderate anomalous trichromacy, the plots allow the observer to make an initial assessment, and provisional diagnosis. The second method of partial error scores categorises red-green error scores from caps 13-33, and 55-75; and blue-yellow error scores from caps 1-12, 34-54, and 76-85. Partial error scores are useful in determining CCVD as they assess error scores along the axes found in CCVD [87, 113]. The third method of 'box error scores' is often used as a simple way of further analysing the FM100 to see pathology or other such variable has a greater effect on certain parts of the spectrum. For example Mantyjarvi et al used the fourth box error scores (caps 64-84 corresponding to blue/purple-red part of the spectrum) in both their study of colour vision in phakic and pseudophakic eyes [160], and also when they investigated normal error scores [128]. However, as there are only four boxes, there was not enough information to ascertain discrimination for each colour. Therefore for this study, ten colour ranges were chosen and their cap ranges determined from the FM100 plot itself. This allowed a quantitative analysis of the colours affected which cannot be obtained by looking at the FM100 plot; and a more detailed analysis than assessing the four boxes. As the colour ranges had unequal numbers of caps in them, the average cap error score in each colour band was calculated. A novel approach was employed in this study to count the number of occasions in each colour band that a cap error score exceeded

four (chosen because the maximum mean cap error score was 4.05, and thus would indicate a significant error), and an average taken in order to remove the cap-number bias that would exist due to unequal band sizes. The purpose of this was to highlight the areas of higher loss of discrimination.

5.8 FM100 Plots

Looking at the plots for the Normal/Control group for the THL (see Figure 4.9 A) it can be seen that there appeared to be three peaks in error scores. The largest of them is at cap 43 (green-green/blue), followed by cap 48 (green/blue-blue), and cap 58 (blue-blue/purple). For the CFL (see Figure 4.9 B) there were again three peaks: at cap 43 (green-green/blue), cap 21 (yellow-yellow/green), and cap 82 (purple/red-red). Whereas for the LED (see Figure 4.9 C), peaks were at cap 42 (green-green/blue), cap 50 (green/blue-blue), and cap 67 (blue/purple-purple). The plots for the CFL and the LED were similar shapes. The spread of peaks was lowest for the THL, and greatest for the CFL. Comparing this with the TESs, the THL had the highest TES and the narrowest range of peaks, but the highest peaks and the greatest range in cap error scores (1.87). This would suggest that in this colour discrimination with the THL between caps 43 and 58 is not as accurate as with the CFL or LED. The CFL had the lowest range of cap error scores (1.25), but had the largest spread of peaks, and the lowest TES; this would suggest that the CFL should provide the best colour discrimination across the whole spectrum.

For the Smoker/Test group the peaks for the THL were at cap 42 (green-green/blue), and cap 47 (green/blue-blue) (see Figure 4.9 D); for the CFL caps 43 (green-green/blue), 81 (purple/red-red), and 64 (blue/purple-purple) (see Figure 4.9 E); and for the LED caps 43 (green-green/blue), 33 (yellow/green-green), and 82 (purple/red-red) (see Figure 4.9 F). As with the Normal/Control group, the THL had the narrowest range of peaks, and in this case only had two significant peaks. The LED had additional smaller peaks, and also had the largest range of peaks. Unlike the Normal/Control group, the range of cap error scores in the Smoker/Test group was smallest with the THL. The cap error score ranges for the other two light sources were very similar, as were the range of peaks on the plots. Thus the conclusions to be drawn from the Smoker/Test group are less clear. The spreads of TESs and cap error scores were narrower than for the Normal/Control group.

When comparing the FM100 plots for the Normal/Control group and the Smoker/Test group for the THL, the shapes of the plots look very similar. The same can be said for this comparison for the CFL and the LED.

Relating this to the wavelength discrimination curve in Figure 1.21, where the two most significant minima are at 490 nm (green/blue) and 590 nm (red/yellow), and there are peaks at approximately 530 nm (green) and 475 nm (purple/blue), some discrepancy can be found. The peak error at cap 42-43 corresponds to 496-498 nm, and the peak $\Delta\lambda$ s are at cap 35 and cap 65. This highlights the difference between the wavelength discrimination and the colour discrimination seen with the FM100.

However, the peaks in the FM100 plots are small (cap error score of <4), and are not large enough to indicate an axis of confusion. The peaks are more likely to be an artefact of the perceptual non-linearity associated with the FM100, for which Farnsworth reduced the number of caps from 100 to 85 [83].

5.9 Colour Band Error Scores

As seen by the plots (see Figure 4.10 A-F), there was good agreement between the colour band error scores (CBESs) and the FM100 plots (see Figure 4.9 A-F). The peak errors occurred in the green-green/blue part of the spectrum for all groups except the Smoker/Test group using the THL (where the peak was in the green/blue-blue band).

When looking at the plots for the Normal/Control group the peak CBESs were highest for the THL. The THL also had higher CBESs for the red-red/yellow green-green/blue, green/blue-blue, blue-blue/purple, and purple-purple/red parts of the spectrum. The CFL had lower CBESs across the whole spectrum (except for yellow-yellow/green – where THL was lowest). This difference between the THL and CFL was most evident in the red-red/yellow, green-green/blue, and the green/blue-blue parts of the spectrum. The LED CBESs lay between the THL and CFL for most of the spectrum (with the exception of yellow/green-green where it had higher errors than both THL and CFL). The CFL had the lowest TES, and the lowest CBESs for most of the colour bands. However, there is considerable overlap of error bars (one standard deviation), which reduces the significance of these findings. This was reinforced by noting the lowest mean CBESs: 2.31 for the THL, 2.09 for the CFL, and 2.19 for the

LED; and the highest mean CBESs: 3.12 for the THL, 2.74 for the CFL, and 2.96 for the LED. That meant that there was a mean CBES difference of <1 between the minimum and the maximum for each light source.

For the Smoker/Test group the plots showed less variation. The CBESs appeared very similar for all three light sources. The THL has higher CBESs for red-red/yellow, green/blue-blue, and blue-blue/purple areas of the spectrum. The CFL had the highest peak in the green-green/blue part of the spectrum, but otherwise had the lowest CBES. The LED had the highest CBES in the yellow/green-green part of the spectrum, but was otherwise similar to the CFL in the red-red/yellow, red/yellow-yellow, and yellow-yellow/green parts of the spectrum; and similar to the THL for blue/purple-purple, purple-purple/red, and purple/red-red parts of the spectrum. This similarity is evident in how similar the TES are with the three light sources. The lowest mean CBESs were 2.33 for the THL, 2.22 for the CFL, 2.21 and for the LED. Whereas the highest mean CBESs were 3.05 for the THL, 3.02 for the CFL, 2.96 and for the LED

When comparing the Normal/Control group with the Smoker/Test group for the THL, the Normal/Control group had higher CBESs in the yellow/green-green, green-green/blue, and the blue-blue/purple parts of the spectrum; but the Smoker/Test had higher CBESs in blue-purple-purple, purple-purple/red, and the purple/red-red parts of the spectrum. However, the graphs look very similar.

When using the CFL the Smoker/Test group had slightly higher CBESs than the Normal/Control group in the red-red/yellow, red/yellow-red, and the purple-purple/red parts of the spectrum. The difference between the two groups seemed to be highest for the green-green/blue, green/blue-blue colour bands, here the smokers had higher CBESs than non-smokers. The Normal/Control group did not appear to have notably higher CBESs than the Smoker/Test group for any of the colours.

For the LED, the Smoker/Test had higher CBESs than the Normal/Control group in the purple-purple/red, and the purple/red-red parts of the spectrum; otherwise the graphs looked very similar.

5.10 Decision Tree Analyses on Colour Band Error Scores

Using DTAs it was found that for some of the colour bands (yellow-yellow/green, green/blue-blue, blue-blue/purple, blue/purple-purple, purple/red-red) neither the 'Light source' nor the 'Pack years' were deemed to be significant (see Table 4.15).

For the red-red/yellow colour band the first split was due to 'Light source' (see Figure 4.11). The THL was on one branch (with the higher CBES), and CFL and LED on the other. This agrees with the plots of CBESs (see Figure 4.10 A-F). There was no further splitting of the THL node; this suggested that smoking had no affect colour discrimination in red-red/yellow colour band if using the THL as the illumination source. The CFL/LED branch underwent another two depths of splits. The first depth off this node was split by pack years. However, what was a little anomalous was that the node with the lowest CBES had the greatest number of pack years (>11.25), in the middle was lowest number of pack years (≤ 7.5), and the highest CBES was found in the remaining group (7.5-11.25 pack years). A possible reason for this was the low number of subjects in the two extreme nodes. The two extreme nodes combined constituted less than 20% of the subjects in that depth of the tree. There was one more depth below this, and this was the split of the largest node on the second depth (pack years ≤ 7.5) by 'Light source'. Here the CFL had a slightly lower CBES than the LED.

In the red/yellow-yellow band the DTA showed that the light source was the most significant variable (see Figure 4.12). As with the first depth on the DTA for the red-red/yellow part of the spectrum, the THL forms one node, while a second node is the combination of CFL and LED. Therefore for these two adjacent colour bands (encompassing red-red/yellow-yellow) the THL resulted in higher error scores, than the grouping of LED and CFL. Ergo, if colour discrimination in colours red-yellow is particularly important, then using an LED or CFL would be the better choice (despite the THL having such a high CRI). This is in good agreement with the CBES plots, where both the Normal/Control group and Smoker/Test group showed an increase in error score in the red-red/yellow-yellow part of the spectrum when using the THL when compared to the CFL and the LED. When looking at the SPDs of the THL (see Figure 3.2) it can be seen that the THL output in the higher wavelengths (that correspond to red and orange) were higher than for the other two lamps

Heading into the yellow-yellow/green part of the spectrum, the results seemed to level out between the three light sources, and smoking was not found to be a significant variable.

For the yellow/green-green part of the spectrum the significant variable was the light source (see Figure 4.13). However, here the LED resulted in the higher error scores, and the THL and the CFL were combined in the group with the lower error scores. When looking at the SPDs of the lamps (see Figure 3.2, Figure 3.4, and Figure 3.6), it can be seen that for the yellow/green-green range (wavelengths 525-560 nm) the average output of the LED was greater than that of the THL and CFL. In this range the THL and CFL were similar.

For the green-green/blue band the number of pack years was the significant variable (see Figure 4.14). In particular, a distinction was made between subjects with ≤ 7.5 pack years and those with > 7.5 pack years. This was the same the same as the DTA for the TES. As with the TES it is important to stress that smoking itself did not increase the CBES, but cumulative effect of smoking was significant.

Of great interest was the neighbouring colour band: green/blue-green. The CBESs are near the peak, but this time there is no significant variable found. One would expect a similar effect to be found in this part of the spectrum as in the green-green/blue. This could cast some doubt over either of the colour bands and would require further testing to confirm the results.

For the next two colour bands (blue-blue/purple and blue/purple to purple) the CBESs were decreasing for both groups with all three light sources. The changes in CBESs were similar as neither variable was found to be significant.

The DTA for the purple-purple/red band found the number of pack years to be the significant variable (see Figure 4.15). However, the cut-off found was 3.75 pack years. The group with ≤ 3.75 pack years had a lower error score. This suggested that smoking had its greatest effect in this colour band, and concurred with the CBES plots. The plots show that for all light sources the Smoker/Test group had higher error scores than the Normal/Control group. Looking at the lamp SPDs it was expected that the LED would result in higher CBES due to the large peak.

Finally, for the purple/red-red part of the spectrum no significant variable was found.

In summary, the light source had a significant effect on the red-red/yellow, red/yellow-yellow, and yellow/green-green parts of the spectrum. The THL produced significantly higher error scores for red-red/yellow-yellow region, and the LED significantly higher error scores for the yellow/green-green band. Smoking was significant in the TES and green-green/blue part of the spectrum at the level of 7.5 pack years, and in the purple-purple/red part of the spectrum at a level of 3.75 pack years. Smoking also had an influence on the red-red/yellow part of the spectrum for the CFL and LED, but not the THL.

On the FM100 plot, the green-green/blue is almost opposite the purple-purple/red (it is actually opposite the purple/red-red, and the green/blue-blue is opposite the purple-purple/red). This could indicate the development of an axis of confusion.

5.11 Frequency of Cap Error Scores greater than four

As with the CBES, the frequency of cap error scores greater than four (FCES4) (see Figure 4.16 A-F) showed good agreement with the FM100 plots (see Figure 4.9 A-F). However, with FCES4 there were two plots that peaked in the green/blue-blue part of the spectrum: Smoker/Test subjects using the THL, and the Smoker/Test subjects using the LED. All the other subject groups peaked in the green-green/blue part of the spectrum.

For the Normal/Control group the FCES4s were highest for the THL for the red-red/yellow, red/yellow-yellow, green-green/blue, and the green/blue-blue parts of the spectrum. The scores for the CFL were the lowest for all except the yellow-yellow/green and the blue-blue/purple (where it lay in between the other two sources), and the purple/red-red (where it had the highest FCES4).

For the Smoker/Test group the results with the THL and CFL followed similar paths. The exceptions to this lay in the red-red/yellow and the blue-blue/purple bands (where the THL FCES4 was higher), and the positions of the peaks (with the THL peaking in the green/blue-blue, and the CFL peaking in the green-green/blue). The significant change from the previous plots is the change in peak for the LED from green-green/blue to green/blue-blue. This is due to the results of this method not being biased by very high cap error scores.

When comparing Normal/Control group with Smoker/Test group for the THL the plots looked very similar to those found with the CBES plots. The Normal/Control group had a higher peak in the green-green/blue band, otherwise they were very similar.

For the CFL are roles are reversed, with the Smoker/Test group had the higher FCES4 that the Normal/Control group. This concurred with the CBES plots.

The plots for the LED were also very similar for Normal/Control and Smoker/Test groups. The only notable differences when compared to the CBES plots were that there was a higher FCES4 for the Normal/Control group in the yellow-yellow/green band (this is the other way round for the CBES plot), there was a slight shift in the peak for the Smoker/Test group, and that the Normal/Control and Smoker/Test groups were closer purple-purple/red and purple/red-red bands for the FCES4.

All the plots (be they CBES or FCES4) showed low error in the yellow bands, peak errors green-blue, a dip in errors in the purple band, before a slight increase in the red band. However, as with the CBES plots there is substantial overlap of the error bars across all plots.

5.12 Decision Tree Analyses on Frequency of Cap Error Scores greater than four

As with the DTAs for CBES, the DTAs for FCES4 in the red-red/yellow band and the red/yellow-yellow band separated the THL from the CFL and LED (see Figure 4.17 and Figure 4.18). The THL had a significantly higher FCES4 than either the CFL or the LED for the red-red/yellow-yellow part of the spectrum. Unlike the DTA for CBES which has three depths, there was only one depth to this DTA for FCES4 for the red-red/yellow band. This was the expected result when looking at the SPDs of the lamps (see Figure 3.2, Figure 3.4, and Figure 3.6).

There were no significant variables found for the next two colour bands: yellow-yellow/green, and yellow/green-green (see Table 4.21). The yellow-yellow/green result was in agreement with the CBES, whereas the yellow/green-green there was a difference between the two methods. This suggests that there were a significant

number of small cap error scores when using the LED in yellow/green-green band which the FCES4 deemed as insignificant.

The DTA for the green-green/blue for FCES4 was the same as for CBES. The threshold for significance was again 7.5 pack years (see Figure 4.19).

There were no significant variables found for the remaining colour bands: green/blue-blue, blue-blue/purple, blue/purple-purple, purple-purple/red, and purple/red-red (see Table 4.21). The difference here lies in the purple-purple/red band; for CBES the threshold for significance was only 3.5 pack years, but for FCES4 pack years were not found to be significant.

5.13 Comparison between Methodologies

By counting the frequency of significant errors, the FCES4 method reduces the influence of extreme error scores. Thus error scores of four or less were not counted, and therefore small transpositions did not penalise the subject. The score for subjects that has made a very large error (a misplaced a cap), but had otherwise scored well, was not biased either. This suggests that FCES4 was not as sensitive as CBES in detecting changes. What was difficult to determine was whether CBES introduces a type 1 error, or whether FBES4 introduces a type 2 error. It is more likely that the FCES4 method reduces the type 1 error of the CBES method.

The correlation between CBES and FCES4 is good for both groups with all three light sources. Although the coefficient was not 1, the probability in all cases was less than 0.005. FCES4 may provide a suitable alternative to CBES in assessing which colours are being poorly discriminated (see Table 4.22).

5.14 Correlation between Pack Years and Colour Vision

Having seen a significantly higher TES in smokers with >7.5 pack years, it was surprising not to find a correlation between pack years and TES (Table 4.23). The scatter plots did not show any correlation between TES and pack years (see Figure 4.20). For the THL the Spearman Rho coefficient was 0.00, which suggests that smoking had no effect on colour discrimination under the THL. The coefficients were

a little higher for the LED, and higher still for the CFL. However, neither was statistically significant. There are a few explanations for the discrepancy between the DTA of TES producing a significant difference, without correlations being present. Firstly, the correlations may be influenced by outliers. When looking at the DTA of the CBES for the red-red/yellow, the node with the highest number of pack years (>11.25) had a lower error score than that found in the node with 7.5-11.25 pack years. Secondly, the relationship between pack years and TES may not be linear. The analysis was carried out using both the Normal/Control group and the Smoker/Test group; as a result the number of pack years is very positively skewed. However, conducting the same analyses on the Smoker/Test group, the Spearman Rho coefficients and probabilities are still not significant: THL (0.11, 0.66), CFL (0.36, 0.14), and LED (0.25, 0.31). The study requires expansion, not just in the number of smokers recruited, but also a more even distribution of pack years.

Looking at the correlation between pack years and the CBES (see Table 4.23), the only statistically significant result was found in for the LED in the purple-purple/red. There was no significant correlation found for the green-green/blue band (which showed a threshold of 7.5 pack years for the DTA). The reasons for this lack of correlation when pack years appeared to be a significant variable are shared with the TES correlations noted above. The result in the purple-purple/red for the LED, may suggest an anomalous result as it is in isolation.

Not surprisingly, the correlations using the FCES4 for the colour bands, shows a similar result (see Table 4.24). However, this time the only statistically significant finding was with the CFL in the purple-purple/red group. This may suggest that there is some issue in this part of the spectrum for smokers with higher pack years (as it did with the CBES correlations), however this band was not found to have any significant variables in the DTA of FCES4.

There does not appear to be any significant correlation between pack years and colour discrimination. As mentioned above, this does not rule out a detrimental effect on colour vision by smoking, but suggests further research is required using a larger Smoker/Test group with pack years that are more evenly distributed.

5.15 Proposed Mechanism for Colour Vision Defects in Smokers

As the differences between the Normal/Control group and the Smoker/Test group were subtle, it is difficult to draw many conclusions on the mechanism for any differences found. Smoking was shown to be significant when it exceeded 7.5 pack years for the TES, and in the green-green/blue part of the spectrum for both CBESs and FCES4. Green/blue-blue are caps 36-45, and may indicate the start of a Type 3a defect as the axis of confusion for this would be around cap 45-46 (see Table 1.5 and Table 5.2). This is contradiction to the red-green defect found by Bimler and Kirkland on the D15 and desaturated D15 [150], and Erb did not find any clear axis of confusion [149]. At this stage the mechanism can only be speculated upon. One such mechanism is the development of very early lens opacities which may be induced by smoking [136, 149]. Lens opacities have been shown to result in type 3 defects as they absorb a greater proportion in the short-wavelength light [62]. Another mechanism is the change to macular pigment. Changes to macular pigment have been suggested as a cause for colour vision changes in an aging eye [87]. Smokers may have reduced macular pigment, which then results in an increase to oxidative damage to the retina and RPE, which in turn leads to RPE atrophy, and ultimately ARMD [136, 148]. However, mild ARMD was not found to cause a colour vision defect [62]. Vascular abnormalities are found in smokers [141, 143], and reduced blood flow may impact on the metabolism of the retinal tissue [149]. If this results in hypoxia and damage to the photoreceptors, then a type 3 defect may be expected, as proposed by Bimler and Kirkland due the S-cone fragility [150].

5.16 Case Study Group

All the subjects in the Case Study group had colour vision defects, and were deemed to be deuteranomalous trichromats. As can be seen from Table 1.3, the most prevalent CCVD is deuteranomalous trichromatism, and with a higher frequency in the male population compared with the female population [10, 19, 45, 152], therefore it was not a surprise that the Case study group comprised mainly of males with deuteranomalous trichromatism. The TESs were 197 ± 82.8 for the THL, 127 ± 56.3 for the CFL, and 160 ± 60.0 for the LED. When examining 117 deuteranomalous subjects with an average age of 26.5, Birch found an average TES of 112.5 ± 62.5 [110]. As TES increases with age 22 years old [113], the higher TESs in the Case

Study group, compared to Birch's results, were expected as the average age of the Case Study group was higher than in Birch's study [110].

The degree of defect measured using the Ishihara PIC varied within the group. The subject with the highest number of correct Ishihara PIC identifications (11) was the only subject to have a TES of <100 for all three light sources (see Figure 4.24 A-C). As the maximum normal TES at the 95% confidence limit in the age group 30-39 years old is 80-133 [113, 117, 158] (see Table 5.1), then it is possible to have classed this subject as having normal colour vision as their TESs were 60 (THL), 48 (CFL), and 78 (LED). Farnsworth's own grading would have classed this subject as having 'average colour discrimination' [111]. If comparing this subject's combined TES for all three light sources with the subjects from the Normal/Control group, they would be ranked 14th out of 19. As an aside, one of the subjects in the Normal/Control classed as having normal colour vision with the Ishihara PIC had TESs of 120 (THL), 136 (CFL), 96 (LED) i.e. defective colour discrimination using the FM100 [111, 113]. This is an example of the discrepancy that exists between the two colour vision tests, and why the FM100 is not designed for screening [110].

A great deal of variation was seen across the subjects when looking at their individual the FM100 plots (see Figure 4.21, Figure 4.22, Figure 4.23, Figure 4.24, Figure 4.25, and Figure 4.26). Subject 1 had large errors around caps 10 and 58, and low errors in regions of caps 25-48 and 66-9 for the THL. A much smaller plot was produced for the CFL with peaks at caps 14 and 58. The LED plot is a little larger than the CFL, but had a pronounced error at cap 58. A similar picture is seen for subject 2; the THL has peaked at caps 10 and 54, the CFL at cap 54, and the LED at caps 13, 56, and 64. The plots for subject 3 were a little more even. For the THL the plot was smaller than for the previous two subjects, and the peak at cap 14 was smaller than that seen at caps 54 and 63. The plot for the LED was a little larger than that for the CFL. Subject 4 had the smallest plots which look almost normal; there was a slight peak seen at caps 52-53 for the THL and LED. The plot for subject 5 was the second smallest; however, they appear abnormal for the THL and LED due to their peaks at cap 17 and 52-60 (THL), and 17 and 52-58 (LED). Subject 6's FM100 plots were similar in size to subject 1's. Again there were peaks for the THL at cap 13, but this time there was a large error seen at caps 58-62. The CFL had a large error through caps 50-58; and the LED at caps 11-15, 50, 58-64, and 70. As can be seen in Table 5.2 all the subjects followed the deuteranopic confusion axes.

Defect	Centre Cap	Cap Range	Colour
Protanopic	17	15-26	Yellow-Yellow/Green
	64	58-68	Blue/Purple
Deutanopic	15	12-17	Red/Yellow-Yellow
	58	53-60	Blue-Blue/Purple
Tritanopic	5	4-6	Red-Red/Yellow
	45.5	45-46	Green/Blue

Table 5.2 Cap positions for the axes of confusion [117]

The Friedman's test revealed a statistically significant difference between the three light sources. Using a series of Wilcoxon signed-rank tests a difference was found between the THL and the CFL, and between the CFL and the LED, but not the THL and the LED. This suggests that using the CFL resulted in lower TES than either the THL or the LED, and that there was no significant difference in the TESs of the THL and LED.

Looking at the combined FM100 plots (Figure 4.28 A-C), a slightly different picture emerges. The plots for the CFL and LED looked very similar. The smallest plot appeared to be the CFL, and the largest plot was the THL. The axis of confusion for the THL ran through caps 10-11 and 53-54. For the CFL the axis was through 14-15 and 58, and for the LED it ran through caps 15 and 59. Table 5.2 shows that for a deuteranomalous individual the expected axis goes through caps 15 and 58 [117]. There appeared to be very good agreement with the CFL and the LED, and the THL was not far off.

5.16.1 Colour Bands

The CBES graphs for all three light sources had similar shapes. There were two peaks: a small peak in the red/yellow-yellow, and a larger peak in the blue/purple-purple. The THL had the highest peaks, followed by the LED. The troughs for all three sources were in the yellow/green-green-green/blue region of the spectrum, and had similar CBES. The lowest CBES appear in the purple-purple/red-red part of the spectrum. The lowest CBESs were 2.72 for the THL, 2.34 for the CFL, and 2.42 for

the LED; and the peak CBESs were 8.26 for the THL, 5.58 for the CFL, and 6.94 for the LED.

Conducting Friedman's tests in each of the colours bands revealed on CBES revealed a significant difference between the three light sources in the blue-blue/purple colour band. Here Wilcoxon signed-rank tests found the CBES for the THL was significantly higher than that for the CFL. The differences between the THL and LED, and CFL and LED, were not statistically significant. However, as this was the only colour band to show a significant difference this may be a type 1 error (see Table 4.26).

When conducting the same analyses using FCES4, there was a similar bimodal graph. The difference between the two methods was that for the FCES4 the CFL graph peaked in the yellow-yellow/green band rather than the red/yellow-yellow as it did with the CBES (see Figure 4.29 D-F). As with the CBES, for the FCES4 plots of all three light sources had their highest peak in the blue-blue/purple. The lowest FCES4 appeared in the purple-purple/red-red band, and a trough in yellow/green-green-green/blue region.

For the FCES4 the Friedman's tests of the revealed a statistically significant difference in the red/yellow-yellow, and purple-purple/red colour bands (see Table 4.27). Wilcoxon signed-rank tests found the THL to have a significantly higher FCES4s compared to both the CFL and the LED for the red/yellow-yellow colour band. Here the CFL and the LED were not significantly different. For the purple-purple/red colour band, the Wilcoxon signed-rank tests were not significantly different for any of the light sources. As with CBESs these are most likely type 1 errors.

The correlation between the two methods was high for all three light sources, as it was with the Normal/Control and Smoker/Test groups (see Table 4.28).

5.16.2 Comparing the Case Study Group to the Normal/Control Group

For both the Case study group and the Normal/Control group the light source resulting in the lowest TES was the CFL, and the highest TES was the THL (see Figure 4.7A, Table 4.3, Figure 4.27, and Table 4.25). The difference was the position

of the LED. The LED in the Normal/Control group was paired with the CFL, and for the Case Study group it was paired with the THL.

When plotting the CBESs for the Case Study along with the Normal/Control CBESs, it can be seen that there were colour bands in which the scores were very different, and colour bands which the scores were very similar (see Figure 4.30, Figure 4.31, and Figure 4.32). It appears that the peaks seen with the Normal/Control group coincided with the troughs seen with the Case Study group, and with the LED the lines crossed (the CBES for the Normal/Control group was higher than that found in the Case Study group). The Mann-Witney U tests in this colour band (green-green/blue), and the final colour band (purple/red-red) showed that there was no significant difference in the CBESs between the Case Study group and the Normal/Control group for all three light sources (see Table 4.29, Table 4.30, Table 4.31, and Table 5.3). This means that in these areas of the spectrum deuteranomalous trichromats and normal trichromats discriminated colours equally well. This similarity in CBES extended into green/blue-blue colour band for the CFL, and into the yellow/green-green colour band for the THL.

For all three light sources there were a significant differences seen in the red-red/yellow, red/yellow-yellow, yellow-yellow/green, blue-blue/purple, and blue/purple-purple colour bands. Further to this these, the THL had a significant difference in the green/blue-blue band, the CFL had a significant difference in yellow/green-green band, and the LED had significant differences in the yellow/green-green, green/blue-blue, and the purple-purple/red bands. The LED had the greatest number of colour bands with significant difference between the Case Study group and the Normal/Control group. This suggests that the LED would highlight the differences between normal trichromats and deuteranomalous trichromats and so may be more useful in differentiating the two groups (see Table 4.29, Table 4.30, Table 4.31, and Table 5.3).

Colour bands	DTAs showing significant differences		
	THL	CFL	LED
Red-Red/Yellow	✓	✓	✓
Red/Yellow-Yellow	✓	✓	✓
Yellow-Yellow/Green	✓	✓	✓
Yellow/Green-Green	×	✓	✓
Green-Green/Blue	×	×	×
Green/Blue-Blue	✓	×	✓
Blue-Blue/Purple	✓	✓	✓
Blue/Purple-Purple	✓	✓	✓
Purple-Purple/Red	×	×	✓
Purple/Red-Red	×	×	×

Table 5.3 Summary of the Mann-Witney U tests showing significant differences comparing scores in each colour band for the Normal/Control group and the Case study group for all three light sources

5.17 Summary of Results

5.17.1 Normal/Control Group

The light source which allowed the best discrimination (lowest TES) was the CFL, and the worst colour discrimination (highest TES) was the THL.

5.17.2 Smoker/Test Group

No significant difference existed between the three light sources.

5.17.3 Smoker/Test compared to the Normal/Control group

The significant variable between the groups was 'Pack years', with a threshold of 7.5 pack years for the TES.

5.17.4 Colour Band Error Scores

Overall, all three lamps had a similar 'W' shape highlighting the perceptual non-linearity of the FM100. When looking at the SPDs the THL resulted in poorer discrimination in the red-red/yellow-yellow colours as expected, and the LED resulted in poorer discrimination for the yellow/green-green. However the LED resulted in better colour discrimination in the purple colour bands than expected. Pack years were significant for only two of the colour bands: green-green/blue (threshold of 7.5 pack years), and purple-purple/red (threshold of 3.5 pack years).

5.17.5 Frequency of Error Scores greater than four

The alternative method showed good agreement with CBES for the red-red/yellow-yellow colour bands with the THL resulting in poorer colour discrimination. For the green-green/blue colour band pack years was a significant variable (threshold 7.5 pack years) with FCES4 as it was for CBESs. It appears to be less affected by type 1 errors, and may provide a suitable alternative to CBES.

5.17.6 Correlation between CBES and Pack Years

There was no significant correlation.

5.17.7 Correlation between FES4 and Pack Years

There was no significant correlation.

6.8 The Best Light Source for Colour Discrimination

The CFL was the best overall light source to use shown by the Normal/Control group and the DTAs.

5.17.9 The Effect of Smoking on Colour Vision

There was a relationship between smoking and colour vision when pack years exceeded 7.5. The colour band of green-green/blue was most affected; however the relationship between error scores at pack years may not be linear.

5.17.10 Case Study Group

The CFL resulted in lower TESs than the THL and LED.

There were no significant differences found between the light sources for each colour band using either the CBES or the FCES4.

When compared to the Normal/Control group, the Case Study group performed most similarly using the CFL and THL, and had the greatest differences when using the LED. There colour bands where the CBES for the Case Study group were the same as for the Normal/Control group for all three light sources were, green-green/blue, and purple/red-red.

5.17.11 The best Light Source for Colour Discrimination

For environments where deuteranomalous trichromats operate the CFL (or a lamp with a similar SPD) was the best light source to use. This concurs with the Normal/Control group.

For colour vision testing the CFL (or a lamp with a similar SPD) should be used as it resulted in the lowest TESs. However, the LED would differentiate deuteranomalous trichromats from normal trichromats by a greater degree, which may be advantageous if that is the aim of the test. The LED may increase the sensitivity of the test at the cost of its specificity, and therefore the CFL is the better choice. In households containing normal trichromats and deuteranomalous trichromats, this particular LED should be avoided.

5.18 Addressing the Questions in the Aims

- 1.1. Can a cheap and readily available daylight source be found for colour vision testing? *Yes. All the sources used were under £10 per lamp, and produced TESs comparable with other studies*
- 1.2. Do any of these illumination sources perform differently with respect to the areas of the spectrum where errors are made? *Yes. The THL consistently resulted in poorer discrimination in the red-red/yellow- yellow part of the spectrum.*
- 2.1. Does smoking affect colour vision? *Perhaps. There was a significant difference found in TESs when pack years exceeded 7.5, however, no significant correlation was between pack years and TES.*
- 2.2. Is the colour vision of smokers affected in the same way as non-smokers under different sources of illumination? *Yes. Smokers showed similar patterns of TES, CBES, and FCES4 to the group of non-smoking trichromats for all three light sources.*
- 2.3. Do smokers have higher errors in certain parts of the spectrum compared to non-smokers? *Perhaps. There was a significant difference found in both CBESs and FCES4s in the green-green/blue part of the spectrum when pack years exceeded 7.5, however, no significant correlation was between pack years and either CBES or FCES4.*
- 3.1. How do deuteranomalous trichromats compare with normal trichromats under each light source? *For all three light sources the deuteranomalous trichromats displayed poorer colour discrimination in the red-red/yellow-yellow-yellow/green and blue-blue/purple-purple parts of the spectrum. The LED had the greatest number of colour bands that were significantly different*
- 3.2. Is there light source recommended for deuteranomalous trichromats to use? *The CFL (or a lamp with a similar SPD) is recommended as it resulted in the lowest TES.*

6 CONCLUSIONS

6.1 Impact on of this Study

This study has shown that a suitable alternative can be found for the discontinued MacBeth Easel lamp. Using a lamp whose SPD is similar the CFL used in this study results in TESs comparable with other studies. The lamp cost less than £10 (although three were needed to ensure an even spread of illumination on the test area). They were easy to install, however, being CFLs needed time to reach a steady state before commencing examination. The LED may provide an alternative for patients wanting to a lamp with rapid re-strike capability, under which to conduct their colour sensitive tasks. Both lamps are power efficient as very little energy is wasted as heat.

The study found that smoking, when beyond 7.5 pack years, had a detrimental effect on colour discrimination. There was no correlation between pack years and TES found either diagrammatically or by statistical analysis. However, with a larger sample size the relationship may become more evident. Although there appeared to be a statistically significant higher CBES and FCES4 in the green-green/blue part of the spectrum when pack years exceeded 7.5, it was not clinically significant. This colour band coincides with the peak in the Normal/Control group as well, and is a result of the inequality in the perceptual steps between the caps in the FM100. As there was no clear axis area of reduced colour discrimination, any explanation for the reduce TES would be speculative at best. This area requires further investigation.

The Case Study group consisted of deuteranomalous subjects as expected. The size of this group was much smaller than the other two, and more varied. The lamp allowing the best colour discrimination was the CFL, and the worst was the THL (as found with the Normal/Control group). The greatest deviation from the Normal/Control group was with the LED. However, as the sample size was small, conclusions drawn from the results need to be interpreted with caution. The FM100 plots (Figure 4.28 A-C) show clearly that through section of the FM100, deuteranomalous subjects perform as well as normal trichromats.

6.2 Limitations

The study would be enhanced by increasing the number of smokers and having a more even spread of pack years. By limiting the age range of the study in order to limit the effects of age, there was a limitation on the higher pack years.

There was a difficulty in recruiting smokers as their numbers are in decline. Recruiting from around the university may have been more fruitful; however, the pack years in this group will most likely be concentrated at the lower end. Attracting office workers in the 23-39 year old age group was particularly difficult as there was no financial incentive for them to give up 2-3 hours of their time. In order to counteract the difficulties posed by have a small sample size the technique of data mining was employed. This was done using DTAs. As with any data mining technique, there can be a violation of the degrees of freedom when analysing repeated measures. Where possible this was avoided by selecting the appropriate options in the CHAID analyses.

Larger groups would allow greater power when looking for small changes. This would aid the identification of outliers, and subsequently a correlation between error score and pack years may have been found. Approaching the local group that helps individuals stop smoking may have been an avenue to explore. Such a group of subject has shown an interest in their health, and may be more inclined to participate. However, the use other sources of nicotine (patches, gum, tablets, the use of e-cigarettes, and the process of cessation itself adds another variable requiring exploration.

Although the smoker's choice of brand was noted, it was not possible to define, as that choice changed over time from one brand to another. Therefore, it was not possible to examine the effects of different brands or their tar content. This is a variable that is very difficult to account for due to the changes in cigarette preferences of a smoker. Their choices may be based on cost, flavour, availability, or even health if switching to a brand with a lower tar content.

The use of a MacBeth Easel lamp as a control would have been ideal if it were still commercially available. Without a true control, the lamps used could only be compared to each other. Alternative controls could have been sourced at the cost of one of the other lamps. Reducing the study to one test lamp would also have reduced the burden on the subject, and would have allowed for monocular testing. An alternative would have been an approximation to the MacBeth Easel lamp. And may have introduced another source of error in the analyses

The Normal/Control and Smoker/Test groups were not gender matched. Dain found that males had significantly lower TES than females despite having larger pupils [153]. The higher number of females in the Normal/Control group may have increased their TESs, and therefore masked an increase in TES due to smoking. Unfortunately, as the sample size was small, it was difficult to match the genders. This solution to this is more efficient recruitment of subjects within the restricted time frame, or an extension of the time frame for recruitment.

As the Ishihara PIC only screens for red-green defects [10, 83, 84], none of the subjects were screened for tritan defects. Tritan defects are very rare (prevalence of 0.0001 %) [10, 19, 45], and it was felt that any tritan defect would be picked up during the FM100. None of the subjects in the Normal/Control group showed the tritan axes of confusion.

The tests were conducted binocularly which is suitable for assessing the lamps, but is not for assessing the ACVDs from smoking. As ACVDs can be monocular or binocular but asymmetric, doing the test binocularly could allow masking of a defect. By conducting the tests binocularly, only those subjects with ACVDs in their dominant eye, or in both eyes, would have been identified.

The choice to conduct the test binocularly was taken to ensure that the two groups were comparable without increasing the burden to the subject. Research objective 2.1.1, and 2.1.2 are examining the affect of the lamp on colour discrimination in subjects without any CCVD or know risk of ACVD. The aim is to give advice on lighting for colour vision testing, and to provide patients with advice on the characteristics of light installed when colour discrimination is of importance. In this group of subjects (the Normal/Control group) there is no suspicion of any asymmetry in colour discrimination, examining them binocularly is appropriate. Testing this group monocularly would have resulted in each subject performing eight FM100s, and may have disadvantaged the subjects that were amblyopic, and would have introduced an element of noise to the results where a small asymmetry was detected. The choice to conduct binocular testing in the Smoker/Test group reduced the study's sensitivity to ACVDs, however, allowed the direct comparison of the two groups. If the Smoker/Test were tested monocularly then the learning effect would have been different in this group. Their TESs may have been significantly lower on repetition; Hardy et al found that the learning effect takes 5-10 repetitions to saturate [114]. With

the Smoker/Test group repeating the test on four more occasions, then the reduction in the TES may mask the depth of the defect.

Doing the test monocularly may have allowed discovery of smaller changes, and would have allowed more accurate investigation of a ACVD in the Smoker/Test group. A method to accommodate the challenges of learning effect would need to be employed. One option is to use only one source of illumination. As this study has found the CFL to produce the lowest TESs, thus conducting future studies using a lamp with a similar SPD should remove any errors resulting from an inappropriate source of illumination. The subjects can be split into two protocols. The first protocol conducts the FM100 monocularly four times: right eye, left eye, left eye, right eye. The second protocol also conducts the FM100 monocularly four times, but starting with the left eye: left eye, right eye, right eye, left eye. Results would need to assess for both a reduction in colour discrimination in both eyes, and the difference between the two eyes. As established by this study, and Erb et al [149], the effect of smoking on colour discrimination is likely to be dose dependant, then measuring 'pack years' as the dependant variable would be a valuable.

6.3 Future Studies

Further exploration of effects of smoking on colour discrimination is required. This can take the form of a more stringent assessment of ACVDs in subjects that smoke (as described in section 6.2). A possible cause for an ACVD in smokers may relate to the macular pigment density. Work by Woo and Lee examined Caucasians and Asians with the FM100 [161]. They found that an increase in blue-yellow defect was greater with age in the Asian group than the Caucasian group. They linked that the difference in pigmentation in the macula as a reason for this. However, they conducted that the FM100 binocularly, and did not measure the pigment density. Further work by Davison et al used a densitometer to measure macular pigment optical density [162]. They did not find a significant difference in TES or partial error scores with macular pigment optical density. Moreland and Westland concluded that increasing macular pigment optical density in normal subjects could improve colour discrimination along the red-green axis at the cost of the blue-yellow axis [163]. The results on macular pigment density and colour discrimination are inconclusive. Tobacco smoke induced oxidative stress was shown to reduce the concentration on macular pigments in vitro by 10% [164], and smokers were found to have significantly

lower concentrations on macular pigment density than non-smokers [165]. An avenue for further exploration is the affect on macular pigment density on FM100 CBES (rather than just partial error scores). The variation seen in the Normal/Control age group examined in this study may be caused by variations in macular pigment density. Some of the smokers in the Smoker/Test group may have naturally high densities of macular pigment resulting in difference in FM100 scores.

An alternative direction to take with colour vision testing with smokers is to use two anomaloscopes: one utilising the Raleigh equation, and the other the Mooreland equation. An alternative is the *Oculus Heidelberg multi-colour anomaloscope* (*Oculus, Wetzlar, Germany*) which matches for both equations. Studies have been done to establish age-related normals, which may allow for extending the age range of the study [166]. Although these devices only examine the axes for CCVDs, the position and the size of the matching range will give an indication on how the match compares with normal subjects, making them an alternative for testing ACVDs [83]. Davison et al used the FM100 along with an anomaloscope using the Mooreland match in their study on macular pigment and colour vision [162]. Anomaloscopes have the advantage of being much quicker to administer than the FM100.

A future study into light sources may reveal help reveal a lamp under which deuteranomalous subjects perform better than under 'daylight'. Studies in to the appliances such as the X-Chrom lens have found some patients benefit in certain occupations, but no improvement was found in the FM100 [167]. Some individuals with CCVDs have found some benefit when looking at PIC plates with selective filters after a period of adaptation [168]. Therefore is it possible for to adjust the spectral output of illumination to reduce increase the colour discrimination in a specified area colour band for deuteranomalous subjects? This may be of use when such an individual is working in quality assurance.

REFERENCES

1. Duncan, T., *Physics: A Textbook for Advanced Level Students*. 1982, London: John Murray Ltd.
2. Mansfield, M. and C. O'Sullivan, *Understanding Physics*. 2nd ed. 2011, Chichester: John Wiley & Sons Ltd.
3. Cutnell, J. and K. Johnson, *Physics*. 7th ed. 2006: John Wiley & Sons Ltd.
4. Nelkon, M. and P. Parker, *Advanced Level Physics*. 4th ed. 1977, London: Heinemann Educational Book Ltd.
5. Le Grand, Y., *Light, Colour and Vision*. 2nd ed. 1968, London: Chapman and Hall Ltd.
6. Smith, N.A., *Lighting for Occupational Optometry*. HHSC Handbook, ed. D. Hughes. 1999: H and H Scientific Consultants Ltd.
7. Zahiruddin, K., et al., *Effect of Illumination on Colour Vision Testing with Farnsworth-Munsell 100 Hue Test: Customized Colour Vision Booth versus Room Illumination*. Korean J Ophthalmol, 2010. **24**(3): p. 159-62.
8. *CIBS Code for Interior Lighting*, ed. V.P. Rolfe. 1985, London: Yale Press Ltd.
9. Davson, H., *Physiology of the Eye*. 5th ed. 1990, Basingstoke: Macmillan Academic and Professional Ltd.
10. Birch, J., *Diagnosis of Defective Colour Vision*. 2nd ed. 2001, Oxford: Butterworth-Heinemann. 160.
11. Marsden, A.M., *History of the CIE: 1913-1988*. 1999, Vienna: Commission Internationale de l'Eclairage.
12. Mollon, J.D., *Color-Vision*. Annual Review of Psychology, 1982. **33**: p. 41-85.
13. Broadbent, A.D., *A critical review of the development of the CIE1931 RGB color-matching functions*. Color Research and Application, 2004. **29**(4): p. 267-272.
14. Shaw, M. and M. Fairchild, *Evaluating the 1931 CIE colour-matching functions*. Color Research and Application, 2002. **27**(5): p. 316-329.
15. Hunt, R.W.G., *The heights of the CIE colour-matching functions*. Color Research and Application, 1997. **22**(5): p. 335-335.
16. Fairman, H.S., M.H. Brill, and H. Hemmendinger, *How the CIE 1931 color-matching functions were derived from Wright-Guild data*. Color Research and Application, 1997. **22**(1): p. 11-23.
17. Stiles, W.S., *Interim report to the Commission Internationale de l'Eclairage, Zurich, 1955, on the National Physical Laboratory's investigation of colour matching*. Optica Acta, 1955. **2**(4): p. 168-181.

18. Smith, N.A., *Light Sources for Use in Areas used for Colour Vision Examination*. Optometry in Practice, 2004. **5**(4): p. 173-181.
19. Holmes, W., *Colour Vision Testing: What can be Achieved in Everyday Practice?* Optometry in Practice, 2011. **12**(4): p. 167-178.
20. Macadam, D.L., *Uniform Color Scales*. Journal of the Optical Society of America, 1976. **66**(10): p. 1103-1104.
21. Li, C., et al., *Evaluation of the CIE Colour Rendering Index*. Coloration Technology, 2011. **127**(2): p. 129-135.
22. Webvision, The Organization of the Retina and Visual System, H. Kolb, et al., <http://webvision.med.utah.edu/>
23. Bhutto, I. and G. Luty, *Understanding Age-Related Macular Degeneration (AMD): Relationships between the Photoreceptor/Retinal Pigment Epithelium/Bruch's Membrane/Choriocapillaris Complex*. Molecular Aspects of Medicine, 2012. **33**(4): p. 295-317.
24. Wimmers, S., M.O. Karl, and O. Strauss, *Ion channels in the RPE*. Progress in Retinal and Eye Research, 2007. **26**(3): p. 263-301.
25. Klettner, A., et al., *Cellular and Molecular Mechanisms of Age-Related Macular Degeneration: From Impaired Autophagy to Neovascularization*. International Journal of Biochemistry & Cell Biology, 2013. **45**(7): p. 1457-1467.
26. Parver, L.M., *Temperature Modulating Action of Choroidal Blood Flow*. Eye (London), 1991. **5**(2): p. 181-185.
27. Auker, C.R., et al., *Choroidal Blood-Flow .1. Ocular Tissue Temperature as a Measure of Flow*. Archives of Ophthalmology, 1982. **100**(8): p. 1323-1326.
28. Winkler, B.S., et al., *Oxidative damage and age-related macular degeneration*. Molecular vision, 1999. **5**: p. 32-32.
29. Snell, R.S. and M.A. Lemp, *Clinical Anatomy of the Eye*. Second ed. 1998, Oxford: Blackwell Science.
30. Wenkel, H. and J.W. Streilein, *Evidence that retinal pigment epithelium functions as an immune-privileged tissue*. Investigative Ophthalmology & Visual Science, 2000. **41**(11): p. 3467-3473.
31. Steinberg, R.H., R.A. Linsenmeier, and E.R. Griff, *3 Light-Evoked Responses of the Retinal-Pigment Epithelium*. Vision Research, 1983. **23**(11): p. 1315-1323.
32. Thompson, D.A. and A. Gal, *Vitamin A metabolism in the retinal pigment epithelium: genes, mutations, and diseases*. Progress in Retinal and Eye Research, 2003. **22**(5): p. 683-703.
33. Osterberg, G., *Topography of the Layer of Rods and Cones in the Human Retina*. Acta Ophthal Suppl. , 1935. **13**(6): p. 1-103.

34. Deng, W.T., et al., *Functional interchangeability of rod and cone transducin alpha-subunits*. Proceedings of the National Academy of Sciences of the United States of America, 2009. **106**(42): p. 17681-17686.
35. Hubel, D.H., *Eye, Brain, and Vision*. 2nd ed. 1995: Henry Holt and Company.
36. Wang, W.J., J.H. Geiger, and B. Borhan, *The photochemical determinants of color vision*. Bioessays, 2014. **36**(1): p. 65-74.
37. Song, H.X., et al., *Variation of Cone Photoreceptor Packing Density with Retinal Eccentricity and Age*. Investigative Ophthalmology & Visual Science, 2011. **52**(10): p. 7376-7384.
38. Conway, B.R., *Color Vision, Cones, and Color-Coding in the Cortex*. Neuroscientist, 2009. **15**(3): p. 274-290.
39. Conway, B.R., et al., *Advances in Color Science: From Retina to Behavior*. Journal of Neuroscience, 2010. **30**(45): p. 14955-14963.
40. Jayakumar, J., B. Dreher, and T.R. Vidyasagar, *Tracking blue cone signals in the primate brain*. Clinical and Experimental Optometry, 2013. **96**(3): p. 259-266.
41. Curcio, C.A., et al., *Distribution and Morphology of Human Cone Photoreceptors Stained with Anti-Blue Opsin*. Journal of Comparative Neurology, 1991. **312**(4): p. 610-624.
42. Bowmaker, J.K., *Visual pigments and molecular genetics of color blindness*. News in Physiological Sciences, 1998. **13**: p. 63-69.
43. Solomon, S.G. and P. Lennie, *The Machinery of Colour Vision*. Nature Reviews Neuroscience, 2007. **8**(4): p. 276-286.
44. Merbs, S.L. and J. Nathans, *Absorption-Spectra of Human Cone Pigments*. Nature, 1992. **356**(6368): p. 433-435.
45. Cole, B., *Assessment of Inherited Colour Vision Defects in Clinical Practice*. Clinical and Experimental Optometry, 2007. **90**(3): p. 157-175.
46. Bergmanson, J., *Clinical Anatomy and Physiology*. 11th ed. 2004, Houston: Texas Eye Research and Technology Center.
47. Kolb, H., et al., *Are There 3 Types of Horizontal Cell in the Human Retina*. Journal of Comparative Neurology, 1994. **343**(3): p. 370-386.
48. Ahnelt, P. and H. Kolb, *Horizontal Cells and Cone Photoreceptors in Human Retina - a Golgi-Electron Microscopic Study of Spectral Connectivity*. Journal of Comparative Neurology, 1994. **343**(3): p. 406-427.
49. Kolb, H., *Organization of Outer Plexiform Layer of Primate Retina - Electron Microscopy of Golgi-Impregnated Cells*. Philosophical Transactions of the Royal Society of London Series B-Biological Sciences, 1970. **258**(823): p. 261-&.

50. Boycott, B.B. and H. Wassle, *Morphological Classification of Bipolar Cells of the Primate Retina*. European Journal of Neuroscience, 1991. **3**(11): p. 1069-1088.
51. Mariani, A.P., *The Neuronal Organization of the Outer Plexiform Layer of the Primate Retina*. International Review of Cytology-a Survey of Cell Biology, 1984. **86**: p. 285-320.
52. Kolb, H., K.A. Linberg, and S.K. Fisher, *Neurons of the Human Retina - a Golgi-Study*. Journal of Comparative Neurology, 1992. **318**(2): p. 147-187.
53. Hubel, D. and M. Livingstone, *Color Puzzles*, in *Brain /*. 1990. p. 643-649.
54. Popovic, Z. and J. Sjostrand, *The relation between resolution measurements and numbers of retinal ganglion cells in the same human subjects*. Vision Research, 2005. **45**(17): p. 2331-2338.
55. Gouras, P., *Identification of cone mechanisms in monkey ganglion cells*. The Journal of physiology, 1968. **199**(3): p. 533-47.
56. Hendry, S.H.C. and R.C. Reid, *The koniocellular pathway in primate vision*. Annual Review of Neuroscience, 2000. **23**: p. 127-153.
57. Hubel, D.H. and M.S. Livingstone, *Color and Contrast Sensitivity in the Lateral Geniculate-Body and Primary Visual-Cortex of the Macaque Monkey*. Journal of Neuroscience, 1990. **10**(7): p. 2223-2237.
58. Rohrschneider, K., *Determination of the location of the fovea on the fundus*. Investigative Ophthalmology & Visual Science, 2004. **45**(9): p. 3257-3258.
59. Chui, T.Y.P., et al., *Foveal Avascular Zone and Its Relationship to Foveal Pit Shape*. Optometry and Vision Science, 2012. **89**(5): p. 602-610.
60. Schwartz, S.G. and C.T. Leffler, *Uses of the word "macula" in written English, 1400-present*. Survey of Ophthalmology, 2014. **59**(6): p. 649-654.
61. Balashov, N.A. and P.S. Bernstein, *Purification and identification of the components of the human macular carotenoid metabolism pathway*. Iovs, 1998. **39**(4): p. S38-S38.
62. Formankiewicz, M., *Acquired Colour Vision Deficiencies*. Optometry Today, 2009. **49**(21): p. 37-42.
63. Kuffler, S.W., *Neurons in the retina; organization, inhibition and excitation problems*. Cold Spring Harbor symposia on quantitative biology, 1952. **17**: p. 281-92.
64. Schiller, P.H., *The ON and OFF channels of the mammalian visual system*. Progress in Retinal and Eye Research, 1995. **15**(1): p. 173-195.
65. Uchiyama, H., K. Goto, and H. Matsunobu, *ON-OFF retinal ganglion cells temporally encode OFF/ON sequence*. Neural Networks, 2001. **14**(6-7): p. 611-615.

66. Campbell, F.W. and J.G. Robson, *Application of Fourier Analysis to the Visibility of Gratings*. The Journal of physiology, 1968. **197**(3): p. 551-66.
67. Dacey, D.M., *Circuitry for Color Coding in the Primate Retina*. Proceedings of the National Academy of Sciences of the United States of America, 1996. **93**(2): p. 582-588.
68. Lennie, P., J. Krauskopf, and G. Sclar, *Chromatic Mechanisms in Striate Cortex of Macaque*. Journal of Neuroscience, 1990. **10**(2): p. 649-669.
69. *John Dalton's Colour Vision Legacy*, ed. C. Dickinson, I. Murray, and D. Carden. 1996, London: Taylor and Francis.
70. Lee, B.B., et al., *An Account of Responses of Spectrally Opponent Neurons in Macaque Lateral Geniculate-Nucleus to Successive Contrast*. Proceedings of the Royal Society Series B-Biological Sciences, 1987. **230**(1260): p. 293-314.
71. Schwartz, S., *Visual Perception: A Clinical Orientation*. 1998: Appleton & Lange
72. Livingstone, M.S. and D.H. Hubel, *Anatomy and Physiology of a Color System in the Primate Visual-Cortex*. Journal of Neuroscience, 1984. **4**(1): p. 309-356.
73. Thorell, L.G., R.L. Devalois, and D.G. Albrecht, *Spatial-Mapping of Monkey V1-Cells with Pure Color and Luminance Stimuli*. Vision Research, 1984. **24**(7): p. 751-769.
74. Conway, B.R., D.H. Hubel, and M.S. Livingstone, *Color contrast in macaque V1*. Cerebral Cortex, 2002. **12**(9): p. 915-925.
75. Roe, A.W., et al., *Toward a Unified Theory of Visual Area V4*. Neuron, 2012. **74**(1): p. 12-29.
76. Bedford, R.E. and G.W. Wyszecki, *Wavelength discrimination for point sources*. Journal of the Optical Society of America, 1958. **48**(2): p. 129-35.
77. Bowmaker, J., D. Hunt, and J. Mollon, *Primate Visual Pigments: Their Spectral Distribution and Evolution*, in *John Dalton's Colour Vision Legacy*. 1997, Taylor and Francis: London. p. 37-46.
78. Cole, B.L., *The Handicap of Abnormal Colour Vision*. Clinical & experimental optometry : journal of the Australian Optometrical Association, 2004. **87**(4-5): p. 258-75.
79. Health and Safety Executive, *Colour Vision examination: A Guide for Employers*. 2005.
80. Health and Safety Executive, *Colour Vision Examination: A Guide for Occupational Health Providers*. 2006.
81. Birch, J., *Colour Vision Deficiency Part 3 - Occupational Standards*. Optometry Today, 2014. **54**(2): p. 44-48.

82. Steward, J.M. and B.L. Cole, *What Do Color-Vision Defectives Say About Everyday Tasks*. Optometry and Vision Science, 1989. **66**(5): p. 288-295.
83. Dain, S., *Clinical Colour Vision Tests*. Clinical and Experimental Optometry, 2004. **87**(4-5): p. 276-293.
84. Formankiewicz, M., *Assessment of Colour Vision*. Optometry Today, 2009. **49**(20): p. 28-34.
85. Pacheco-Cutillas, M., A. Sahraie, and D.F. Edgar, *Acquired Colour Vision Defects in Glaucoma - Their Detection and Clinical Significance*. British Journal of Ophthalmology, 1999. **83**(12): p. 1396-1402.
86. Marré, M., *The Investigation of Acquired Colour Vision Deficiencies*, in *Colour 73: Survey Lectures and Abstracts of the Papers Presented at the Second Congress of the International Colour Association, University of York 2-6 July 1973*, R.W.G. Hunt, Editor. 1973, Adam Hilger: London. p. 99-135.
87. Beirne, R., L. McIlreavy, and M. Zlatkova, *The Effect of Age-related Lens Yellowing on Farnsworth Munsell 100 Hue Error Score*. Ophthalmic & Physiological Optics, 2008. **28**: p. 448-465.
88. Cheng, A.S. and A.J. Vingrys, *Visual Losses in Early Age-Related Maculopathy*. Optometry and Vision Science, 1993. **70**(2): p. 89-96.
89. Maaranen, T.H., K.T. Tuppurainen, and M.I. Mantyjarvi, *Color vision defects after central serous chorioretinopathy*. Retina-the Journal of Retinal and Vitreous Diseases, 2000. **20**(6): p. 633-637.
90. Kanski, J.J., *Clinical Ophthalmology*. Fourth ed. 1999, Oxford: Butterworth-Heinemann.
91. American Academy of Ophthalmology, *Glaucoma*. 2005-2006.
92. Gupta, D., *Glaucoma: diagnosis and management*. 2005.
93. Sample, P.A., R.M. Boynton, and R.N. Weinreb, *Isolating the Color-Vision Loss in Primary Open-Angle Glaucoma*. American Journal of Ophthalmology, 1988. **106**(6): p. 686-691.
94. Papaconstantinou, D., et al., *Acquired color vision and visual field defects in patients with ocular hypertension and early glaucoma*. Clinical ophthalmology (Auckland, N.Z.), 2009. **3**: p. 251-7.
95. Drance, S.M., et al., *Acquired Color-Vision Changes in Glaucoma - Use of 100-Hue Test and Pickford Anomaloscope as Predictors of Glaucomatous Field Change*. Archives of Ophthalmology, 1981. **99**(5): p. 829-831.
96. Rodgers, M., et al., *Colour Vision Testing for Diabetic Retinopathy: A Systematic Review of Diagnostic Accuracy and Economic Evaluation*. Health Technology Assessment, 2009. **13**(60).
97. Schneck, M.E. and G. Haegerstrom-Portnoy, *Color Vision Defect Type and Spatial Vision in the Optic Neuritis Treatment Trial*. Investigative Ophthalmology & Visual Science, 1997. **38**(11): p. 2278-2289.

98. Pearlman, A.L., J. Birch, and J.C. Meadows, *Cerebral Color-Blindness - Acquired Defect in Hue Discrimination*. *Annals of Neurology*, 1979. **5**(3): p. 253-261.
99. Lawrenson, J.G., et al., *Acquired Colour Vision Deficiency in Patients receiving Digoxin maintenance Therapy*. *British Journal of Ophthalmology*, 2002. **86**(11): p. 1259-1261.
100. Pula, J.H., A.M. Kao, and J.C. Kattah, *Neuro-ophthalmologic side-effects of systemic medications*. *Current Opinion in Ophthalmology*, 2013. **24**(6): p. 540-549.
101. Verrotti, A., et al., *Color vision in epileptic adolescents treated with valproate and carbamazepine*. *Seizure-European Journal of Epilepsy*, 2004. **13**(6): p. 411-417.
102. Nousiainen, I., R. Kalviainen, and M. Mantyjarvi, *Color vision in epilepsy patients treated with vigabatrin or carbamazepine monotherapy*. *Ophthalmology*, 2000. **107**(5): p. 884-888.
103. Sorri, I., R. Kalviainen, and M. Mantyjarvi, *Color vision and contrast sensitivity in epilepsy patients treated with initial tiagabine monotherapy*. *Epilepsy Research*, 2005. **67**(3): p. 101-107.
104. Fine, B.J. and L. McCord, *Oral-Contraceptive Use, Caffeine Consumption, Field-Dependence, and the Discrimination of Colors*. *Perceptual and Motor Skills*, 1991. **73**(3): p. 931-941.
105. Hulka, L.M., et al., *Blue-yellow colour vision impairment and cognitive deficits in occasional and dependent stimulant users*. *International Journal of Neuropsychopharmacology*, 2013. **16**(3): p. 535-547.
106. Birch, J., *Colour Vision Deficiency Part 2 - Assessment in Clinical Practice*. *Optometry Today*, 2014. **54**(1): p. 48-52.
107. Moreland, J.D. and J. Kerr, *Optimization of a Rayleigh-Type Equation for the Detection of Tritanomaly*. *Vision Research*, 1979. **19**(12): p. 1369-1375.
108. Birch, J., *Efficiency of the Ishihara test for identifying red-green colour deficiency*. *Ophthalmic and Physiological Optics*, 1997. **17**(5): p. 403-408.
109. Birch, J. and L.M. McKeever, *Survey of the Accuracy of New Pseudoisochromatic Plates*. *Ophthalmic and Physiological Optics*, 1993. **13**(1): p. 35-40.
110. Birch, J., *Use of the Farnsworth-Munsell 100-Hue Test in the Examination of Congenital Color-Vision Defects*. *Ophthalmic and Physiological Optics*, 1989. **9**(2): p. 156-162.
111. Farnsworth, D., *The Farnsworth-Munsell 100- Hue Test for the Examination of Color Discrimination Manual*. 1957: MacBeth, A Division of Kollmorgen Corp.

112. Seshadri, J., V. Lakshminarayanan, and J. Christensen, *Farnsworth and Kinnear Method of Plotting the Farnsworth Munsell 100-Hue Test Scores: A Comparison*. *Journal of Modern Optics*, 2006. **53**(11): p. 1643-1646.
113. Kinnear, P.R. and A. Sahraie, *New Farnsworth-Munsell 100 Hue Test Norms of Normal Observers for Each Year of Age 5-22 and for Age Decades 30-70*. *British Journal of Ophthalmology*, 2002. **86**: p. 1408-1411.
114. Hardy, K., et al., *Extent and Duration of Practice Effects on Performance with the Farnsworth-Munsell 100-Hue Test*. *Ophthalmic & Physiological Optics*, 1994. **14**: p. 306-309.
115. Breton, M.E., D.E. Fletcher, and T. Krupin, *Influence of Serial Practice on Farnsworth-Munsell 100-Hue Scores - the Learning Effect*. *Applied Optics*, 1988. **27**(6): p. 1038-1044.
116. Birch, J., *Pass Rates for the Farnsworth D15 Colour Vision Test*. *Ophthalmic and Physiological Optics*, 2008. **28**(3): p. 259-264.
117. Birch, J., *Clinical use of the City University Test (2nd edition)*. *Ophthalmic and Physiological Optics*, 1997. **17**(6): p. 466-472.
118. Oliphant, D. and J.K. Hovis, *Comparison of the D-15 and City University (second) Color Vision Tests*. *Vision Research*, 1998. **38**(21): p. 3461-3465.
119. Hovis, J.K., *Repeatability of the Holmes-Wright Type A Lantern Color Vision Test*. *Aviation Space and Environmental Medicine*, 2008. **79**(11): p. 1028-1033.
120. Ashurst, W., *Physics*. 2nd ed. General Science for Schools. 1962, London: John Murray.
121. Smith, N.A., *Light-Emitting Diodes as a Universal Light Source*. *Optometry in Practice*, 2001. **2**(2): p. 121-128.
122. Mayr, S., M. Kopper, and A. Buchner, *Comparing Colour Discrimination and Proofreading Performance under Compact Fluorescent and Halogen Lamp Lighting*. *Ergonomics*, 2013. **56**(9): p. 1418-1429.
123. Gilman, J.M., M.E. Miller, and M.R. Grimaila, *A Simplified Control System for a Daylight-matched LED Lamp*. *Lighting Research & Technology*, 2012. **45**(5): p. 614-629.
124. Mahler, E., J.-J. Ezrati, and F. Vienot, *Testing LED Lighting for Colour Discrimination and Colour Rendering*. *COLOR Research and Application*, 2008. **34**(1): p. 8-17.
125. Dain, S., *Daylight Simulators and Colour Vision Tests*. *Ophthalmic & Physiological Optics*, 1998. **18**(6): p. 540-544.
126. *Interior Lighting Design*. 6th ed, ed. D.C. Pritchard. 1986, London: Lighting Industry Federation Ltd. & The Electricity Council.
127. Long, G.M. and J.P. Tuck, *Color-Vision Screening and Viewing Conditions - the Problem of Misdiagnosis*. *Nursing Research*, 1986. **35**(1): p. 52-55.

128. Mantyjarvi, M., *Normal Test Scores in the Farnsworth-Munsell 100 Hue Test*. Documenta Ophthalmologica, 2001. **102**: p. 73-80.
129. Johnson, D.D., *The True Daylight Illuminator (TDI): a less expensive source of illumination for color vision screening*. Journal of the American Optometric Association, 1992. **63**(7): p. 491-5.
130. Committee on Vision, Assembly of Behavioral and Social Sciences, and National Research Council, *Procedures for Testing Color Vision: Report of Working Group 41*. 1981, Washington: National Academy Press.
131. Pokorny, J., V. Smith, and J. Trimble, *A New Technique for Proper Illumination for Color Vision Tests*. American Journal of Ophthalmology, 1977. **84**(3): p. 429.
132. Higgins, K.E., A. Moskowitz-Cook, and K. Knoblauch, *Color vision testing: an alternative 'source' of Illuminant C*. Modern problems in ophthalmology, 1978. **19**: p. 113-21.
133. Smith, N.A., *Lighting for the High-Street Practice*. Optometry in Practice, 2003. **4**(1): p. 55-64.
134. All Party Parliamentary Group on Smoking and Health, *Inquiry into the Effectiveness and Cost-effectiveness of Tobacco Control: Submission to the 2010 Spending Review and Public Health White Paper Consultation Process*. 2010.
135. Department of Health, *Smoking Kills : A white Paper on Tobacco*. 1998: The Stationery Office.
136. Painter, J. and M. Crossland, *Smoking, Eye Disease and Smoking Cessation Strategies*. Optometry in Practice, 2007. **7**(4): p. 147-154.
137. Chakravarthy, U., et al., *Cigarette Smoking and Age-Related Macular Degeneration in the EUREYE Study*. Ophthalmology, 2007. **114**(6): p. 1157-1163.
138. Church, D.F. and W.A. Pryor, *Free-Radical Chemistry of Cigarette-Smoke and Its Toxicological Implications*. Environmental Health Perspectives, 1985. **64**: p. 111-126.
139. Lawrenson, J.G. and J.R. Evans, *Advice about Diet and Smoking for People with or at Risk of Age-Related Macular Degeneration: A Cross-Sectional Survey of Eye Care Professionals in the UK*. BMC Public Health, 2013. **13**.
140. Lois, N., et al., *Environmental Tobacco Smoke Exposure and Eye Disease*. British Journal of Ophthalmology, 2008. **92**(10): p. 1304-1310.
141. Action on Smoking and Health, *Smoking and Peripheral Aterial Disease*. 2014.
142. Uz, E., et al., *The relationship between serum trace element changes and visual function in heavy smokers*. Acta Ophthalmologica Scandinavica, 2003. **81**(2): p. 161-164.

143. U.S. Department of Health and Human Services, *U.S. Department of Health and Human Services. How Tobacco Smoke Causes Disease: The Biology and Behavioral Basis for Smoking-Attributable Disease: A Report of the Surgeon General*, U.S. Department of Health and Human Services. Centers for Disease Control and Prevention. National Center for Chronic Disease Prevention. Health Promotion Office on Smoking and Health, Editor. 2010.
144. Wang, J.B., et al., *Estimation of cancer incidence and mortality attributable to smoking in China*. *Cancer Causes & Control*, 2010. **21**(6): p. 959-965.
145. Action on Smoking and Health, *The Health Effects of Exposure to Secondhand Smoke*. 2014.
146. Law, M.R. and N.J. Wald, *Environmental tobacco smoke and ischemic heart disease*. *Progress in Cardiovascular Diseases*, 2003. **46**(1): p. 31-38.
147. van Staden, S.R., et al., *Carboxyhaemoglobin levels, health and lifestyle perceptions in smokers converting from tobacco cigarettes to electronic cigarettes*. *South African medical journal = Suid-Afrikaanse tydskrif vir geneeskunde*, 2013. **103**(11): p. 865-8.
148. Cong, R.H., et al., *Smoking and the Risk of Age-Related Macular Degeneration: A Meta-Analysis*. *Annals of Epidemiology*, 2008. **18**(8): p. 647-656.
149. Erb, C., et al., *Colour Vision Disturbances in Chronic Smokers*. *Graefes Archive for Clinical and Experimental Ophthalmology*, 1999. **237**(5): p. 377-380.
150. Bimler, D. and J. Kirkland, *Multidimensional scaling of D15 caps: Color-vision Defects among Tobacco Smokers?* *Visual Neuroscience*, 2004. **21**(3): p. 445-448.
151. Shimada, S., et al., *High Blood Viscosity Is Closely Associated With Cigarette Smoking and Markedly Reduced by Smoking Cessation*. *Circulation Journal*, 2011. **75**(1): p. 185-189.
152. Formankiewicz, M., *Normal Colour Vision and Inherited Colour Vision Deficiencies*. *Optometry Today*, 2009. **49**(18): p. 32-39.
153. Dain, S., *Differences in FM100-Hue Test Performance Related to Iris Colour may be due to Pupil Size as well as Presumed Amounts of Macular Pigmentation*. *Clinical and Experimental Optometry*, 2004. **87**(4-5): p. 322-325.
154. Lan, L. and Z. Lian, *Application of statistical power analysis - How to determine the right sample size in human health, comfort and productivity research*. *Building and Environment*, 2010. **45**(5): p. 1202-1213.
155. Faul, F., et al., *G*Power 3: A Flexible Statistical Power Analysis Program for the Social, Behavioral, and Biomedical Sciences*. *Behavior Research Methods*, 2007. **39**(2): p. 175-191.

156. Prajapati, B., M. Dunne, and R. Armstrong, *Sample Size Estimation and Statistical Power Analyses*. Optometry Today, 2010. **50**(14).
157. Field, A., *Discovering Statistics using SPSS*. 3rd ed. 2011, London: Sage Publications Ltd.
158. Verriest, G., J. Laethem, and A. Uvijls, *A New Assessment of the Normal Ranges of the Farnsworth-Munsell 100 Hue Scores*. American Journal of Ophthalmology, 1982(93): p. 635-642.
159. Dain, S.J., *Skewness and Transformations of Farnsworth-Munsell 100-Hue Test Scores*. Vision Research, 1998. **38**(21): p. 3473-3476.
160. Mantyjarvi, M., et al., *Colour Vision through Intraocular Lens*. Acta ophthalmologica Scandinavica, 1997. **75**(2): p. 166-169.
161. Woo, G.C. and M.-H. Lee, *Are ethnic differences in the F-M 100 scores related to macular pigmentation?* Clinical & experimental optometry : journal of the Australian Optometrical Association, 2002. **85**(6): p. 372-7.
162. Davison, P., et al., *Macular Pigment: Its Associations with Color Discrimination and Matching*. Optometry and Vision Science, 2011. **88**(7): p. 816-822.
163. Moreland, J.D. and S. Westland, *Macular pigment and color discrimination*. Visual Neuroscience, 2006. **23**(3-4): p. 549-554.
164. Hurst, J.S. and F.J.G.M. van Kuijk, *Macular Pigment Stability after Exposure to Heat and Tobacco Smoke*. ARVO Annual Meeting Abstract Search and Program Planner, 2003. **2003**: p. 1789.
165. Hammond, B.R., B.R. Wooten, and D.M. Snodderly, *Cigarette smoking and retinal carotenoids: Implications for age-related macular degeneration*. Vision Research, 1996. **36**(18): p. 3003-3009.
166. Rufer, F., et al., *Age-corrected reference values for the Heidelberg multi-color anomaloscope*. Graefes Archive for Clinical and Experimental Ophthalmology, 2012. **250**(9): p. 1267-1273.
167. Hartenbaum, N.P. and C.M. Stack, *Color vision deficiency and the X-Chrom lens*. Occupational health & safety (Waco, Tex.), 1997. **66**(9): p. 36-40, 42.
168. Supe, I. and V. Grabovskis, *Selective filters for improvement of color discrimination, in Advanced Optical Devices, Technologies, and Medical Applications*. 2002, Spie-Int Soc Optical Engineering: Bellingham. p. 339-342.

APPENDIX A



AUDIOLOGY & OPTOMETRY ETHICS FORM

All parts of the *Ethics Application* must be written concisely using terminology that would be understandable to an educated lay person on an ethics committee.

Title: The influence of different illumination sources on colour discrimination for normal, colour defective and smoking subjects

Principal Investigator: Mr Kalpen Mistry

Contact Details: [REDACTED], [REDACTED] mistryk4@aston.ac.uk tel [REDACTED]

Other Staff / Students involved: Dr Robert Cubbidge, ORG, ext 4107, r.p.cubbidge@aston.ac.uk

A. PROJECT OBJECTIVES / BACKGROUND

A1. What are the primary research questions / objective?

Lighting during the testing of colour vision is important as the spectral distribution of the light source influences the colour perception task. Ideally, colour vision testing is conducted under lighting which is equivalent to a lightly overcast north sky^{1,4}. However in modern optometric practice this is not always achievable due to the constraints of window placement within the practice⁵. As the previous "gold standard" illumination in the form of the Macbeath Easel lamp is now commercially unavailable, a practical alternative needs to be found for Optometric practice.

It needs to be determined whether the choice of illumination has a greater effect on subjects that have a pre-existing colour vision compared to subjects with normal colour vision. The influence of smoking on ocular pathology has been of ongoing interest in ophthalmology. Studies have shown that cigarette smoking can increase the risk of eye disease, especially macular degeneration⁶. Certain drugs have also been shown to induce an acquired colour vision deficiency⁷. It is possible that smoking may reduce the ability of an individual to discriminate colours and consequently may need be examined more regularly for colour vision problems.

The recommended illumination source for colour vision testing is standard illuminant C^{2,8}. The Macbeath lamp provided this using a 100W tungsten filament light source with a specific blue filter of correlated colour temperature (CCT) 6800-7500 K, yielding 300-400 lux. However, as technology has improved, illuminant D₆₅ (CCT 6500 K) is also recommended when high levels of colour discrimination are required^{3,4}. The CCT needs to be 6500 K or higher⁸ and the source needs a broad spectral power distribution. Many optical practices do not have access to either standard illuminant C or illuminant D₆₅. The aims of this investigation are to firstly evaluate three easily accessible artificial daylight sources (halogen, fluorescent and LED) under standardized conditions to firstly evaluate their suitability as substitutes for standard illuminant light sources and secondly to investigate their influence on colour vision discrimination in normals, colour defectives and subjects who are chronic smokers. It is hoped that recommendations can be made on the optimal lighting conditions required for colour vision testing in optometric practice.

1. Cole B (2007). Assessment of inherited colour vision defects in clinical practice. *Clin Exp Optom* 90: 157-175
2. Farnsworth D (1957). The Farnsworth-Munsell 100-hue test for the examination of color discrimination manual. MacBeath, A division of Kollmorgen Corp.
3. Dain S (1998). Daylight simulators and colour vision tests. *Ophthal Physiol Opt* 18: 540-544
4. Smith NA (2004) Light sources for use in areas used for colour vision examination. *Optom in Pract* 5: 173-181.
5. Smith NA (2003) Lighting for the high-street practice. *Optom in Prac* 4: 55-64
6. Painter J and Crossland M (2007) Smoking, eye disease and smoking cessation strategies. *Optom in Pract* 7: 147-154

7. Formankiewicz M (2009) Acquired colour vision deficiencies. *Optom Today* 49: 37-42
8. Birch J (2001) *Diagnosis of defective colour vision 2nd Ed.* Butterworth-Heinemann, Oxford, p 160

A2. Where will the study take place?

In Optometry Practice: Lesley Arkin Optometrists, Stony Stratford and Herons Opticians, Newport Pagnell

A3. Describe the statistical methods and/or other relevant methodological approaches to be used in the analysis of the results (e.g. *methods of masking / randomization*)

The protocol will be randomised between volunteers in order to minimise any order effects. Each participant will be assigned an order of examination which will remain constant for that individual but will be randomized between subjects. A learning effect is known for the 100-hue test and there will be an initial training visit, the results of which will be excluded from the main analysis. Any further learning effect will be minimized from averaging readings.

A4. List the clinical techniques to be conducted on patients as part of the study and indicate whether they fall within the scope of normal professional practice of the individual to perform them

Colour vision tests: Farnsworth-Munsell 100-hue, Ishihara and City Colour Vision Tests which are all part of an Optometrist's professional practice. The investigator Mr Mistry is a registered Optometrist.

ENCLOSE AN OUTLINE OF THE STUDY RATIONALE AND METHODOLOGY

B. RESEARCH PARTICIPANTS

B1. How many participants will be recruited? Please provide justification (power analysis software available from <http://www.psych.uni-duesseldorf.de/abteilungen/aap/gpower3/>)

Using the known error in 100-hue scores, the sample size would require has been calculated to require 30 volunteers in each of the normal, colour defective and smoking groups, based on implementing a confidence level of 95%

B2. What restrictions will there be on participation (age, gender, language comprehension etc)?

The exclusion criteria are as follows

- Significant lens yellowing
- Medications and ocular conditions which are known to give rise to acquired colour vision defects (with the exception of smoking)
- Manual dexterity problems which will hinder arrangement of tiles in the 100-hue test.

B3. How will potential research participants in the study be (i) identified, (ii) approached and (iii) recruited? *If research participants will be recruited via advertisement then attach a copy of the advertisement in the appendix of the ethics report.*

Participants will be recruited through verbal and written invitation both within and outside the practice of local optometrists. Local optometrists will be provided with details of the study so that they can refer subjects into the study if they deem it appropriate. The recruits will be free to aid in the recruitment process.

B4. Will the participants be from any of the following groups? *Tick as appropriate and justify any affirmative answers.*

- | | |
|--|-------------------------------------|
| Children under 16: | <input type="checkbox"/> |
| Adults with learning disabilities: | <input type="checkbox"/> |
| Adults who are unconscious or very severely ill: | <input type="checkbox"/> |
| Adults who have a terminal illness: | <input type="checkbox"/> |
| Adults in emergency situations: | <input type="checkbox"/> |
| Adults with mental illness (particularly if detained under Mental Health Legislation): | <input type="checkbox"/> |
| Adults suffering from dementia: | <input type="checkbox"/> |
| Prisoners: | <input type="checkbox"/> |
| Young Offenders: | <input type="checkbox"/> |
| Healthy volunteers: | <input checked="" type="checkbox"/> |
| Those who could be considered to have a particularly dependent relationship with the investigator, e.g. those in care homes, audiology students: | <input type="checkbox"/> |
| Other vulnerable groups: | <input type="checkbox"/> |

B5. What is the expected total duration of participation in the study for each participant?

A maximum of 6 weeks

B6. Will the activity of the volunteer be restricted in any way either before or after the procedure (e.g. diet or ability to drive)?
If so then give details.

NO

B7. What is the potential for pain, discomfort, distress, inconvenience or changes to life-style for research participants during and after the study?

NONE

B8. What levels of risk are involved with participation and how will they be minimized?

There are no risks associated with the normal and colour defective groups. In the smoking group, it is possible that they may be identified with a congenital or acquired colour vision defect. Congenital defects will be counseled under the normal remit of an optometrist. If an acquired defect is discovered, the subject will be referred to an ophthalmologist via their GP.

B9. What is the potential for benefit for research participants?

NONE

B10. If your research involves individual or group interviews/questionnaires, what topics or issues might be sensitive, embarrassing or upsetting? Is it possible that criminal or other disclosures requiring action could take place during the study?

The smoking group will be asked questions relating to the length of smoking and the amount of tobacco product used daily. No other disclosures are required outside those which constitute a routine eye examination.

B11. How will participants be de-briefed after the study? [See separate guidance notes on designing a De-briefing Sheet]

Volunteers will be de-briefed verbally. Information sheets supplied to volunteers express the opportunity for participants to request copies of any associated published material

B12. Describe any arrangement that have been made for indemnity insurance, if you have reason to think it is not already covered by the University's policy. [NOTE: We have been advised by the Risk & Insurance officer that research on Aston campus, or undertaken by Aston OD students, is covered by the University's professional indemnity policy, currently provided by Zurich Municipal Insurance with a £10 million limit.]

This research will be covered by both the University's professional indemnity policy as Mr Mistry is an OD student. He also carries his own professional indemnity insurance associated with his practice as an Optometrist

C. CONSENT

C1. Will a signed record of informed consent be obtained from the research participants? *If consent is not to be obtained, please explain why not.*

Yes.

ENCLOSE A PARTICIPANT'S INFORMATION SHEET (including a clear statement of what will happen to a volunteer) & A CONSENT FORM

C2. *Who will take consent and how it will be done?*

Prospective volunteers will be supplied with information sheet. An investigator and prospective volunteer will convene at least 24 hours after to discuss any issues raised by the prospective volunteer before signing of consent form by both investigator and volunteer.

C3. *How long will the participant have to decide whether to take part in the research? Justify your answer.*

24 hours. Volunteers will be supplied with an information sheet. This is the minimum period of time recognized by the NHS National Research Ethics Service guidance for participation to qualify as informed consent.

C4. *What arrangements are in place to ensure participants receive any information that becomes available during the course of the research that may be relevant to their continued participation?*

In the normal and smoking groups, it is possible that they may be identified with a congenital or acquired colour vision defect. Congenital defects will be counseled under the normal remit of an optometrist. If an acquired defect is discovered, the subject will be referred to an ophthalmologist via their GP.

C5. Will individual research participants receive any *payments/reimbursements* or any other *incentives* or *benefits* for taking part in this research? *If so, then indicate how much and on what basis this has been decided?*

No

C6. How will the results of research be made available to research participants and communities from which they are drawn?

Information sheets supplied to volunteers express the opportunity for participants to request copies of any associated published material

D. DATA PROTECTION

D1. Will the research involve any of the following activities? *Delete as appropriate and justify any affirmative answers.*

Electronic transfer of data by e-mail:

Use of personal addresses, postcodes, faxes, emails or telephone numbers:

Communication between the supervisor and principle investigator will involve data transmission by email. However, the data will not contain any personal details with respect to patients so the data will not be traceable to participants.

Mr Mistry will have details of personal addresses, postcodes, emails and telephone numbers of the participants of the study. This information will only be known to him and will be kept under lock and key. Where electronically kept, the data will be encrypted with password access.

D2. Will data be stored in any of the following ways? *Delete as appropriate and justify any affirmative answers.*

Manual files: YES

Home or other computers: YES

University computers: YES

Data collection will take place one-to-one with the investigator. Paper copies of colour vision testing results will be placed in a file and stored securely. Colour vision data used for analysis will principally be stored in password encrypted files on computers held by the investigators and only accessible by them.

D3. What measures have been put in place to ensure confidentiality of personal data? *Give details of whether any encryption or other anonymisation procedures will be used, and at what stage.*

All personal data will be anonymised and stored securely, only accessible by the investigators. Each subject will be assigned an identification number which will be the only link between the personal data and the results of the colour vision testing. No identifiable information will be published. Spreadsheets and personal computer login will be via password protection.

D4. If the data are not anonymised, where will the analysis of the data from the study take place and by whom will it be undertaken?

N/A

D5. Other than the study staff, who will have access to the data generated by the study?

None

D6. Who will have control of, and act as the custodian for, the data generated by the study?

Mr Kalpen Mistry

D7. For how long will data from the study be stored [minimum 5 years]? *Give details of where and how the data will be stored.*

Data will be stored for at least 7 years. Data will be stored on computer machines. Access to data on machines will be password protected.

E. GENERAL ETHICAL CONSIDERATIONS

E1. What do you consider to be the main ethical issues or problems that may arise with the proposed study, and what steps will be taken to address these?

In the normal and smoking groups, it is possible that they may be identified with a congenital or acquired colour vision defect. Congenital defects will be counseled under the normal remit of an optometrist. If an acquired defect is discovered, the subject will be referred to an ophthalmologist via their GP.

APPENDIX B



Response from AOREC

21st February 2011

Our Ref: AO2011.02

Project title: The influence of different illumination sources on colour discrimination for normal, colour defective and smoking subjects

Application Number: AO2011.02

Researchers: Dr Robert Cubbidge, Mr Kalpen Mistry
Ophthalmic Research Group
Aston University, B4 7ET

Dear Dr Cubbidge,

On behalf of the Audiology/ Optometry Research Ethics Committee (AOREC), I am pleased to inform you that the AOREC are happy to give approval to the above study and the following documents:

- Kalpen Mistry OD Blank_Ethics_Application_Form(amended21_02_2011).doc
- Kalpen Mistry- Information Sheet & Consent.docx
- Kalpen Mistry Protocol.docx

The details of the investigation will be placed on file. You should notify the Committee of any difficulties experienced by the volunteer subjects, and any significant changes which may be planned for this project in the future.

Yours sincerely,

A handwritten signature in blue ink, appearing to read "L. Davies".

Dr Leon N. Davies
Chair AOREC

APPENDIX C

CONSENT FORM

RESEARCH WORKERS, SCHOOL, SUBJECT AREA RESPONSIBLE:

Mr. Kalpen Mistry, Life & Health Sciences, Vision Sciences

TITLE:

The effect of different illumination sources on colour discrimination.

INVITATION:

You are being invited to take part in a research study. Before you decide whether you will participate it is important for you to understand why the research is being done and what it will involve. Please take time to read the following information carefully.

WHAT IS THE PURPOSE OF THE STUDY?

The purpose of this study is to determine whether the ability to discriminate between different colours is affected by the type of lamp used to illuminate the task area. This will give information to whether there is a difference between some commonly available light sources when discriminating colours, and which one provides the best environment for colour discrimination.

WHY HAVE I BEEN CHOSEN?

You have been chosen because you have normal colour vision and are free from any eye disease. The study is only open to adults between the ages of 20 and 39 years old.

WHAT WILL HAPPEN TO ME IF I TAKE PART?

The study will take place at location convenient for the subject, and will run for 18 months in total although your participation may only take a couple of hours. The first part of the study will involve a short screening test that will last 5 minutes to ensure that your colour vision is normal. During this test you will be required to identify the numbers that you see on a series of pages. Once this is complete the main part of the study can begin and you will be assigned an identification number. You will then be asked to arrange discs in colour order under a particular light source. There are 85 discs to arrange. This will be repeated for each light source. There are three different light sources that are being investigated during this study, and their combinations. All the light sources do not have to be tested on the same day; you will be free to return on a separate day to complete the task. Once all four light sources have been tested your participation in the study will be complete.

ARE THERE ANY POTENTIAL RISKS?

There are no physical risks from the study. All four light sources are commonly available to the public, and carry the CE marking. All personal data will be securely stored and destroyed once the study is completed. Your identification number will stay with the data. However, no link will remain between your identification number and your personal details.

DO I HAVE TO TAKE PART?

No. Participation is on a purely voluntary basis, and you will be free to exit the study at any stage without penalty.

EXPENSES AND PAYMENT:

There are no expenses or payments for participation in this study.

WILL MY TAKING PART IN THIS STUDY BE KEPT CONFIDENTIAL?

Yes. Any personal details collected at the beginning of the study will be securely stored, and will be destroyed at the end of the study. This information will only be used for this study and will not be made available to anyone outside of this study.

WHAT WILL HAPPEN TO THE RESULTS OF THE RESEARCH STUDY?

The results of the study will be collated, analysed and submitted as part of an Ophthalmic Doctorate. This will be available for your viewing from the Aston University Optometry Department library. The published material will contain the assigned identification number, but no personal data will be made available.

WHO IS ORGANISING AND FUNDING THE RESEARCH?

The research is organised in conjunction with Aston University. There is no funding for this study.

WHO HAS REVIEWED THIS STUDY?

The research has been submitted for approval by Aston University's Ethics Committee.

WHO DO I CONTACT IF SOMETHING GOES WRONG OR IF I NEED FURTHER INFORMATION?

Please feel free to contact Mr. Kalpen Mistry (mistryk4@aston.ac.uk).

WHO DO I CONTACT IF I WISH TO MAKE A COMPLAINT ABOUT HOW THE RESEARCH IS CONDUCTED?

If you have any concerns about the way in which the study has been conducted, then you should contact Secretary of the University Research Ethics Committee on j.g.walter@aston.ac.uk or telephone 0121 204 4665.

VOLUNTEER CONSENT FORM:

Title of Project: The effect of different illumination sources on colour discrimination.

Name of Chief Researcher: Mr. Kalpen Mistry.

		Tick Box
1	I confirm that I have read and understand the information sheet for the above study. I have had the opportunity to consider the information, ask questions and have had these answered satisfactorily.	
2	I understand that my participation is voluntary and that I am free to withdraw at any time without giving any reason, without my medical care or legal rights being affected.	
3	I agree to take part in the above study.	

Name of volunteer

Date

Signature